Selection and Characterization of DNA Aptamers for Therapeutic Monitoring of Lenalidomide, 6-Mercaptopurine, Dabrafenib and Venetoclax

Prepared by:

Mubark M. Alabudahash

Supervised by:

Dr. Ibrahim Khadra

A Thesis Submitted in Fulfilment of the Requirements for the Award of Degree of Doctor of Philosophy in Strathclyde Institute of Pharmacy and Biomedical Sciences at the University of Strathclyde, 2025

August 2025

Declaration

This thesis is the result of the author's original research. It has been composed by the author and has not been previously submitted for examination leading to the award of a degree.

Signed:

Date: 29 / 08 / 2025

Dedication

- To my parents, without whose endless prayers and encouragement, I would never have been able to complete this work. I love you both and I appreciate everything you have done for me.

- To my wife, who has walked every step of this journey with me and who pushes me to reach for the stars.

- To my son (Muhammed), the light of my life.

- To my brothers and sisters, for their emotional support.

Acknowledgments

First and foremost, I wish to express my sincerest gratitude to Allah, the Omniscient for providing me with health, commitment and patience to complete this study.

I would like to express my deepest appreciation to my supervisor, Dr. Ibrahim Khadra, for his support, continuous motivation and encouragement throughout my PhD study, despite his significant work with Strathclyde University. Words cannot express my gratitude to him.

I am extremely grateful to Prof. Mohammad Zourob for providing me with research ideas, guidance for research structure and valuable suggestions for improvement of my work. I could not have undertaken this journey without his support, advice and patience.

I also extend my appreciation and gratitude to staff in Prof. Zourob's lab – Dr. Shimaa Eissa, Dr. Raja Chinnappan and Dr. Maysoon Saleh – and my colleagues – Dr. Maram Sandouka and Dr. Haya Abdulkareem – for their cooperation and assistance with my lab work.

I would like to extend my sincere thanks to Dr. Christine Dufès, Dr. Steven Ford, Dr. Lina Akil and Grace Tedman in SIPBS at Strathclyde University.

Table of Contents

List of Tables

List of Figures

List of Abbreviations

Abbreviation	Full Name
6-MP	6-Mercaptopurine
ADRs	Adverse Drug Reactions
ALL	Acute Lymphoblastic Leukemia
AML	Acute Myeloid Leukemia
BCG	Bacillus Calmette-Guérin
BCL-2	B-cell lymphoma 2 protein
CAR	Chimeric Antigen Receptor
CD19	Cluster of Differentiation 19 protein
CD20	Cluster of Differentiation 20 protein
CD3	Cluster of Differentiation 3 protein
CD34+	Cluster of Differentiation 34
CE	Capillary Electrophoresis
CLL	Chronic Lymphocytic Leukemia
CTLA-4	Cytotoxic T-lymphocyte–associated antigen 4
DMSO	Dimethylsulphoxide
DNA	Deoxyribonucleic Acid
dNTP	Deoxynucleoside triphosphate
DVT	Deep vein thrombosis
EDTA	Ethylenediamine tetraacetic acid
ELISA	Enzyme-Linked Immunosorbent Assay
EMA	European Medicines Agency
ESI	Electrospray ionization
FDA	Food and Drug Administration
FLC	Fluorescamine
GC	Gas chromatography
G-CSF	Granulocyte colony-stimulating factor
GM-CSF	Granulocyte-macrophage colony-stimulating factor
HbF	Foetal Haemoglobin
HGPRT	Hypoxanthine-Guanine Phosphoribosyl Transferase
HPLC	High-performance liquid chromatography
I-131	Radioactive iodine
IFN-γ	Interferon gamma
IL-12	Interleukin-12
IL-1β	Interleukin-1 beta
IL-6	Interleukin 6
ILs	Interleukins
INFs	Interferons
IP	Intraperitoneal
IS	Internal standard
ISFET	Ion-Sensitive Field-Effect Transistor
IV	Intravenous

Kd	Dissociation constant
LC-MS	Liquid chromatography-mass spectrometry
LC-MS/MS	Liquid chromatography-mass/mass spectrometry
LMD	Lenalidomide
LOD	Limit of detection
LOQ	Limit of quantification
MAPK	Mitogen-activated protein kinase
MDS	Myelodysplastic syndromes
MM	Multiple myeloma
MS	Mass spectrometry
MST	Microscale thermophoresis
NMIBC	Non–muscle-invasive bladder cancer
PCR	Polymerase chain reaction
PD-1	Programmed Cell Death Protein -1
PD-L1	Programmed Cell Death Ligand 1
PE	Pulmonary embolism
pH	Potential of hydrogen
PZ	Piezoelectric
RNA	Ribonucleic acid
RP-HPLC	Reversed-phase high-performance liquid chromatography
SELEX	Systematic Evolution of Ligands by Exponential Enrichment
SLL	Small Lymphocytic Lymphoma
SPE	Solid-phase extraction
SPR	Surface plasmon resonance
SRM	Single reaction monitoring
ssDNA	Single Strand Deoxyribonucleic Acid
TDM	Therapeutic drug monitoring
TILs	Tumour-infiltrating lymphocytes
TLS	Tumour Lysis Syndrome
TNF-α	Tumour Necrosis Factor Alpha
UPLC	Ultra-performance liquid chromatographic
AF Solution	Ammonium Formate

Abstract

Adverse drug reactions associated with some anticancer medicines are a significant reason for patient compliance; therefore, healthcare providers have invested substantial effort in the last four decades in therapeutic drug monitoring (TDM) research to maximize therapeutic results, minimize toxicity or to achieve both of these. Therapeutic drug monitoring (TDM) is extremely important for anticancer drugs which often have serious adverse effects and whose optimum dosage can differ significantly between patients. Most analytical techniques applied for TDM are chromatographic methods, such as HPLC, LC-MS and LC-MSMS. Since these current methods have some challenges, such as time consuming, financial cost, and the need for high skilled personnel, it was beneficial to search for better methods.

Therefore, the aim of this research to study the developing and synthesizing of an aptamer model to approach monitoring of Lenalidomide (LDM), 6-Mercaptopurine (6-MP), Dabrafenib (DFB) and Venetoclax (VENX) via the Sequential Evolution of Ligands by Exponential Enrichment (SELEX) process.

In this work, DNA aptamers against four commonly used anticancer – Lenalidomide (LDM), 6-Mercaptopurine (6-MP), Dabrafenib (DFB) and Venetoclax (VENX) – have been selected, identified and characterized through the systematic evolution of ligands by exponential enrichment (SELEX) technique. Ten cycles of selection have been applied for each medicine. Many different Lenalidomide, 6-Mercaptopurine, Dabrafenib and Venetoclax-specific aptamer sequences were successfully obtained.

For the Lenalidomide, 19 aptamers were isolated, identified and aligned through SELEX and cloning then three of these were synthesized and the binding affinity of these three candidate's ssDNA aptamers to Lenalidomide were individually tested by a microscale thermophoresis (MST) technique and their dissociation constants calculated (Kd for the candidate aptamer number 1 = 653.46 ± 0.23 nM; Kd for the candidate aptamer number 2 = 15.18 ± 0.37 nM; and Kd for the candidate aptamer number 3 = 7.75 ± 0.09 nM). For the 6-Mercaptopurine, 10 aptamers were isolated, identified and aligned through SELEX and cloning and then three of these were synthesized. The binding affinity of these three candidate's ssDNA aptamers to 6-Mercaptopurine were individually tested by microscale thermophoresis (MST) and their dissociation constants calculated (Kd for the candidate aptamer number 1 = 2.30 ± 0.22 nM; Kd for the candidate aptamer number 2 = 46.8 ± 0.23 nM; and Kd for the candidate aptamer number 3 = 0.1552 ± 0.37 nM). For Dabrafenib, 28 aptamers were isolated, identified and

aligned through SELEX and cloning, then three of these were synthesized and the binding affinity of these three candidate's ssDNA aptamers to Dabrafenib were individually tested by microscale thermophoresis (MST) with their dissociation constants calculated (Kd for the candidate aptamer number 1 = 0.324 ± 0.23 nM; Kd for the candidate aptamer number 2 = 0.153 ± 0.23 nM; and Kd for the candidate aptamer number 3 = 2.016 ± 0.23 uM). Finally, for the Venetoclax, eight aptamers were isolated, identified and aligned through SELEX and cloning. Three of these were synthesized and the binding affinity of these three candidate's ssDNA aptamers to Venetoclax were individually tested by microscale thermophoresis (MST). Their dissociation constants calculated (Kd for the candidate aptamer number 1 = 29.06 ± 0.28 nM; Kd for the candidate aptamer number 2 = 11.66 ± 0.24 nM; and Kd for the candidate aptamer number 3 = 13.87 ± 0.29 uM). This work reports the first oligonucleotide aptamers selected for Lenalidomide, 6-Mercaptopurine, Dabrafenib and Venetoclax with Kd in the nanomolar range. These aptamers can be used for both basic research and clinical purposes. The sub-nanomolar range of Kds indicate that these aptamers have very high affinity for their respective drugs. These aptamers could be an emerging molecular recognition receptor for the construction of highly specific and very sensitive aptamer-based biosensors for therapeutic drug monitoring applications.

Chapter One: Research Background

Chapter One: Research Background

1.1 Introduction

Cancer is a disease occurring when cells in the human body divide uncontrollably and spread into surrounding tissues. Cancer is primarily caused by changes to DNA. Most cancer-causing DNA changes occur in a part of the DNA called genes; therefore, such changes are called genetic changes (National Cancer Institute, 2019). Changes in DNA can transform genes that regulate normal cell growth into oncogenes. Unlike normal genes, oncogenes cannot be stopped, so they cause uncontrolled cell growth. Genetic changes related to cancer tend to affect three main kinds of genes: proto-oncogenes, DNA repair genes and tumour suppressor genes. In normal cells, proto-oncogenes are involved in the process of growth and division. However, when these genes are altered in abnormal ways, they might change to cancer-causing genes (or oncogenes), allowing cells to grow and divide in uncontrolled way. Tumour suppressor genes are similarly involved in the growth and division of normal cell. Cells that are exposed to certain alterations in tumour suppressor genes might divide in an uncontrolled process. DNA repair genes are mainly responsible for fixing damaged DNA; therefore, cells with mutations in these genes are likely to develop additional mutations in other genes. Cancer cells differ from normal cells in many aspects that permit them to grow out of control and become invasive. They can break away from the original tumour cell and spread through the blood or lymph system to other locations in the body to form additional tumours (National Cancer Institute, 2019).

Most cancers form solid tumours which consist of masses of tissue. However, cancers of the blood, such as leukaemia, usually do not form solid tumours. Tumours are either malignant or benign. Cancerous tumours are mostly malignant, which means they have the ability to spread, or invade, nearby tissues. Moreover, as these tumours grow, some cancer cells can break off and move to other places in the human body through the blood or the lymph system and form new tumours away from the original tumour. Unlike malignant tumours, benign tumours do not have the ability to spread or invade the near tissues (Jemal et al., 2007). Metastatic cancer is a term used when cancer spreads from the place it first started to another place in the human body; the process by which cancer cells spread to other parts of the human body is called a metastasis. Metastatic cancer has the same name and the same type of cancer cells as the original cancer. For example, lung cancer that spreads to and forms a metastatic tumour in the breast is metastatic lung cancer, not breast cancer. Metastatic cancer cells generally look the

same as cells of the original cancer when examined under the microscope. In addition, cells of the original cancer and metastatic cancer cells typically have similarity in molecular features, such as the presence of specific chromosome changes (National Cancer Institute, 2019).

Most of medicines that dispensed to treat tumors, have some advers effects, so most of healthcare provider monitoring the therapeutic level(s) of the treatment in the patients. The chromatographic techniques are the most wide applied technique for this porpuse, however some analyrical technique can be applied, such as aptasensors.

In the last decade, the aptamer technology field has progressed significantly, and is regarded as a more efficient technology as the number of studies in the application of aptamers is speedily increasing. Aptamers hold great potential in many of medical applications, such as therapeutic drug monitoring, target-based drug discovery, diagnostics, drug delivery and imaging. In 2017, a DNA-aptamer for Tenofovir (an antiviral medicine for HIV treatment) detection have been developed and verified through both negative and positive controls in full human serum (Tzouvadaki et al., 2017). Moreover, electrochemical Carbamazepine (antiepileptic) aptasensor was developed for therapeutic drug monitoring purposes (Chung et al., 2022).

Many of aptasensors have been developed for detection and monitoring of some antibiotics in serum, such as gentamicin (Rowe et al., 2010), tobramycin (González-Fernández et al., 2011; Cappi et al., 2015), kanamycin (Li et al., 2014), and streptomycin (Danesh et al., 2016; Emrani et al., 2016) detection in serum.

Singh et al. have reported a significant advance by developing a noninvasive, wearable electrochemical aptasensor for real-time cortisol monitoring (Singh et al., 2023). Furthermore, Ye, Cui et al reported a remarkable progress in the field by engineering a wearable aptasensor for noninvasive monitoring of female hormones from sweat, which were previously difficult to monitor noninvasively and continuously (Cui et al., 2024).

Although aptamers have many advantages, such as high affinity and specificity for their targets, ease of generation, minimal batch-to-batch variation, low manufacturing costs, and low immunogenicity, the development and application of aptamers face some challenges. The SELEX process is often inefficient and labor-intensive. This method requires multiple cycles of selection and amplification to enrich high-affinity aptamers, which might introduce biases, such as the loss of rare binding sequences and non-

specific or unintended amplification of non-target sequences. These issues can affect the binding affinity and quality of the selected aptamers (Haixiang et al., 2021).

In addition, incomplete release of target molecules during regeneration cycles, leaves binding sites partially occupied, which reduces the aptasensor's performance and sensitivity. Another critical limitation is the performance discrepancy between in vitro and in vivo conditions. Aptamers selected in vitro may fail to function ineffective in biological systems due to their intrinsic physicochemical properties, such as pH, ionic strength, and the presence of competing molecules.

Additionally, they may lose their binding capability under extreme temperatures, limiting their functionality in diverse sensing environments. Therefore, in vivo applications depend on animal models to develop aptamers compatible with complex biological conditions, along with chemical modifications to improve the stability and resistance to nuclease degradation and prolong action (Yizhen et al., 2024).

1.2 Statistics

Although statistical studies are usually not directly applicable to individual patients, they are essential for governments, health professionals, policy makers and researchers to analyze and understand the impact of cancer on the population and to design and develop strategies overcome the challenges cancer poses. Statistical studies are also important for measuring the achievement and success of efforts to control and manage cancer. The most common in 2020 (in terms of new cases of cancer) were breast (2.26 million cases); lung (2.21 million cases); colon and rectum (1.93 million cases); prostate (1.41 million cases); skin (non-melanoma) (1.20 million cases); and stomach (1.09 million cases) (Ferlay et al., 2020). The total number of reported newly diagnosed cancer cases in Saudi Arabia in 2020 was 14,050 (SCR, 2020).

Table 1.1: Most common cancers among Saudi nationals, 2020 (SCR, 2020)

Type	Number	%
Breast	2499	17.8
Colorectal	1729	12.3
Thyroid	1044	7.4
Leukaemia	835	5.9
Non-Hodgkin Lymphoma	756	5.4
Hodgkin's Lymphoma	581	4.1
Corpus Uteri	494	3.5
Brain, CNS	488	3.5
Lung	458	3.3
Liver	450	3.2

Table 1.2: Most common cancers among Saudi nationals by gender, 2020 (SCR, 2020)

Male	6209	%	Female	7841	%
Colorectal	966	15.6	Breast	2459	31.4
Leukaemia	494	8.0	Thyroid	816	10.4
Non-Hodgkin Lymphoma	420	6.8	Colorectal	763	9.7
Prostate	366	5.9	Corpus Uteri	494	6.3
Lung	353	5.7	Leukaemia	341	4.3
Hodgkin's Lymphoma	347	5.6	Non-Hodgkin Lymphoma	336	4.3
Liver	291	4.7	Ovary	234	3.0
Bladder	291	4.7	Hodgkin's Lymphoma	234	3.0
Brain, CNS	283	4.6	Brain, CNS	205	2.6

1.3 Cancer Classifications

There are more than 100 types of cancer. Cancer types are usually named for the organs or tissues where the cancer cells form. For example, liver cancer starts in cells of the liver, and lung cancer starts in cells of the lung. Cancers may occasionally be described by the type of cell that formed them, such as a squamous cell or an epithelial cell (Song, 2008). The following sections describe cancers that begin in specific types of cells.

1.3.1 Carcinoma

Carcinomas are the most common kind of cancer. They are formed by epithelial cells, which are the cells that cover the outside and inside surfaces of the body (Helman and Meltzer, 2003). According to Murphy et al. (2018) carcinomas that begin in different epithelial cell types have specific names.

i. *Adenocarcinoma* is a cancer that forms in epithelial cells and produces mucus or fluids. Tissues with this type of epithelial cell are sometimes called glandular tissues. Most cancers of the prostate, colon and breast are adenocarcinomas.

ii. *Basal cell carcinoma* is a cancer that forms in the lower or basal layer of the epidermis, the outer layer of skin in humans.

iii. *Squamous cell carcinoma* is a cancer that begins in squamous cells, which are epithelial cells located just beneath the outer surface of the skin. Squamous cells also line many organs, including lungs, stomach, intestines, bladder and kidneys.

iv. *Transitional cell carcinoma* is a cancer that begins in a type of epithelial tissue called transitional epithelium. This tissue, composed of multiple layers of epithelial cells that can expand and contract, is found in the linings of the ureters, bladder and part of the kidneys, especially the renal pelvis. Some cancers of the bladder, ureters and kidneys are transitional cell carcinomas.

1.3.2 Sarcoma

Sarcomas are cancers that begins in bone and soft tissues, including muscle, blood vessels, lymph vessels and fibrous tissue (such as tendons and ligaments). The most common cancer of bone is osteosarcoma, while the most common types of soft tissue sarcoma are Kaposi sarcoma, leiomyosarcoma and liposarcoma (Fletcher et al., 2013).

1.3.3 Leukaemia

Cancers that form in the blood-forming tissue of the bone marrow are called leukaemia. These cancers do not create solid tumours. However, large numbers of abnormal white blood cells (leukemic blast cells and leukaemia cells) build up in the blood and bone marrow.

According to Borowitz et al. (2008), there are four common kinds of leukaemia, categorized based on how quickly the disease worsens (acute or chronic) and on the type of blood cell in which the cancer begins (lymphoblastic or myeloid).

1.3.4 Lymphoma

Lymphoma is cancer that forms in lymphocytes (B cells or T cells). These are white blood cells that are part of the immune system. In this type of cancer, abnormal lymphocytes build up in lymph vessels and lymph nodes (Swerdlow et al., 2016).

There are two main types of lymphoma as following**:**

i. *Hodgkin lymphoma:* Patients with this disease have abnormal lymphocytes called Reed-Sternberg cells. These cells mainly form from B cells.

ii. *Non-Hodgkin lymphoma:* This cancer starts in lymphocytes and grows quickly or slowly and can form either from B cells or T cells.

1.3.5 Multiple Myeloma

Multiple myeloma is cancer that forms in plasma cells, another type of immune cells. The abnormal plasma cells, called myeloma cells, synthesized in the bone marrow and form tumours in bones throughout the human body (Sirohi and Powles, 2004).

1.3.6 Melanoma

Melanoma is cancer that forms in cells that become melanocytes, which are the cells responsible for producing melanin (the pigment that gives skin its colour). While the majority

of melanomas form on the skin, melanomas can also form in some other pigmented tissues, such as the eye (Balch et al., 2009).

1.3.7 Brain and Spinal Cord Tumours

There are many types of brain and spinal cord tumours. These tumours are named according to the types of cells in which they formed and where the tumour first started in the central nervous system (Lewandrowski et al., 2011).

1.4 Cancer Treatment

There are many forms of cancer treatment. Treatment typically depends on the type of cancer and how advanced it is. In some patients, only one treatment is enough, while most of patients require a combination of treatments, such as surgery with radiation and chemotherapy. Moreover, some patients might have immunotherapy, hormone therapy or targeted therapy (National Cancer Institute, 2003).

1.4.1 Surgery

Surgery is applied to treat many types of cancer. Surgery gives better results when used for solid tumours that are localized in one area. It is a local treatment, which means that it treats only the part of the body with the cancer; therefore it is not used for leukaemia (a type of blood cancer) or for cancers that have spread to more than one organ (Lange et al., 2013). There are many techniques of performing surgery.

i. Cryosurgery

Cryosurgery is a type of treatment in which extreme cold generated by liquid nitrogen or argon gas is utilized to destroy abnormal tissue. Cryosurgery is typically used to treat early-stage skin cancer, precancerous growths on the skin, cervix and retinoblastoma. Cryosurgery is sometimes referred to as cryotherapy (Gage, 1995).

ii. Lasers

This is a technique in which beams of laser are used to cut through tissue. Lasers have the ability to be focused extremely accurately on tiny areas, so they can be utilized for precise surgeries. In addition, lasers can be used to shrink or destroy tumours or growths that might convert to cancer (Stafford et al., 2010). Lasers are typically used in case of tumours on the surface of the human body or on the inside lining of internal organs (Meijer et al., 2007).

iii. Photodynamic Therapy

Photodynamic therapy is a kind of treatment that uses specific drugs which react to a certain type of light. When that specific light focuses on a tumour, these drugs become active and kill the surrounding cancer cells. Photodynamic therapy is used most often topically to treat or relieve symptoms resulting from skin cancer.

Although surgery is considered the primary method for treating cancer, there are potential risks: pain, damage to nearby tissues, bleeding, and reactions to the anaesthesia (Dougherty et al., 1998).

1.4.2 Radiation Therapy

Radiation therapy is a technique using high doses of radiation to kill cancer cells or slow their growth by damaging their DNA, which will prevent dividing or cause the death of these cancer cells (Delaney et al., 2005).

Radiation therapy is used to treat cancer and to ease cancer symptoms, but it does not kill cancer cells instantly. It may take days or weeks of treatment before the DNA is damaged completely after which cancer cells continue dying for weeks or months even after the radiation therapy course ends. Radiation therapy has many advantages because it can treat cancer, prevent its return, or stop or slow its growth. Moreover, it can be used as a palliative treatment, shrinking tumours by external beam radiation to relive pain and other problems caused by the tumour, such as difficulty breathing or loss of bladder control (Eriksson and Stigbrand, 2010). Pain resulting from cancer that has spread to the bone can be cured with systemic radiation therapy agents called radiopharmaceuticals (Jonathan et al., 1999).

There are two main kinds of radiation therapy, internal and external beam.

i. The type of radiation therapy selected depends on a plethora of factors, including the type of cancer, size of the tumour, tumour location in the body, closeness of the tumour to normal tissues that are sensitive to radiation, and a patient's age and health condition (Brown, 2001).
ii. External beam radiation therapy is produced by a machine that aims radiation at the tumour. Usually the radiation is directed towards the tumour from many directions. In contrast, internal radiation therapy is a technique in which a source of radiation is put inside patient's body. The radiation source can be liquid or solid (Le et al., 2015).

Internal radiation treatment with a liquid source is called systemic therapy, which means that the treatment distributes through the blood to tissues that contain cancer cells. The administration route is either by swallowing, or through a vein via an IV line, or through an injection. In contrast, the internal radiation treatment with a solid source is called brachytherapy. In this kind of treatment, capsules, ribbons or seeds that contain a radiation source are placed in the patient's body, in or near the tumour. Brachytherapy is typically used to treat cancers of the head and neck, breast, prostate, cervix and eye (Dolgin, 2016).

A systemic radiation therapy called radioactive iodine (I-131) is most often used to treat specific types of thyroid cancer. Targeted radionuclide therapy is another type of systemic radiation therapy for treating some cases of advanced prostate cancer or gastroenteropancreatic neuroendocrine tumour (Haymart et al., 2011).

In some cases, radiation may be the only treatment used. However, in most cases, radiation therapy is combined with other cancer treatments, such as surgery, immunotherapy and chemotherapy (Mouridsen and Overgaard, 1990). Radiation therapy might be given before, during or after these other treatments. When combined with surgery, radiation therapy may be given beforehand to shrink the cancer, making it easier to remove and reducing the risk of recurrence. In some cases, it can be given during surgery, applied directly on the tumour without passing through the skin. In such cases, it is called intraoperative radiation (Gebski et al., 2006).

Radiation not only kills or slows the growth of cancer cells, it can also affect nearby normal cells. Damage to normal cells can cause many side effects, such as fatigue, nausea, vomiting, headache, swelling (oedema), tenderness, skin changes and hair loss (Stubbe and Valero, 2013).

1.4.3 Chemotherapy

Chemotherapy works by slowing or halting the growth of cancer cells which otherwise grow and divide rapidly. Chemotherapy is used to treat cancer or to ease cancer symptoms. It is used to treat many types of cancer (DeVita and Chu, 2008). In some cases, chemotherapy may be the only treatment given to the patient, but in most of cases, it is accompanied by other cancer treatments. When used with other treatments, chemotherapy can shrink a tumour before surgery or radiation therapy, which is called neoadjuvant chemotherapy. When it is used to destroy cancer cells that may remain after treatment with radiation therapy or surgery, it is called adjuvant chemotherapy (Mayer and Janoff, 2007).

Chemotherapy may be given in different ways, such as oral (pills, capsules or liquids) or through intravenous or intramuscular or intrathecal (injected between the layers of tissue that cover the brain and spinal cord) or intraperitoneal (IP), intra-arterial or topical (Abraham and Allegra, 2001).

Intravenous chemotherapy is usually given through catheters (a thin, soft tube) or ports (a small, round disc placed under the skin during minor surgery), and sometimes with the aid of a pump (often attached to catheters or ports to control how much and how fast chemotherapy goes into a catheter or port, allowing a patient to receive chemotherapy outside the hospital) (National Comprehensive Cancer Network, 2000).

There are many side effects for chemotherapy. It affects the bone marrow, which can cause anaemia. Chemotherapy increases the risk of bleeding and bruising. These treatments can lower the number of platelets (cells that help blood to clot and stop bleeding) in the blood. When the platelet count is low, the patient will bleed very easily and have tiny purple or red spots on his skin. This condition is called thrombocytopenia (Carelle et al., 2002).

1.4.4 Immunotherapy

Immunotherapy is a type of cancer treatment that supports immune system to fight cancer. Immunotherapy is a kind of biological therapy. Biological therapy is a type of treatment that utilize substances made from living organisms to treat cancer (Old, 1996).

As part of its normal function, the immune system detects and destroys abnormal cells and prevents the growth of many cancers. For instance, immune cells are sometimes accumulated around tumours. These cells, called tumour-infiltrating lymphocytes, or TILs, are indicator that the immune system is responding to the tumour. Patients whose tumours contain TILs often have better outcomes than patients whose tumours do not contain them (Rosenberg, 2014). Although the immune system can prevent or suppress cancer growth, cancer cells have certain ways to avoid destruction by the immune system. For example, cancer cells may have proteins on their surface that inactivate immune cells. In addition, they can change the normal cells around the tumour so they interfere with how the immune system responds to the cancer cells (Yang, 2015).

There are five major types of immunotherapies: immune checkpoint inhibitor, T cell transfer therapy, targeted therapy, treatment vaccines and immune system modulators (Klener et al., 2015).

Immune checkpoints are normal points of the immune system. Their role is to prevent the immune response from becoming so strong that it damages healthy cells. Immune checkpoints are involved in the process when proteins on the surface of T cells recognize and attach to partner proteins on other cells, such as some tumour cells. These types of proteins called immune checkpoint proteins. When the checkpoint and partner proteins attach together, they send an 'off' signal to the T cells, preventing the immune system from fighting the cancer (Ribas and Wolchok, 2018).

Some immunotherapy drugs acts against a checkpoint protein called CTLA-4. On the other hand, some immune checkpoint inhibitors act against a checkpoint protein called PD-1 or its partner protein PD-L1. Some tumours inhibit the T cell response by producing plenty of PD-L1 (Leone et al., 2015).

Many immune checkpoint inhibitors have been approved to treat patients with a variety of cancer types, including bladder, breast, liver, rectal, colon, cervical, stomach and Hodgkin lymphoma cancers (Lipson and Drake, 2011). The most common side effects of immune checkpoint inhibitors are fatigue, rash, nausea and trouble breathing (Heinzerling and Goldinger, 2017).

The second major type of immunotherapy is T cell transfer therapy. The principle of this type of treatment depends on taking immune cells from the tumour, especially those most active against cancer. They are selected and isolated in the lab to grow in large batches and injected in the patient through a needle in a vein. The process of growing T cells in the lab usually takes from two to eight weeks (Wherry, 2011).

There are two major types of T cell transfer therapy: tumour-infiltrating lymphocytes (TIL) therapy and chimeric antigen receptor (CAR) therapy (Eshhar et al., 2014). TIL therapy utilizes T cells called tumour-infiltrating lymphocytes that are found in a patient's tumour. Oncologists test these lymphocytes in the lab looking for the best ones that recognize the tumour cells. Then, these selected lymphocytes are treated with substances that make them rapidly increase to large numbers (Kershaw et al., 2013).

The idea behind this technique is that lymphocytes in or around the tumour have already shown the ability to recognize tumour cells, but there may not be enough to fight the tumour or to stop the signals the tumour is releasing to suppress the immune system. Therefore, when a patient is given large numbers of lymphocytes that react best with the tumour, the response is enhanced to overcome these obstacles (Kershaw et al., 2013).

CAR T cell therapy is similar to TIL therapy but the T cells in this technique are changed in the lab so that they express a type of protein known as CAR before they are grown and given back to the patient. CARs are designed to allow T cells to bind to specific proteins on the surface of the cancer cells, increasing their ability to attack the cancer cells (Haji-Fatahaliha et al., 2016).

T cell transfer therapy was first applied for the treatment of metastatic melanoma because melanomas often cause a severe immune response and often have many TILs. The use of TIL therapy has been effective for some patients diagnosed with melanoma and has produced promising results in other cancers, such as cervical squamous cell carcinoma and cholangiocarcinoma. However, this treatment is still experimental (Rosenberg et al., 1988). Two CAR T cell therapies have been approved by the Food and Drug Administration in the USA, both for blood cancers: Tisagenlecleucel (Kymriah®) (FDA, 2019) and Axicabtagene ciloleucel (Yescarta®) (FDA, 2018).

CAR T cell therapy can cause a serious adverse reaction known as cytokine release syndrome. This syndrome happens when the transfer of T cells, or other immune cells responding to the new T cells, results in the production and release of a large number of cytokines into the blood. Cytokines are immune substances with multiple functions in the human body. A sudden increase in their levels can cause trouble breathing, rapid heartbeat, low blood pressure, fever and rash.

The significant problem related to TIL therapy is capillary leak syndrome. This syndrome causes fluid and proteins to leak out of tiny blood vessels and flow into surrounding tissues, resulting in low blood pressure, which may lead to multiple organ failure and shock (Wang and Liu, 2017).

Targeted therapy is a kind of cancer treatment that targets changes in cancer cells that enhance them to grow, divide and spread. Many targeted therapies are either small-molecule drugs or monoclonal antibodies. Small-molecule drugs are small enough to enter cells easily, so they are utilized for targets inside cells, while monoclonal antibodies are proteins produced in the

lab. These proteins are designed to bind and interact with specific targets localized on cancer cells (Gerber, 2008).

Some monoclonal antibodies are working as immunotherapy because they support the immune system against cancer. For example, some monoclonal antibodies mark cancer cells so that the immune system will better recognize and attack them. An example is rituximab, which attaches to a protein called CD20 on B cells (type of white blood cells) and some types of cancer cells, causing the immune system to attack and fight them (Trapani and Darcy, 2017).

Some other monoclonal antibodies bring T cells near to cancer cells, helping the immune cells attack and fight the cancer cells. Blinatumomab (Blincyto®) is one of these examples, which binds to both CD19, a protein located on the surface of leukaemia cells, and CD3, a protein on the surface of T cells. This mechanism enables T cells get close enough to the leukaemia cells to respond to and destroy them (Yip and Webster, 2018).

To test a tumour and identify the targets, oncologists may require a biopsy. A biopsy is a procedure in which a piece of the tumour is taken for testing in the lab. There are some risks to having a biopsy, however. These risks vary according to the size of the tumour and the tumour's location. Targeted therapy has many advantages because of its selectivity and specificity.

One reason that cancer cells thrive is because they have the ability to hide from the immune system. Some specific targeted therapies can mark cancer cells so it is easier for the immune system to track, find and attack them.

Healthy normal cells in the human body usually divide to create new cells only when they receive signals to do so. These signals attach to proteins on the cell surface, telling the cells to divide. This process ensures new cells form only as a body needs them. Nevertheless, some cancer cells have changes in the proteins on their surface that direct them to divide whether or not signals are present. Some targeted therapies interfere with these proteins, thereby preventing them from ordering the cells to divide. This process suppresses the uncontrolled growth of a cancer.

Angiogenesis is the process by which tumours stimulate the formation of new blood vessels, allowing them to grow beyond a certain size in response to signals from the tumour. Some targeted therapies called angiogenesis inhibitors are designed to interfere with these signals and hinder the blood supply, thereby shrinking the tumour.

Some monoclonal antibodies have a synergetic effect when they combine with chemotherapy agents or radiation and when they attach to targets on the surface of cancer cells, the cells take up the cytotoxic substances, causing them to shrink and die (Hudson, 1999).

Another advantage of targeted therapy is represented in their ability to work in two ways, especially in breast and prostate cancers which require certain hormones to grow. Hormone therapy, a type of targeted therapy, can prevent the human body from making specific hormones needed by cancer cells to grow (Fay and Scott, 2011).

Targeted therapy does have some drawbacks, however.

- Cancer cells can become resistant to targeted therapy. Therefore, certain therapies may be more useful when taken with other types of targeted therapy or with other cancer treatments, such as chemotherapy and radiation.
- There may be difficulty developing drugs for some targets because of a target's structure, the target's function in the cell, or both.

The most common side effects of targeted therapy are diarrhoea and liver problems. Other adverse reactions might include problems with blood clotting and wound healing, fatigue, high blood pressure, mouth sores, nail changes, loss of hair colour, skin reactions like dry skin and rash and flu-like symptoms (Imai and Takaoka, 2006).

Cancer treatment vaccines are a kind of immunotherapy that treat cancers by enhancing the body's immunity against the cancer. Unlike cancer immunization vaccines, cancer treatment vaccines are designed for patients who already have cancer. It rests on the principle that cancer cells contain specific substances, called tumour-associated antigens, which are not available in normal cells or, if present, are at very low levels. Treatment vaccines can assist the immune system to recognize and react with these antigens and destroy cancer cells that contain them.

Cancer treatment vaccines can be synthesized in three main ways. The first way is by making them from patient's tumour cells, which means they are custom-made so that they stimulate a reaction against features unique to the patient's cancer. The second way is by making them from tumour-associated antigens present on cancer cells of many patients with a specific type of cancer. Such a vaccine can yield an immune response in any patient whose cancer produces that specific antigen. However, this type of vaccine is still under experimental process. The last way of making the treatment vaccines is by producing them from a patient's dendritic cells, a

type of immune cell. Dendritic cell vaccines stimulate the immune system to respond to an antigen on tumour cells. One dendritic cell vaccine has been approved, sipuleucel-T, which is now used to treat some patients with advanced prostate cancer.

Oncolytic virus therapy is a different type of cancer treatment and sometimes classified as a type of cancer treatment vaccine. It depends on utilization of an oncolytic virus, which is a virus that infects and destroys cancer cells without any harm to normal cells (Vonderheide and Nathanson, 2013).

The first FDA-approved oncolytic virus therapy was Talimogene laherparepvec (T-VEC, or Imlygic®) in 2015 (FDA, 2015). It is made by modifying the herpes simplex virus type 1 to treat melanoma in the skin or lymph glands. Although this virus can infect both normal and cancer cells, normal cells are able to resist the virus while cancer cells cannot.

Cancer treatment vaccines can cause some side effects, such as flu-like symptoms, nausea, vomiting and fatigue. One adverse reactions reported for T-VEC is tumour lysis syndrome. When tumour cells die, they break apart and release their content into the blood, causing a change in specific chemicals in the blood, potentially harmful to some organs, including the kidneys, liver and heart (Kohlhapp and Kaufman, 2016).

The last major type of immunotherapy, immune system modulators, enhance the body's immune response against cancer. Some of these agents support specific parts of the immune system, whereas others support the immune system in a more general way (Lee et al., 2010).

There are three classes of immune-modulating agents.

- *Cytokines* are proteins made by white blood cells. They play important roles in a body's normal immune responses and in the immune system's ability to respond to cancer (Ardolino et al., 2015). Many different cytokines are used to treat cancer, such as the following:
    a. *Interferons (INFs).* INF-alpha is one type of interferon that enhances the immune response to slow the growth of cancer cells or accelerate their death (Kirkwood and Ernstoff, 1984).
    b. *Interleukins (ILs)* are classified as cytokines. There are more than 12 interleukins, including IL-2, which is also called T cell growth factor. IL-2 increases the number of white blood cells in the human body, increasing

support for the immune response against the cancer (Floros and Tarhini, 2015).

c. *Hematopoietic growth factors,* classified as cytokines, are used to minimize the side effects from cancer treatment by promoting the growth of blood cells damaged by chemotherapy. They include erythropoietin, which increases the creation of red blood cells; IL-11, which promotes the production of platelets; and granulocyte-macrophage colony-stimulating factor (GM-CSF) and granulocyte colony-stimulating factor (G-CSF), which both raise white blood cell numbers. Increasing the white blood cell count reduces the risk of infections. G-CSF and GM-CSF can also support the immune system response against cancer through increasing the number of cancer-fighting T cells (Bociek and Armitage, 1996).

- *Bacillus Calmette-Guérin (BCG)* vaccine, an attenuated form of the bacteria that causes tuberculosis, is developed from Mycobacterium Bovis. It does not cause disease in humans, however. BCG is used to treat bladder cancer. When inserted directly into the bladder with a catheter, BCG causes an immune response against cancer cells. By 2015, there were more than seven different biosimilar agents or strains used in the treatment of non-muscle-invasive bladder cancer (NMIBC). It is also being studied in other types of cancer, such as colon cancer (Herr and Morales, 2008).
- *Immunomodulatory drugs* (also called biological response modifiers), boost the immune response. They have co-stimulating potent effects with the induction of IL-2 and IFN-γ production, which increases the number of natural killer (NK) cells. In addition, immunomodulatory agents have a significant impact in stopping tumours from forming new blood vessels (Sharma et al., 2011). They include the following:
  a. Thalidomide (Thalomid®)
  b. Lenalidomide (Revlimid®)
  c. Pomalidomide (Pomalyst®)
  d. Imiquimod (Aldara®, Zyclara®)

Imiquimod, a cream rubbed on the skin, boosts skin cells to release cytokines (Eklind et al., 2003). Most immune-modulating agents are used clinically to treat advanced cancer. In some cases, they are used to improve and manage side effects resulting from other cancer treatments. There many different dosage forms of immunotherapy that can be administered in different

routes: intravenously (IV), orally, topically and intravesical (i.e., the immunotherapy agent injected directly into the bladder). Some types of immunotherapies are dispensed in cycles, a period of treatment followed by a period of rest. The rest period allows the body to recover, respond to the immunotherapy and produce new healthy cells (Mellman et al., 2011).

Although many oncologists have begun prescribing immune-modulating agents with more frequency because of their potent efficacy, these agents have some side effects such as flu-like symptoms, weakness, fatigue, trouble breathing, blood clots and significant variations in mood and behaviour (Srinivas and Meier-Kriesche, 2008).

1.5 Therapeutic Drug Monitoring

Therapeutic drug monitoring (TDM) is the process of measuring a drug or its metabolites in the blood at scheduled time intervals to maintain a relatively constant concentration of the medication in the blood. Therapeutic drug monitoring (TDM) is used to determine the dose at which a drug will be the safest and more effective (MacDougall et al., 1992).

In the 1960s and early 1970s, researchers began promoting the concept of clinical pharmacokinetics, and by the 1970s, practitioners were designing drug treatment strategies based on blood drug concentrations in clinical settings (Oellerich et al., 1997). The original meaning of therapeutic drug monitoring (TDM) is to administer drugs in an optimal way for each patient by monitoring various factors that affect drug efficacy and adverse drug reactions (Ghiculescu, 2008). Therapeutic drug monitoring is applied in many situations such as optimization of the dosage (usually after reaching a steady state), assessment of adequate loading dose, assessment of compliance (e.g., anticonvulsant concentrations in patients with frequent seizures), dose forecasting to help predict patient dose requirements (e.g., aminoglycosides), prior adjustment of the dose to avoid or minimize toxicity (e.g., cyclosporin, aminoglycosides) and diagnosis of failed therapy, because TDM can help differentiate between ineffective drug treatment, non-compliance and adverse effects that mimic the underlying disease (Innocenti et al., 2000).

Several classes of drugs commonly require therapeutic monitoring, such medicines that have a narrow therapeutic index, which is a ratio between the toxic and therapeutic (effective) dose of medication and medicines that have a significant pharmacokinetic variability. In addition, some classes of drugs are commonly monitored to ensure a correct blood concentration, including antineoplastics, immunosuppressants, antiarrhythmic and antiepileptics (Ghiculescu, 2008).

TDM results are strongly dependent on many factors:

i. *Time sampling:* The process of sample collection should occur at the correct time after a dose of drug administration (errors in time sampling are likely most responsible for mistakes in interpreting results).
ii. *Type of sample and pre-treatment:* Solvents or reagents used in the pre-treatment must be compatible to the properties of the molecules to be quantified; pretreatment can be complex with the processes of extraction and centrifugation.
iii. *Method:* The analytical method or assay applied should be specific, sensitive, reliable and robust (Reynolds and Aronson, 1993).

Drug concentrations are generally measured in whole blood or serum, although saliva, which gives a measure of the unbound drug concentration, may be a useful alternative when blood samples are difficult to collect (Wilhelm et al., 2014).

In general, the sample must be collected at regular intervals to ensure that the effective or the therapeutic concentration of the drug is maintained in the body. For some drugs, maintaining this steady state is not as simple as giving a standard dose of medication. Each patient will absorb, metabolize and eliminate drugs at various rates based upon many factors like age, weight, gender and general state of health (Gross, 2001).

Levels of monitored drugs are tested frequently when a patient starts a drug regimen. When the results are in the therapeutic range and the clinical signs indicate that the treatment is appropriate, the health practitioner may monitor the drug at regular intervals (or as needed to accommodate changes in patient status) to ensure that the drug concentration within the therapeutic range. If the regimen treatment does not appear to be fully effective, or if the patient has either excessive side effects or signs of toxicity, then the health practitioner might order testing aimed at adjusting the drug dosage and maintaining levels within the therapeutic range. Sometimes the health practitioner may need to re-evaluate the use of a specific medication and consider switching to another type of drug to improve the patient's condition (Reynolds and Aronson, 1993).

The ideal application of therapeutic drug monitoring requires more than simply measuring the concentration of a drug in the patient's blood and comparing it with a target range. It begins when the drug is first prescribed and involves determining an initial dosage regimen that is appropriate for the clinical condition under treatment, the patient's clinical characteristics like

age, weight and renal and hepatic functions (Hon and Evans, 1998). Moreover, some factors that must be considered are the sampling time in relation to the dose, the dosage history (i.e., whether or not the result represents the steady state), the patient's response and the desired clinical targets. This information is vitally important for adjusting doses to achieve the optimal response with minimum toxicity (Galpin and Evans, 1993).

The analytical techniques used for TDM must be robust, standardized, validated, reliable, fast and cost-effective. There are many techniques applied to carry out a TDM, classifiable into two main groups, traditional methods and immunoassays methods. Traditional methods include spectrophotometry, fluorimetry, gas chromatography (GC), high-performance liquid chromatography (HPLC), liquid chromatography with mass spectrometry detection (LC-MS) or with double mass spectrometry detection (LC-MS/MS) (Milone, 2024).

On the other hand, immunoassays methods include radio immunoassay (RIA), particle enhanced turbidimetric inhibition immunoassay (PETINIA), enzyme immunoassay (EIA), microparticle enzyme immunoassay (MEIA), enzyme multiplied immunoassay technique (EMIT), fluorescence polarization immunoassay (FPIA), chemiluminescent immunoassays (CLIA), cloned enzyme donor immunoassay (CEDIA) and enzyme linked immunosorbent immunoassay (ELISA) (Esteve-Romero et al., 2016).

LC methods such as high-performance liquid chromatography (HPLC) are widely applied for TDM in many clinical laboratories. A variety of detectors is utilized, from the basic ultraviolet (UV) detector to multi-wavelength photodiode array detectors to mass spectrometry. One main advantage of chromatographic methods is the ability to conjointly analyze multiple drugs in a single assay; these methods typically provide higher specificity for identification of the drug (Snyder et al., 2016). While HPLC methods using UV absorbance detection (HPLC-UV) are generally highly specific, quite robust, precise, and sensitive they are not without their challenges. There are several drawbacks of these methods, such as a required extraction step and column degeneration over time (Shaikh and Guo, 2017).

In spite of these pre-analytical steps, interfering substances can sometimes pose significant challenges. The choice of an internal standard with high similarity to the compound of interest during specimen processing and chromatographically separable from the compound can also be challenging (Vogeser and Seger, 2010).

Although chromatography alone offers a high level of specificity in chemical analysis, the potential of combining liquid chromatography (LC) with the highly specific detection capabilities of mass spectrometry (MS) was recognized early in the field of therapeutic drug monitoring (TDM).

Although LC-MS/MS has high specificity, it still has problems, because it is still subject to interference issues induced by the blood matrix. This is a significant challenge due to ion suppression, where components of the matrix or co-eluting compounds interfere with the ionization and detection of a molecule of interest, leading to falsely high or low results. This persistent problem appears particularly when the analyte molecule and internal standard (IS) are affected quite differently, which is more likely to occur with analogue IS. Additional sources of LC-MS/MS inaccuracy include compound transformations that may occur within the ion source due to molecular degradation, even with relatively weak ionization. This is particularly problematic for target molecule analysis where Phase II conjugates, when the target compound can be converted into the parent compound if inadequate LC separation occurs, result in co-elution from the LC into the ion source (Willoughby et al., 2002).

In spite of the versatility of LC-MS/MS permitting flexible assay development for drug analysis, there are still some barriers that prevent the introduction of LC-MS/MS systems for routine use in clinical laboratories. First and foremost, a significant amount of technical experience is required to operate these complex and advanced systems. Lab technicians require extensive training over a long period to gain appropriate competency to operate and maintain these highly complicated instruments (Vogeser and Seger, 2010). Moreover, LC-MS/MS systems need large space requirements that can add to cost as such space is not always available in all clinical laboratories. In addition, operation requires vacuum pumps and a supply of clean nitrogen gas provided by either nitrogen gas generator or a pressurized tank. These gas sources generate abundant heat and the use of nitrogen generators with an associated air compressor can contribute to ambient noise in the lab (Van Eeckhaut et al., 2009).

Immunoassays are bioanalytical methods that rely on an antibody that will specifically bind to the antigen of interest to detect the presence or concentration of a specific substance using an immunological reaction in biological samples. The general principle of an immune assay depends on competitions between a fixed amount of labelled analyte and an inconstant amount of unlabelled sample analyte for binding a limited number of binding sites of an antibody

specifically raised against the analyte (i.e., antigen); therefore, the antibodies used in the immunoassay test must have a high affinity for the antigen (Salamone et al., 2023).

Immunoassay techniques can be subdivided based on the labelling specifications into two main pathways: label-free, in which the assay does not need any label for quantification; and on-labelled, which means the use of a label for detection (Clarke, 2004).

Furthermore, immunoassays can be classified in two main groups: heterogeneous, which involves a physical separation of bound and free moieties; and homogeneous, which requires only mixing of a sample and immunochemical reagent followed by detection (Ullman, 2013). There are several methods that utilize the principles of immunoassay for detection and quantification of therapeutic drugs in clinical laboratories: radio immunoassay (RIA), particle enhanced turbidimetric inhibition immunoassay (PETINIA), enzyme immunoassay (EIA), microparticle enzyme immunoassay (MEIA), enzyme multiplied immunoassay technique (EMIT), fluorescence polarization immunoassay (FPIA), chemiluminescent immunoassays (CLIA), cloned enzyme donor immunoassay (CEDIA), and enzyme linked immunosorbent immunoassay (ELISA) (Milone, 2024).

Radio immunoassay (RIA) is no longer commonly used because of the high costs of waste disposal and the health concerns from use of radioactive materials. This technique relies on radioactivity to detect the presence of the analyte, where the sample is incubated with an antibody and a radio-labelled drug. The amount of radioactivity measured is compared to the radioactivity present in known standards which are included in each run. Strengths of the RIA method, however, include sensitivity and reliability. In contrast, the special handling and disposal costs of radioactive material are major weaknesses of this method (Alhabbab, 2018).

Particle enhanced turbidimetric inhibition immunoassay (PETINIA) method uses the creation of light scattering particles to measure drug levels. The latex particle-bound drug binds to the drug-specific antibody, forming insoluble light-scattering aggregates. This causes an increase in the turbidity of the reaction mixture. Non-particle-bound drug in the patient sample competes with the particle-bound drug for antibody binding sites, inhibiting the formation of insoluble aggregates. The rate of particle aggregation (turbidity) is inversely proportional to the concentration of drug in the sample. Therefore, the rate of increase of absorbance (hence, the rate of the increase in turbidity) is inversely proportional to the concentration of the drug (Usman and Hempel, 2016).

Enzyme immunoassay (EIA) considered the next generation of immunoassays after RIA. Enzyme immunoassay (EIA) uses a non-radioactive enzyme label, eliminating the need for special handling and reducing disposal costs. Most drug testing today is performed using homogeneous EIA techniques. This refers to the fact that assays are performed in a single step (i.e., only one antibody is used in the procedure), thereby reducing the turnaround time for testing.

Microparticle enzyme immunoassay (MEIA) is a technique in which the solid-phase support consists of very small microparticles to increase the surface area on which the antigen-antibody reaction occurred, resulting in increased assay kinetics and decreased incubation time. Specific reagent antibodies are covalently bound to the microparticles. Antigen, if present, is then 'sandwiched' between bound antibodies and antigen-specific, enzyme-labelled antibodies. Antigen-antibody complexes are detected and quantitated by analysis of fluorescence from the enzyme-substrate interaction (Baktır, 2017).

The enzyme multiplied immunoassay technique (EMIT) is homogeneous and based on competition for the target analyte antibody binding sites. Analyte in the sample competes with the drug in the enzyme reagent that is labelled with G6PDH. Active enzyme G6PBH converts the coenzyme (NAD) in the antibody reagent to NADH, resulting in a kinetic absorbance change that is measured photometrically (Zhao et al., 2022).

Fluorescence polarization immunoassay (FPIA) uses a fluorescent molecule as the label instead of an enzyme, rendering it more sensitive. In FPIA, the patient sample is incubated with a known quantity of the fluorescent-labelled drug and an antibody specific for the drug. As in EMIT, the labelled and unlabelled drugs compete for the binding sites of the antibody. Polarized light is emitted in certain angles depending on whether the fluorescent-labelled drug is bound to antibodies or not. Since this is a competitive assay, the greater the amount of drug in the sample, the lower the amount of fluorescence. While this technique is relatively simple to perform with good precision and good sensitivity, it requires specialized instrumentation that is not routinely available on commonly used, high-throughput clinical analysers (Lea and Simeonov, 2011).

Chemiluminescent immunoassays (CLIA) are based on chemical reactions that emit energy in the form of light. When used in combination with immunoassay technology, the light produced by the reaction indicates the amount of analyte in a sample. The most common

chemiluminescent assay methods are either enzyme-amplified or direct chemiluminescent measurements. The rapid detection times and low background make the chemiluminescent methods faster than RIA or other EIA methods (Wang et al., 2012). Chemiluminescent immunoassays have achieved levels of sensitivity several orders of magnitude better than RIA and fluorometric immunoassays (Snyder et al., 2016).

Cloned enzyme donor immunoassay (CEDIA) technique is based on the bacterial enzyme B-galactosidase, which has been genetically engineered into two inactive fragments. These fragments spontaneously reassociate to form fully active enzymes that, in the assay format, cleave to a substrate, generating a colour change that can be measured spectrophotometrically. Analyte in the sample competes with analyte conjugated to one inactive B-galactosidase fragment for antibody binding sites. If analyte is present, it binds to antibody, leaving the inactive enzyme fragments free to form active enzyme. If analyte is not present, antibody binds to analyte conjugated to inactive fragment, inhibiting reassociation of these inactive B-galactosidase fragments and no enzyme is formed. The amount of active enzyme formed (absorbance change) is directly proportional to the amount of analyte present in the sample (Nishiyama et al., 2019).

Enzyme-linked immunosorbent assay (ELISA) is analytical technique for quantitation of antigen or antibody in which enzyme-labelled antibody or antigen is bound to a solid support (e.g., plastic tines or fins, microtiter plate wells, beads). After addition of a sample test and substrate, antigen, antibody or complex are detected by a colour change expressing the presence of the product of an enzyme-substrate reaction (Clarke, 2004).

Immunoassay methods offer numerous advantages, including the ability to perform tests in a wide range of settings, compatibility with multiplexed and fully automated high-speed clinical analysers, widespread availability in most clinical laboratories, relatively high precision, and the use of inexpensive equipment (Clarke, 2004).

Although immunoassay techniques are now widely used and provide faster turnaround times than traditional analytical methods for measuring a single analyte, they often lack specificity due to cross-reactivity between the parent drug, its metabolites, and structurally similar compounds. Moreover, the presence of endogenous human antibodies or endogenous compounds like bilirubin in the specimen can interfere with components of the assay reagent such as the assay antibodies or the antigen labels. These forms of interference can be source of

positive bias for immunoassays when compared against more specific methods such as liquid chromatography with double mass spectrometry detection (LC-MSMS) (Dasgupta, 2016).

The majority of clinical laboratories have begun implementing TDM by use of immunoassay analysers and immune-based methods, such as chemiluminescent immunoassays (CLIA), enzyme-linked immunosorbent assays (ELISAs) and liquid chromatography with mass spectrometer (LC-MS). LC–MS/MS methods are still considered the gold standard for TDM, as they have high specificity; however, high running costs minimize their routine application in a clinical setting. It should be noted, however, that all these highly specific techniques, except for their significant cost, require properly trained personnel and lengthy preparation time. Instead of these techniques, new-generation biosensor analysis techniques can be utilized, offering direct analysis at a reasonable or reduced cost. Even so, they are still far from being routinely applied in hospitals (Dauphin-Ducharme et al., 2019; Meneghello et al., 2018)

1.5.1 Biosensors

A biosensor is an analytical device that converts biological or chemical response into measurable electrical signals generating signals. The history of this technique dates back to 1906 when M. Cremer proved that the concentration of an acid in a liquid state is directly proportional to the electric potential arising between two portions of the fluid located on opposite sides of a glass membrane (Cremer, 1906).

The major components of the biosensor are as follows:

- *Analyte:* The substance of interest that needs measurement or detection. For instance, glucose is the 'analyte' in a biosensor developed to measure and detect glucose.
- *Bioreceptor:* The molecule that recognizes the analyte in specific matter, for instance cells, enzymes, aptamers, antibodies and deoxyribonucleic acid (DNA). The process of signal generation (in the form of heat, pH, light, mass change or charge) on interaction of the analyte with the bioreceptor is called bio-recognition.
- *Transducer:* An element that changes one form of energy into another. Converting the bio-recognition activity into a measurable signal is the role of the transducer in the biosensor technique. This process of energy conversion is termed signalization.
- *Electronics:* This is the part of a biosensor that produces the transduced signal and readies it for display. It is composed of complex electronic circuitry that operates

signal conditioning such as amplification and translation of signals from analogue into digital form. The processed signals are then measured by the display unit of the biosensor.

- *Display:* Typically consisting of a hardware part and software part. Usually, the display unit composes the interpretation system such as the liquid crystal display of a computer or a direct printer that formulates curves or numbers understandable by the user. There are many forms for the output signal on the display: an image, graphic, tabular or numeric.

Biosensors can be classified as the following:

a. *Resonant biosensor:* In this type, an acoustic wave transducer is attached with an antibody. The mass of the membrane changes when the analyte molecule (or antigen) is bound to the membrane. The producing change in the mass then changes the resonant frequency of the transducer. This frequency change is consequently measured (Reddy et al., 1994).

b. *Optical biosensors:* Light is used as a transduced signal that is measured in this type of biosensor. The biosensor can be designed based on electrochemiluminescence or optical diffraction. Optical transducers are mostly attractive for application for direct detection of bacteria. These sensors have the ability to detect minute changes in the thickness or refractive index which happen when cells attach to receptors immobilized on the transducer surface. Direct changes in characteristics of light correlate according to changes in concentration, number of molecules or mass. Several optical techniques have been designed to detect bacterial pathogens including surface plasmon resonance (SPR), monomode dielectric waveguides, the resonant mirror and the interferometer (Syam et al., 2012). Surface plasmon resonance (SPR) biosensor relies on optical sensors utilizing a thin gold film for sensing applications. The detection of reflection minima on photo-detector array sensors when the probed interaction between the molecule (i.e., analyte) passing over immobilized gold surface occurs. SPR has been applied to the detection of pathogen bacteria (Homola et al., 1999). On the other hand, the main principle of a piezoelectric (PZ) biosensor depends on coating the surface of the PZ sensor with a selectively binding material, such as antibodies to bacteria, and then placing it in a solution to detect the presence of bacteria. The bacteria will bind to the antibodies

and the mass of the crystal will rise while the resonance frequency of oscillation will decline proportionally (Watts et al., 1994).

c. *Thermal biosensors:* This type of biosensor relies on the absorption or production of heat of biological reactions, which leads to changes in the temperature of the medium in which the reaction occurs. They are created by combining temperature sensors with immobilized enzyme molecules. When the analyte attaches with the enzyme, the heat released from reaction of the enzyme is measured and calibrated against the concentration of the analyte. Detection of pesticides and pathogenic bacteria are the most common applications of this type of biosensor (Syam et al., 2012).

d. *Electrochemical biosensors:* Electrochemical biosensors are primarily designed for the detection of DNA binding drugs, glucose concentration and hybridized DNA. Electrochemical biosensors can be classified according to the measuring electrical parameters as conductimetric, amperometric and potentiometric (Wang et al., 1997).

e. *Conductimetric biosensors:* The electrical conductance or resistance of the solution is the main parameter in this kind of biosensor. When electrochemical reactions yield electrons or ions, the overall conductivity or resistivity of the solution changes. This change is measured and calibrated to the appropriate scale (Lazcka et al., 2007). Amperometric biosensors produce a current correlated to the concentration of the analyte to be detected. The Clark Oxygen electrode is an example of an amperometric biosensor (Syam et al., 2012). The principle of potentiometric biosensors depends on the fundamental principle that when voltage is applied to an electrode in solution, a current flow yields from electrochemical reactions. Therefore, the oxidation or reduction potential of an electrochemical reaction is the measured parameter in this kind of biosensors (Syam et al., 2012).

f. *Bioluminescence sensors:* It relies on the ability of specific enzymes to emit photons as a byproduct of their reactions. Therefore, this kind of sensor has been applied for detection of many microorganisms (Syam et al., 2012).

g. *Nucleic acid-based biosensors:* The work principle relies on the integration of an oligonucleotide with a signal transducer. The transducer is immobilized with nucleic acid probe, so it works as the bio-recognition molecule to detect DNA/RNA fragments (Syam et al., 2012).

h. *Nano biosensors:* The work principle is based on nanotechnology. The silver and some other specific noble metal nanoparticles have particular applications in the field of antimicrobial drugs, drug delivery systems and biolabeling (Rai et al., 2012).

There are parameters that affect the performance of the biosensor, such as selectivity, reproducibility, stability, sensitivity and linearity. Selectivity is perhaps the most vital feature of a biosensor. It reflects the ability of a bioreceptor to detect a specific analyte in a sample containing a matrix of other substances. Reproducibility reflects the ability of the biosensor to show identical responses in more than one experiment. It is characterized by the accuracy and precision of the transducer and electronics in a biosensor. Accuracy shows the sensor's capacity to yield a mean value close to the true value when a sample is measured multiple times, while precision indicates the ability of the sensor to give identical results every time a sample is measured (Gibson, 1999).

The stability parameter reflects the degree of susceptibility to ambient turbulences in and around the biosensing system. Turbulence can cause a drift in the released signals of a biosensor under measurement. This can result in errors in the measured concentration and can affect the accuracy and precision of the biosensor. Stability is the most crucial parameter in applications where a biosensor mainly requires long incubation procedures or frequent monitoring. Temperature can influence the response of transducers and electronics, potentially affecting the stability of a biosensor. Therefore, suitable tuning of electronics is crucial to ensure a stable response of the sensor. Another factor that can affect the stability of the receptor is the affinity, the degree to which the analyte binds to the bioreceptor. The degradation of the bioreceptor over time is yet another factor influencing the stability of a measurement (Song et al., 2021).

Sensitivity is a parameter that affects the performance of the biosensor. Occasionally it is termed the 'limit of detection' (LOD), which means the minimum amount or concentration of the analyte that can be detected by a biosensor. The final parameter that can influence biosensor performance is linearity, a feature that shows the accuracy of the measured response (for different of measurements with different concentrations of analyte) to a straight line (Zhou et al., 2025).

Many applications for biosensors are expanded because their unique characterizations. Some of these applications include general healthcare monitoring, screening in disease diagnosis,

drug analysis and discovery, agricultural and veterinary applications, industrial processing and monitoring and environmental pollution monitoring and control (Mehrotra, 2016).

1.5.2 Aptamer

Aptamers can interact with their targets through structural recognition, as in antibodies, though with higher specificity. With this added advantage, they can be useful for clinical applications such as targeted therapy and diagnosis.

Aptamers are short, single stranded nucleic acid/peptide (of ~30 to ~70 nucleotides in length on average), that can be created by a well-established and sophisticated technique known as Systematic Evolution of Ligands by Exponential Enrichment (SELEX). The term *aptamer* derived from the Latin *aptus*, meaning "to fit", and *meros* (Greek), meaning "part", according to Ellington (Ellington and Szostak, 1990). It is fold into three-dimensional structures, interacting and binding to its target with high affinity and selectivity (Sun et al., 2014).

In 1990, Craig Tuerk and Larry Gold were investigating bacteriophage T4 DNA polymerase, demonstrating the process of selecting RNA ligands which bind to target protein in very specific ways (Tuerk and Gold, 1990). Since then, the number of aptamers developed as biosensors has grown exponentially and continues to increase to the present day (Wang et al., 2025).

The development of oligonucleotide screening through the Systematic Evolution of Ligands by Exponential Enrichment (SELEX) facilitated the discovery of many aptamers. With this technique, repetitive cycles of selection, amplification and washing of the nucleotide ligand are carried out until an aptamer appears with high affinity and specificity for the target (Wilson and Szostak, 1999).

The strengths of the SELEX (Systematic Evolution of Ligands by Exponential Enrichment) approach include its ability to produce aptamers with high-affinity and high specificity against diverse targets, which can replace antibodies. In addition, SELEX is more cost-effectiveness compared to antibody production, higher-throughput selection, faster and the ability to be easily modified to improve stability and binding properties (Brown et al., 2024).

However, SELEX suffers from some limitations, including time-consuming, requires significant manual effort, variation between in-vitro and in-vivo efficacy (Xiao et al., 2021).

These limitations have lead researchers sometimes to apply other methods to develop aptamer, such as magnetic bead-assisted screening, competition selection, capillary electrophoresis, centrifugal distribution and In-silico screening.

Magnetic bead-assisted screening for aptamer selection involves using magnetic beads to separate aptamers from a library based on their binding to a target molecule. The principle depends on immobilizing either the molecule (i.e. target) or the aptamer library. The magnetic field is applied onto the magnetic beads, to isolate and wash unbound sequences, and then eluting the bound sequences (i.e. target) for the next round of selection. This technique accelerates the process by simplifying the separation step, which is often a hurdle in the traditional method (Manea et al., 2024). It offers several advantages, including increased speed and efficiency by enabling easy and rapid separation of aptamers from unbound molecules. However, there are some disadvantages for this technique, such as potential for beads to hinder aptamer-target binding, non-specific binding to the bead surface, complex and costly due to the specialized equipment required for separation and labeling (Fang et al., 2024).

The competition selection method has a similar strategy to the classical SELEX, but without the repetitive binding, washing, separation, and amplification processes of traditional competitive SELEX. It relies on competition rather than evolution to screen aptamers, and is suitable for the rapid screening of large nucleic acid libraries, which leads to generate aptamers with higher specificity and affinity for the target molecule (Kushwaha et al., 2019).

One of the main drawbacks of this method is cross-reactivity, which results from using a single solution containing positive and negative targets, so it is possible for the final aptamer to bind to similar, non-target molecules. In addition, the presence of competitive targets, which may not always be easily available or obtainable for all desired aptamers, is one of the main obstacles to apply this method (Kushwaha et al., 2019).

The capillary electrophoresis-based non-SELEX approach is roughly the same as classical SELEX in principle and methodology, but no amplification is required between the two cycles of screening, and the DNA fragment collected in the first cycle is directly used as

the input DNA for the second cycle, which is mixed and incubated with a new aliquot of the target molecule and injected into the capillary to start a new cycle, which accelerates the screening process (Yang et al., 2021).

Beside increasing the speed of the process, reducing sample and solvent consumption are one of the advantages for this method. The high cost of the analytical equipment, such as multi-capillary arrays is one of the disadvantages of this technique, in addition to the training required to operate the system (Yang et al., 2021).

The principle of centrifugal distribution method for aptamer development depends on using a high-speed centrifuge to separate and isolate the aptamer-target complexes from unbound aptamers based on their mass and size (Jeong et al., 2022).

Fast separation is one of the advantages of this method, as well as low sample and reagent volume required. In spite of that, there are many drawbacks for this method, such as equilibrium shifts, unstable pH gradients and high chance to produce false positives (Jeong et al., 2022).

In silico aptamer screening technique utilizes computational methods such as molecular modeling, docking, and dynamics simulations to predict and screen high-affinity aptamers virtually, bypassing or enhancing classical, time-consuming experimental methods like SELEX (Lee et al., 2023).

The main advantages of this technique are that it is faster, cheaper, and more efficient than classical experimental methods such as SELEX (Chen et al., 2023), however, there some disadvantages for this method, such as high cost for the computer, the inability to design and develop aptamers for complex cellular targets and the difficulty and complexity of the modeling (Bavi et al., 2019).

Identification of aptamers in vitro, by SELEX, initially begins with the incubation of a random DNA library pool with the target molecule (which can be amino acids, proteins, antibiotics, peptides, bacteria and virus). Then, the sequences that have been bound to targeted molecules are eluted and incubated with control and concomitant by amplification by PCR. These steps are continuously repeated until the sequences show high affinity and specificity against its target molecules. Later, these enriched pools of sequences with higher affinity and specificity against its targets are cloned into bacteria. The positive clones are utilized for sequencing to obtain the individual sequence of an aptamer (Gopinath, 2007).

As many selection processes, the functional role of an aptamer is related by a stable three-dimensional structure related to the length and sequence of the aptamer. The degree of complexity of three-dimensional structures increases the specificity of aptamer. The process of aptamer binding to its target involves numerous mechanisms, such as electrostatic interactions, hydrogen bonding and Van der Waals forces (Hermann and Patel, 2000). Aptamers are stable, inexpensive to manufacture, non-immunogenic and can be chemically modified to simplify their visualization, absorption and delivery (Ni et al., 2011).

Compared to antibody-based immunoassays like ELISA, the benefits of aptamers in clinical application is higher because of many characteristics, such as low immunogenicity, thermal stability and greater modification. Furthermore, aptamers can be selected for numerous targets ranging from small molecules to even the whole cell (Kim and Gu, 2014). Table 1.3 illustrates the difference between aptamers and antibodies when used for developing biosensors.

Table 1.3: Comparison between using aptamer and antibodies in biosensor development

Parameter	Aptamers	Antibodies
Stability	Withstand repeated rounds of denaturation/renaturation. Temperature resistant: stable at room temperature. Long shelf life (several years). Can be lyophilized. Degradable by nucleases. Resistant to proteases.	Easily denatured. Temperature sensitive and require refrigeration to avoid denaturation. Limited shelf life. Must be refrigerated for storage and transport. Degradable by proteases. Resistant to nucleases.
Synthesis	In vitro SELEX takes only two to eight weeks. No batch-to-batch variation. Cheap to synthesize.	Produced in vivo. More than six months. Batch-to-batch variations. Laborious and expensive.
Target potential	From ions and small molecules to whole cells and live animals.	Targets must cause a strong immune response for antibodies to be produced.
Affinity	High and increased in multivalent aptamers.	Dependent on the number of epitopes on the antigen.
Size	Small molecules.	Relatively large by comparison.
Specificity	Single point mutations identifiable.	Different antibodies might bind the same antigen.
Modifiability	Aptamers can readily and easily be modified without affinity loss.	Modifications often lead to reduced activity.
Tissue uptake/kidney filtration	Fast	Slow

1.6 Research Aim and Objectives

Based on these advantages of aptamers – rapidity, low cost, small size, high specificity and selectivity – it is possible that they be utilized to develop a method for therapeutic drug

monitoring of some antitumour, such as Lenalidomide, 6-Mercaptopurine, Dabrafenib and Venetoclax, allowing for safe and optimal dosing to ensure compliance of a patient to the treatment and to identify patients responding to the drug. This is the aim of this thesis: to study the developing and synthesizing of an aptamer model to approach monitoring of Lenalidomide (LDM), 6-Mercaptopurine (6-MP), Dabrafenib (DFB) and Venetoclax (VENX) in human blood via the Sequential Evolution of Ligands by Exponential Enrichment (SELEX) process.

There many reasons for choose these medicines in the research, such as the high consumption and the request of some oncologists in Saudi Arabia to monitor these medicines. The global lenalidomide market size is USD 10.5 billion in the first, second and third quarters of 2025. The increasing rate of multiple myeloma is expected to increase the sales to reach USD 19.2 billion by 2034 with annual growth rate of 6.9 % (Market Publishers, 2025).

In 2024, the global 6 - mercaptopurine market size was valued at around USD 700 million, and it is expected to reach around USD 1.1 billion by 2032, with growing of 5.7 % during the forecast period. This growth is driven by increasing occurrence of chronic diseases such as leukemia (Data in sights market, 2024).

The global dabrafenib market is currently experiencing high growth, driven by the rising incidence of cancer, particularly melanoma and non-small cell lung cancer, where it has shown hopeful therapeutic results. Dabrafenib market size was estimates at USD 1.5 billion in 2024 and is likely to reach USD 3.1 billion by 2031, with growing of 13.2% during the forecast period. The increasing number of melanoma cases worldwide is an important factor for the dabrafenib market growth (Data in sights market, 2024).

The global venetoclax market size was estimated at USD 1.22 billion in 2024, and it is expected to reach from USD 1.33 billion in 2025 to USD 2.42 billion by 2033, with rising of 2.92% during the prediction period (Data in sights market, 2024).

All these financial data indicate the demand and importance of these medicines in the field of healthcare services, especially in the treatment of some kinds of cancer. In addition to the high demand, these medicines have some serious adverse reactions, therefore the therapeutic drug monitoring for them might be necessary, so they have been chosen to involved in this research project (i.e. developing DNA aptamer for each medicine).

The objectives of this thesis are to select a specific aptamer for these four antitumour medicines (Lenalidomide, 6-Mercaptopurine, Dabrafenib and Venetoclax) and determine the dissociation constants (Kd) for each selected aptamer.

1.7 Lenalidomide

1.7.1 Pharmacology of Lenalidomide

Lenalidomide is a novel compound based on the molecular structure of thalidomide that has been modified with a view to increasing the immunomodulatory effect of the parent compound while also providing a better safety profile (Bartlett et al., 2004).

Lenalidomide (Revlimid®) has been approved by the Food and Drug Administration (FDA) in 2005 (FDA, 2005) and has been approved by the European Medicines Agency (EMA) in 2007 (EMEA, 2007) for treating patients with multiple myeloma.

Currently, Lenalidomide has been approved for the treatment of patients with multiple myeloma whose cancer has relapsed after at least one prior treatment and who have already undergone or are unsuitable for conventional treatment (Tariman, 2007).

Lenalidomide has shown efficacy in several model systems. Pharmacology studies suggest that therapeutic activities of Lenalidomide are classified into the following classes: immunomodulatory, anti-inflammatory, anti-proliferative and anti-angiogenic.

These findings make it difficult to expect the effect of compound in more complex in vivo models and in human disease. In vivo, Lenalidomide has shown to delay tumour growth and extend survival in a mice xenograft model with human lymphoma cells. Lenalidomide has been chemically modified and developed based on the chemical structure and pharmacology of thalidomide. In vitro data shows that Lenalidomide is much more potent than thalidomide. In fact, it was 10-100 times more potent than thalidomide in several in vitro pharmacological studies of anti-proliferative and immunomodulatory activities.

Based on in vitro and in vivo studies, Lenalidomide has been shown to:

- enhance the secretion of anti-inflammatory cytokine Il-10 by monocytes and prevent secretion of pro-inflammatory cytokines TNF-α, IL-1β, IL-6 and IL-12;
- elevate natural killer (NK) cell activities and induce interferon-gamma (IFN-γ) production and T cell proliferation;
- decrease the proliferation of several haematopoietic tumour cell lines, especially the multiple myeloma;

- increase foetal haemoglobin (HbF) expression upon CD34+ erythroid stem cell differentiation; and
- hinder the mechanism steps of angiogenesis by blocking the formation of micro vessels and endothelial cell tubes as well as the migration and adhesion of endothelial cells, which will lead to inhibition in the growth of haematopoietic tumour cells, shrinking solid tumour.

Lenalidomide has the chemical formula ($C_{13}H_{13}N_3O_3$), the molecular weight of 259.26 g/mol and the chemical structure as shown in Figure 1.1 (Celgene, 2008).

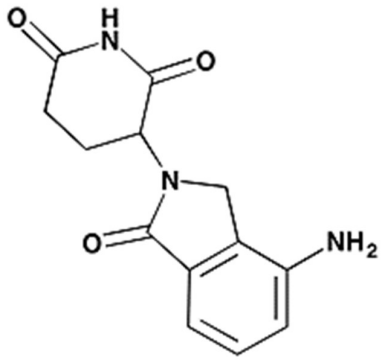

Figure 1.1: Chemical structure of Lenalidomide

While Lenalidomide is more soluble in organic solvents and low pH solutions, it is soluble in organic solvent/water mixtures and buffered aqueous solvents (Celgene, 2008).

Lenalidomide shares the same chemical backbone as thalidomide but differs by the removal of an oxygen atom from the phthaloyl ring and the addition of an amine group. Although it is chiral and has an asymmetric carbon, it has been modified as a racemic mixture since it undergoes racemization under physiological conditions. It is obtained as a hemihydrate form and is non-hygroscopic. It exhibits polymorphism; however, the commercial synthesis process yields only the desired polymorph (Richardson et al., 2002).

Lenalidomide is available in markets in hard capsule with four strengths: 5, 10, 15 and 25 mg per capsule (Celgene, 2008).

1.7.2 Pharmacokinetics of Lenalidomide

Lenalidomide is rapidly absorbed after oral administration in monkeys and rats. Bioavailability varies between 50-75%. The elimination half-life in monkeys and rats is approximately 13 and

two hours, respectively, after a single oral administration. In humans, terminal half-life is dependent on dose (Celgene, 2008).

Lenalidomide can be taken either before or after food, taking into consideration that co-administration with food delays absorption of the active substance.

A comparison of data from several studies with labelled Lenalidomide vs. non-labelled Lenalidomide shows that a vast majority of the administered dose is present as intact Lenalidomide in plasma.

Lenalidomide is not metabolized via cytochrome P450 in humans. Urinary excretion is the main route of elimination of Lenalidomide (90% of radioactive dose), with minor amounts excreted in faeces (7%). Urinary excretion of Lenalidomide is around 27% lower when Lenalidomide is administered with food compared to the fasted state (Celgene, 2008).

Because elderly patients are more likely to have impaired kidney function, care should be taken in dose prescription and it is recommended to monitor renal function.

The recommended dose of Lenalidomide for patients with relapsed or refractory multiple myeloma who have received at least one prior therapy is 25 mg/day in combination with Dexamethasone (40 mg/day). Lenalidomide 25 mg/day is administered orally on days 1 to 21 of each 28-day cycle, and 40 mg/day of dexamethasone on days 1 to 4, 9 to 12 and 17 to 20 of each 28-day cycle for the first four cycles, with reduction to 40 mg/day of Dexamethasone on days 1 to 4 of each cycle thereafter (Chen et al., 2003).

Although combination of Lenalidomide with Dexamethasone shows good results, that combination is associated with a higher incidence of grade 4 neutropenia; therefore, dose adjustment and monitoring may be recommended in such cases. In addition, that combination of Lenalidomide with dexamethasone is linked with raised risk of pulmonary embolism (PE) and deep vein thrombosis (DVT) in patients with multiple myeloma. Concomitant treatment with erythropoietic agents or presence of history of DVT may also elevate thrombotic risk in these patients. Consequently, erythropoietic agents should be used with caution in multiple myeloma patients taking Lenalidomide with Dexamethasone (João et al., 2016).

Dose adjustments during treatment, as summarized below in Table 1.4, are recommended to minimize the incidence of thrombocytopenia and grade 3 or 4 neutropenia related to Lenalidomide.

Table 1.4: Dose reduction steps to minimize incidence of thrombocytopenia related to Lenalidomide

Starting dose	25 mg
Dose level 1	15 mg
Dose level 2	10 mg
Dose level 3	5 mg

From previous observations on the side effects of Lenalidomide, treatment should be initiated and monitored under the supervision of an oncologist experienced in the management of multiple myeloma (MM).

Dose monitoring should be carried out on patient's sample. There are many methods for detection of Lenalidomide.

1.7.3 Literature Review of Detection of Lenalidomide in Human Blood

There are many analytical methods for detecting Lenalidomide in human blood. The first method is liquid chromatography-mass spectrometry using single ion monitoring for determining the Lenalidomide in human plasma (Tohnya et al*.,* 2004).

A high-pressure liquid chromatographic assay with MS detection has been developed for quantitative measurement in human plasma (Guglieri-López et al., 2016). Samples for a pretreatment procedure involved liquid-liquid extraction with acetonitrile/1-chlorobutane (4:1, v/v) solution containing the internal standard, umbelliferone (7-hydroxycouma rin). Separation of the compounds of interest was performed by using C18 Nova-Pak material (4 µm particle size; 300 mm x 3.9 mm internal diameter) using acetonitrile, de-ionized water, and glacial acetic acid in ratios of 20:80:0.1 (v/v/v) (pH 3.5). The flow rate was 1.00 ml/minutes at isocratic system. The run time was eight minutes.

One method for the quantitation of Lenalidomide in human plasma by LC-MS/MS using Box–Behnken experimental design was developed by Hasnain et al*.* (2013). The Carbamazepine used as an internal standard and the samples were prepared by solid-phase extraction. The triple quadruple mass spectrometer was used as a detector operated in the positive ion mode with turbo ion spray ionization. The separation run was by analytical HPLC-RP column, with a 5 µm particle size and a mobile phase flow rate of 1ml/ min. The mobile phase components are ammonium formate (AF) solution and acetonitrile in a ratio of 15:85. The injection volume was 10 µl and three minutes were set as the run time. The retention time of Lenalidomide and Carbamazepine (IS) were observed to be 1.04 and 1.2 min, respectively.

Plasma samples were spiked with Lenalidomide in the range of the 2–1000 ng/ mL and the lower limit of quantification (LLOQ) was analysed to determine the precision and accuracy of the method.

The fourth analytical method developed for the determination of Lenalidomide and flavopiridol as internal standard was by liquid chromatography-mass spectrometry (LCMS/MS) using a gradient elution and a single reaction monitoring (SRM) in a run time of approximately 10 minutes (Liu et al*.,* 2008)

Another method was developed by using ultra-performance liquid chromatographic with tandem mass spectrometry for determination of Lenalidomide in rabbit and human plasma (Iqbal et al*.,* 2013).

The separation was performed on a UPLC system with RP- C18 column (50 × 2.1 mm, i.d., 1.7 µm). The mobile phase was a mixture of acetonitrile: water: formic acid (65:35:0.1%, v/v/v) at a flow rate of 0.2 ml/min. A triple-quadrupole tandem mass spectrometer connected with electrospray ionization (ESI) interface was utilized for analytical detection. The ESI source was set in positive ionization mode. Standard stock solution of Lenalidomide and Carbamazepine as an internal standard (IS) were prepared by dissolving in dimethylsulphoxide (DMSO) and methanol, respectively, to give a final concentration of 1 mg/ml.

Plasma samples stored at around −80 °C were thawed and left for one hour, vortexed for 30 seconds at room temperature before extraction to ensure homogeneity. Accurately, 20 µl of working standard and 25 µl (5 µg/mL) of internal standard (except blank sample) were added to 200 µl of plasma sample. The samples were vortexed and mixed for about 30 seconds and around 750 µl of methanol was added. The samples were vortexed and mixed again gently for two minutes and then cold centrifuged for 10 minutes at 10000 rpm. After centrifugation, 400 µl of supernatant was transferred into HPLC vial, and 5 µl of the sample was injected to be analysed by UPLC–MS/MS using mobile phase composed of acetonitrile:water:formic acid (65:35:0.1%, v/v/v) at a flow rate of 0.2 mL/min and isocratic mode. The run time was 2.5 minutes.

Although data in the previous methods show that methods were rapid, specific, stable, accurate and valid for the determination of Lenalidomide in plasma, the technique used (LC-MS/MS) may not be available in some laboratories or hospitals as it is expensive. Therefore, other accessible techniques are required.

A high-performance liquid chromatography (HPLC) method has been utilized for the determination of Lenalidomide in plasma by non-extractive HPLC procedures with fluorescence detection after pre-column derivatization with fluorescamine (Khalil et al., 2013).

The standard stock solution was prepared with initial concentration of 1 mg/mL by dissolving in methanol. The stock solution was further diluted with deionized water to obtain a working standard solution containing 1.0 µg/mL of Lenalidomide. Five mg of fluorescamine was weighed and dissolved in acetonitrile to produce a stock solution of 0.05% (w/v).

The HPLC system equipped with UV-visible and fluorescence detectors. Hypersil BDS C18 column (250 × 4.6 mm, 5 µm particle size) was used for separation of the derivatized Lenalidomide with mobile phase mixture: phosphate buffer (pH 4): methanol: tetrahydrofuran (70:10:20, v/v) at a constant flow rate of 1.0 mL/min. The derivatized analytes were monitored at an emission wavelength of 495 nm after excitation at a wavelength of 382 nm. The injection volume was 50 µl for standard and test. The fluorescence detector was set at 382 nm as an excitation wavelength, while the emission wavelength was set at 495 nm.

Acetonitrile added to the plasma samples to participate protein precipitation, and then samples were treated with copper acetate to form stable complexes with the biogenic amines and hinder their interference with the derivatization reaction of Lenalidomide. Treated plasma samples containing Lenalidomide (LMD) was derivatized at ambient temperature with fluorescamine (FLC) in aqueous media.

This derivatization was applied, because Lenalidomide has a weak absorbing chromophore in its chemical structure. Moreover, it does not have a native fluorescence, so a pre-column derivatization procedure was carried out.

Fluorescamine is a fluorogenic reagent which reacts instantly with a wide variety of nucleophiles, such as primary amines, even at very low concentrations, making fluorescent pyrrolinone moieties.

Lenalidomide has a primary aromatic amino group which reacts easily with Fluorescamine releasing a highly fluorescent adduct. However, plasma contains plenty of compounds that are rich with nitrogen, such as amino acids. Consequently, interference from such endogenous amino acids is highly predicted. Therefore, the researchers in that study added a copper acetate to form a selective complex between copper ions and to eliminate the interference.

The accuracy and precision of that method was measured by intra-day and inter-day replicate analysis of samples spiked with different concentrations of Lenalidomide covering the working linear range.

Although this method has suggested fluorescent detection as an alternative to mass detectors, the time of procedure (pre-column derivatization with fluorescamine) had increased because Lenalidomide is not a fluorescent. Furthermore, the derivatization procedure will increase the likelihood of variable results.

Furthermore, some methods were developed by using high performance liquid chromatography alone for determination of the Lenalidomide in plasma (Guglieri-López et al., 2016).

The concentration of standard stock solution was 0.5 mg/ ml using acetonitrile as a solvent. The stock solution was further diluted with water to obtain a working standard solution containing 2.0 µg/ml.

Accurately measured aliquots of standard working solution (2.0 µg/m) were transferred into 10 separate test tubes, each containing 525 µl plasma. The volume in all tubes were completed to 1.0 ml with deionized water. This obtained a series of Lenalidomide-spiked plasma solutions covering the working range of 100 to 950 ng/ml. A blank solution containing 525 µl plasma and water was also prepared. The test tubes were ultrasonicated for 20 min at room temperature and then centrifuged for 10 min at 3000 rpm. A solid-phase extraction (SPE) was performed before injecting the solutions in the HPLC using cyano-bonding cartridges. The cartridges were conditioned with 2 ml of methanol, then the solid phase equilibrated with 2 ml of 0.03 M phosphate buffer (pH 7.4). One ml of serum or plasma spiked with Lenalidomide was loaded after that on the cartridges, then washed with 2 ml of 0.03 M phosphate buffer (pH 7.4). The elution was then carried out with 2 ml of mobile phase. The eluted samples were evaporated to dryness at 60 ± 1 °C under a vacuum of 600 mm Hg for one hour. The solid yielded was further diluted in 110 µl of mobile phase and centrifuged at 10,200 rpm for two minutes. The supernatant obtained was transferred into an HPLC vial, and a volume of 80 µL of that solution was injected into the HPLC system.

Separation was performed by using RP C18 (250 mm length × 4.6 mm i.d., 5 µm) using a mobile phase composed of phosphate buffer/acetonitrile (85:15, v/v, pH 3.2) at a constant flow rate of 0.5 ml/min. The injection volume was 80 µl. The separation was monitored at a wavelength of 311 nm and the retention time of Lenalidomide observed at 10.8 minutes.

Although this method does not use a mass technique and does not need any derivatization, it has many disadvantages, such as the extended length of the procedure for evaporation and dryness and the lengthy retention time (10 minutes).

The reviewed literature on detection methods for Lenalidomide in plasma highlights several shortcomings and limitations. Therefore, there is a need for a method that is cost-effective, reliable, and capable of delivering rapid and linear results. Such requirements can be addressed through the development of a biosensor based on the Systematic Evolution of Ligands by Exponential Enrichment (SELEX) technique.

1.8 6-Mercaptopurine

1.8.1 Pharmacology of 6-Mercaptopurine

6-Mercaptopurine was synthesized and discovered by Nobel Prize winning scientists George H. Hitchings and Gertrude B. Elion and at Burroughs Wellcome Research laboratories in Tuckahoe, USA (Mukherjee S., 2010).

6-Mercaptopurine (6-MP) is an antineoplastic drug belonging to antimetabolite drugs and widely used in childhood acute lymphoblastic leukaemia (ALL) medication in single or combination dose (Hunger et al., 2015). It is typically used in combination with other anticancer drugs and interferes with the synthesis of adenine and guanine ribonucleo-sides, important precursors of DNA and RNA (McCormack and Johns, 1982). 6-Mercaptopurine (6-MP), a sulphur analogue of adenine and sold under (PURINETHOL), is known chemically as 1,7-dihydro-6H-purine-6-thione monohydrate. Figure 1.2 shows its chemical structure, which is considered an analogue of the purine bases adenine and hypoxanthine (Elion, 1967).

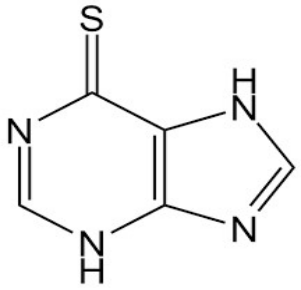

Figure 1.2: Chemical structure of 6-Mercaptopurine

1.8.2 Pharmacokinetics of 6-Mercaptopurine

The half-life of 6-Mercaptopurine in plasma is short, ranging from 1-3 hours. It is excreted through renal excretion minimally at conventional doses. The oral absorption of 6-MP is

incomplete and highly variable (5-35%) largely because of first pass metabolism in the liver, which is suggested as one of the possible reasons for relapse in children with leukaemia receiving maintenance chemotherapy (Whalen et al., 1986).

It is metabolized by hepatic system 5 by hypoxanthine-guanine phosphoribosyl transferase (HGPRT), resulting in thiopurine nucleotides as active metabolites and 6-methyl mercaptopurine as inactive metabolite (Elion, 1967).

High levels of active metabolite have been linked with good therapeutic efficacy and haematology toxicity, whereas high levels of inactive metabolite are associated with hepatotoxicity, enhancing the importance of therapeutic drug monitoring, particularly in the first stages of treatment (Philips et al., 1954).

1.8.3 Literature Review of Detection of 6-Mercaptopurine in Human Blood

Various analytical methods have been published for the determination of 6-MP and its metabolites in human albumin, such as high performance liquid chromatography (Van Os et al., 1996; Narang et al., 1982; Fell and Plag, 1979), mass spectrometry (Hofmann et al., 2012; Tibor et al., 2010; El-Yazigi and Wahab, 1992; Albertioni et al., 1995; Maddocks, 1979; Teck and Leslie, 1979; Sahnoun et al., 1990; Torsten et al., 1996; Tsutsumi et al., 1982), gas chromatography (Bailey et al., 1975; Wypior et al., 1982), UV spectrophotometry (Gorog and Gorog, 1988), Raman assays (Yang et al., 2005), capillary electrophoresis (Rabel et al., 1995; Lu et al., 2015), chemiluminescence and electrochemical methods (Sato et al., 2005; Sun et al., 2013; Li et al., 2005; Zhou et al., 2025).

HPLC assay utilizing the monobromobimane derivative of 6-MP was developed by Burton, Aherne and Marks (1984). This method requires overnight incubation, which is time consuming.

HPLC and MS are always employed together to detect 6-MP. Protein precipitation, SPE (solid phase extraction) and LLE (liquid-liquid extraction) are the sample preparation techniques frequently used to process plasma (Prashant et al., 2011). Although the LC-MS technique is sensitive and selective, it requires expensive equipment and toxic reagents and often involves complicated extraction or derivatization procedures.

Rosenfeld, Taguchi, Hillcoat and Kawal (1977) developed a gas liquid chromatography mass spectrometric assay for 6-MP which appears specific, but the cost of instrumentation and using toxic solvents, however, will limit its availability in clinical practice.

Spectroscopic methodologies can be suitable for routine analysis. However, UV spectrophotometry procedures are subject to low sensitivity. The main drawback for spectroscopic methodologies is the effect of potential interference of biological background as well as from other unexpected sample components. Capillary electrophoresis (CE) and Raman methods require advanced and expensive equipment, minimizing their suitability to be used to monitor drug levels.

Recently, the electrochemical assays are most widely reported, and several modified electrodes have been used in 6-MP detection. However, the complexity of the electrode modification process and poor repeatability have limited their application in biological real samples.

Hence, developing fast, simple, costless, sensitive, convenient and reliable method to detect 6-MP in human blood is necessary to assess efficacy and safety.

1.9 Dabrafenib

1.9.1 Pharmacology of Dabrafenib

Dabrafenib is a protein kinase inhibitor which blocks or slows the cancer growth blocker by targeting certain proteins made by mutation called a BRAF V600 gene that involves stimulating cell division and therefore helps the growth and spread of the cancer cells (Rheault et al., 2013). It has approved by both the European Medicines Agency (EMA) and US Food and Drug Administration (FDA) as monotherapy or in combination with other mitogen-activated protein kinase (MAPK) inhibitors for the treatment of adult patients with melanoma, advanced non-small cell lung and anaplastic thyroid cancers (Menzies, Long and Murali, 2012).

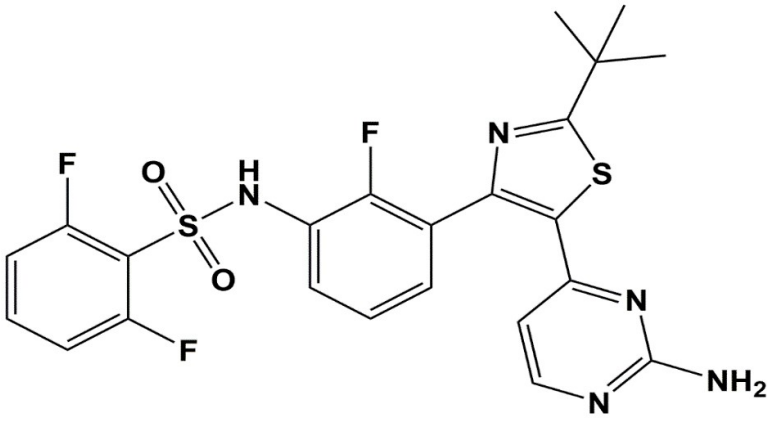

Figure 1.3: Chemical structure of Dabrafenib

The most common side effects for Dabrafenib include hyperkeratosis, pyrexia, headache, arthralgia, alopecia, fatigue, skin papilloma and hand-foot syndrome (Falchook et al., 2014).

1.9.2 Pharmacokinetics of Dabrafenib

Dabrafenib is an orally administered medicine almost entirely absorbed after administration with mean terminal half-life of eight hours after oral administration (Puszkiel et al., 2018).

The mean absolute bioavailability of oral Dabrafenib is 95% (decreased with food) and the median time for achieving peak plasma concentration (Tmax) is two hours. It shows around 99.7% binding to human plasma proteins (Ouellet et al., 2014).

Dabrafenib is metabolized by CYP3A4 and CYP2C8 enzymes; therefore, drug interactions are probable with strong inhibitors or inducers of these enzymes (Suttle et al., 2015).

Around 71% of Dabrafenib, excreted in faeces, which is the major route of elimination, while about 23% through urinary excretion (Bershas et al., 2013).

Oral administration of some anti-cancers such as Dabrafenib is associated with a better quality of life but also exhibits a complex pharmacokinetic profile, because it metabolized by CYP3A4 and CYP2C8 (Mikus and Foerster, 2017).

This pharmacokinetic variability leads to significant variable drug exposure between patients, resulting in too low or too high plasma concentrations, thereby enhancing the occurrence of adverse drug effects or treatment failures. This variation increases in some cases, such as in hepatic impairment, concomitant administration of CYP inhibitors or inducers, which is common in patients who use more than two medicines daily such as cancer patients (Van Erp et al., 2009).

Considering the impaired patient's quality of life, severe prognosis of the disease, the pharmacokinetic complexity, the high cost of the medicine, the chronic use, therapeutic drug monitoring (TDM) of Dabrafenib could be a useful approach to assist clinicians with individual dose adjustment and monitoring adherence to minimize the risks of dose-related adverse effects or under-therapeutic exposure (Verheijen et al., 2017).

1.9.3 Literature Review of Detection of Dabrafenib in Human Blood

Many analytical methods have developed to measure Dabrafenib in human serum or plasma. Most depend on liquid chromatography (LC) with mass or double mass detection techniques (Aghai et al., 2021; Balakirouchenane et al., 2021; Cardoso et al., 2018; Herbrink et al., 2018; Huynh et al., 2017; Krens et al., 2020; Merienne et al., 2018; Nijenhuis et al., 2016; Rousset et al., 2017; Vikingsson et al., 2017) in human plasma.

All published methods use liquid-liquid extraction, solid-phase extraction or a mixture of both, but this is more time-consuming because they include a generic plasma protein precipitation with organic solvents followed by a step of evaporation/reconstitution of supernatants. Moreover, the need for deuterated internal standards and LC-MS/MS grade solvents is just one difficulty of the LC-MS/MS technique. In addition, another drawback of the LC-MS/MS technique is its use of harmful organic solvents in the sample preparation.

Capillary electrophoresis (CE) coupled to UV/Vis detection has already been developed to the quantification of Dabrafenib in biological samples, but the sample treatment has many steps including sonicating the sample for 15 minutes then centrifuging for eight minutes for the suspension, then sonication for eight minutes after centrifugation. Finally, the extract is transferred to a glass tube and dried under nitrogen gas stream at room temperature (Rodríguez et al., 2016).

Although CE or LC-MS/MS meet the requirements of sensitivity and selectivity for the quantification of Dabrafenib, it is an expensive instrument, rendering these approaches unaffordable for most routine laboratories. In addition, published methods have not confirmed the type of anticoagulants used for blood collection and have not demonstrated the influence on Dabrafenib quantification, except the method developed by Cardoso et al. (2018). It shows the concentrations of medicine at the three QCs levels measured either in serum, in heparinized or EDTA plasma, which did not differ significantly from those measured in citrate plasma used as a reference value.

1.10 Venetoclax

1.10.1 Pharmacology of Venetoclax

Venetoclax is a selective inhibitor of B cell lymphoma-2 (BCL-2), which is an anti-apoptotic protein that is associated with many cancer progressions (Cao et al., 2023). Overexpression of that anti-apoptotic molecule (i.e., BCL-2) has been demonstrated in Chronic Lymphocytic Leukaemia (CLL) and Acute Myeloid Leukaemia (AML) cells where it mediates tumour cell growth and has been associated with resistance to some chemotherapeutics (McBride et al., 2019). Venetoclax supports restore the process of apoptosis by binding directly to the BCL-2 protein molecules, dislocating pro-apoptotic proteins like BCL-2 Interacting Mediator (BIM), enhancing mitochondrial outer membrane permeabilization and the initiation of caspases (Lasica and Anderson, 2021). It has a potent cytotoxic activity in tumour cells that overexpress B cell lymphoma-2 (BCL-2) (Deeks, 2016).

The European Medicines Agency (EMA) and Food and Drug Administration (FDA) approved it as monotherapy or in combination with other anticancer to treat adults with Acute Myeloid Leukaemia (AML), Chronic Lymphocytic Leukaemia (CLL) and Small Lymphocytic Lymphoma (SLL) (Zhong et al., 2021). Its chemical structure contains a combination of benzamide moiety with a morpholino and chloro substituent (as shown in Figure 1.4), which can significantly influence its biological activity (Scott et al. 2016).

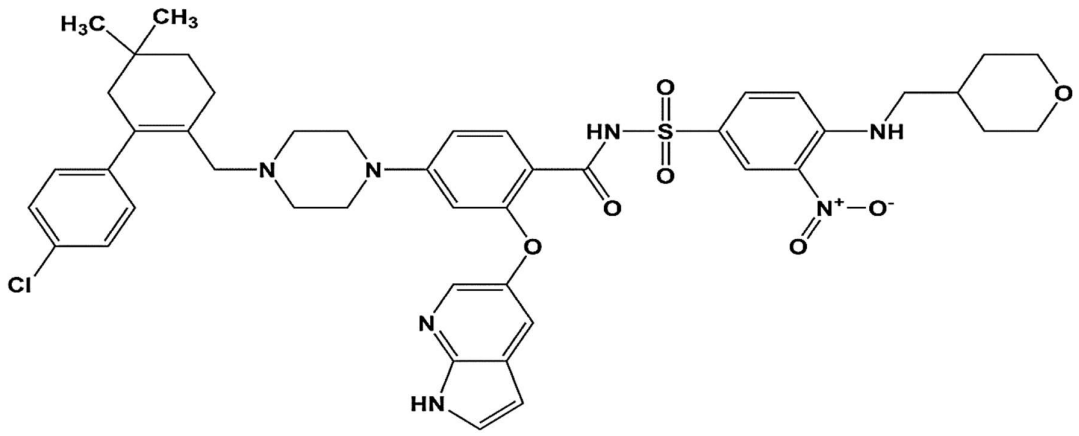

Figure 1.4: Chemical structure of Venetoclax

The most commonly occurring side effects in patients receiving Venetoclax were neutropenia, pneumonia, upper respiratory tract infections (such as nose and throat infections), thrombocytopenia, hyperkalaemia, fatigue, diarrhoea and anaemia. Additionally, Venetoclax may cause fertility problems in males (Waggoner et al., 2022).

The chance of Tumour Lysis Syndrome (TLS) is high with patients receiving Venetoclax, especially in case of Acute Myeloid Leukaemia (AML). Tumour Lysis Syndrome (TLS) occurs when contents of tumour cells have released into the bloodstream, leading to the characteristic findings of hyperkalaemia, hypocalcaemia, hyperphosphatemia, and hyperuricemia (Fischer et al., 2020).

1.10.2 Pharmacokinetics of Venetoclax

Venetoclax, an orally administered medicine, is almost entirely absorbed after administration with a mean terminal half-life of 14-18 hours after oral administration (Salem et al., 2016).

The mean bioavailability of oral Venetoclax is reported to be 5.4% in fasting status; therefore, it is recommended that Venetoclax be taken with food with the median time to reach peak plasma concentration (Tmax) at five to eight hours after the dose. It shows around 99.9% binding to human plasma proteins (Cheung et al., 2017).

Principally, Venetoclax is metabolized by CYP3A4/5 enzymes; therefore, drug interactions are probable with strong inducers and moderate or strong inhibitors of these enzymes (Freise et al., 2017).

Around 99.9% of Venetoclax if excreted in faeces, which is the major route of elimination, while about 0.1% through urinary excretion (Juárez-Salcedo et al., 2019).

Oral administration of some anticancer, such as Venetoclax, is associated with better quality of life but also exhibits a complex pharmacokinetic profile, because it metabolizes by CYP3A4/5 enzymes (Liu et al., 2016). This pharmacokinetic variability leads to significant variable drug exposure between patients, resulting in too low or too high plasma concentrations, which enhances the occurrence of adverse drug effects or treatment failures. This variation increases in some cases, such as in hepatic impairment, concomitant administration of strong inducers and moderate or strong CYP3A4/5 enzymes inhibitors or inducers, which is common in patients who use more than two medicines daily such as cancer patients (Salem et al., 2019).

Concomitant administration of Venetoclax with strong CYP3A4/5 enzymes inhibitors or inducers contraindicated in patients with Chronic Lymphocytic Leukaemia (CLL) and Small Lymphocytic Lymphoma (SLL) because of the potential for increased risk of Tumour Lysis Syndrome (Mukherjee et al., 2023).

Considering an impaired patient's quality of life, severe prognosis of the diseases, the pharmacokinetic complexity, the high cost of the medicine, and chronic use, therapeutic drug monitoring (TDM) of Venetoclax could be a useful approach to assist clinicians with individual dose adjustment and monitoring the adherence to minimize the risks of dose-related adverse effects or under-therapeutic exposure.

Venetoclax has a significant variability between patients with nonlinearity in relative bioavailability (Kaufman et al., 2021; Freise et al., 2017; Yang et al., 2022) and shows a severe drug-drug interaction with azole antifungals such as posaconazole (Bhatnagar et al., 2021). Therefore, monitoring the plasma exposure of Venetoclax in patient is recommended.

1.10.3 Literature Review of Detection of Venetoclax in Human Blood

Few analytical methods have developed to determine and measure Venetoclax in human serum or plasma. Most depend on liquid chromatography (LC) with mass-mass detection technique (Reddy et al., 2022; Yang et al., 2022; Yang et al., 2023).

Although that LC-MS/MS meet the requirements of sensitivity and selectivity for the quantification of Venetoclax, it is an expensive instrument, rendering these approaches unaffordable for most routine laboratories.

Another challenge of LC-MS is the complicated assay procedure, such as digestions steps that result in low throughput and added variability. Moreover, internal standard selection and long time in sample preparation are drawbacks for LC-MS techniques.

In addition, another drawback of LC-MS/MS technique is its use of harmful organic solvents in the sample preparation.

Finally, published methods have not shown the type of anticoagulants used for blood collection, nor have they shown the influence on Venetoclax quantification.

Chapter Two: Materials, Reagents, Instruments and Methodology

Chapter Two: Materials, Reagents, Instruments and Methodology

2.1 Materials and Reagents

Lenalidomide reference material, 6-Mercaptopurine reference material, Dabrafenib reference material, dimethyl sulfoxide (DMSO), sodium chloride, sodium acetate, sodium bicarbonate, sodium azide, hydrochloric acid (37%), sodium carbonate anhydrous, dipotassium hydrogen orthophosphate, potassium dihydrogen orthophosphate, urea, boric acid, Ethylenediaminetetraacetic acid (EDTA), tetramethyl ethylenediamine (TEMED), acetic acid, free Nuclease water, agarose and Ethanol absolute 99% were all purchased from Sigma-Aldrich (Schnelldorf, Germany).

Kanamycin reference material and Venetoclax reference material were obtained from LGC (Teddington, UK).

NHS (N-hydroxysuccinimide)-activated Sepharose™ 4 Fast Flow was obtained from GE Healthcare (Wisconsin, USA).

A DNA library with 72 bases (5'-TCC CTA CGG CGC TAA CNN NNN NNN NNN NNN NNN NNN NNN NNN NNN NNN NNN NNN NNG CCA CCG TGC TAC AAC-3'), forward primer with 16 bases (5'- TCC CTA CGG CGC TAA C-3'), reversed primer with 16 bases (5'-GTT GTA GCA CGG TGG C-3'), M13 forward primer with 17 bases (5'-GTA AAA CGA CGG CCA GT-3') and M13 reversed primer with 17 bases (5'-CAG GAA ACA GCT ATG AC-3') were all ordered, synthesized and purchased from Metabion (Planegg, Germany).

A thermal buffer, PCR master mix, DNA gel loading dye 6X, formamide solution, acrylamide 40% solution, ammonium persulfate powder (APS), super optimal medium with optimal broth with catabolite repression (SOC) medium, X-Gal '5-Bromo-4-chloro-3-indolyl β-D-galactopyranoside' solution and TBE buffer 5X (pH of 8.3) have been purchased from Thermo Fisher Scientific GmbH (Dreieich, Germany).

A cloning kit (TOPO TA Cloning™ Kit with pCR™2.1 Vector and One-Shot MAX Efficiency DH5α-T1 competent cells), Luria-Bertani (LB) broth agar medium, and DNA ladder (100bp - 12,000bp) have been purchased from Invitrogen by Fisher Scientific (Dresdner, Germany).

An Amicon Ultra Centrifugal Filter (3 kDa) and Spin-X filters were purchased from Merck Millipore (Massachusetts, USA).

A TE buffer (1X, pH 8.0), TBE buffer (10X, pH 8.5), binding buffer (pH 7.4), dNTP (10 mM), magnesium chloride solution (25 mM), tween 20 solution, and DNA Polymerase (5 ug/µl) were purchased from Promega (Wisconsin, USA).

2.2 Instrumentation

All weighing processes in this research were carried out by calibrated and verified semi-micro lab balance from Sartorius (Goettingen, Germany).

A laboratory rotator was purchased from Bellco Glass (New Jersey, USA), while the shaker was obtained from Scilogex (Connecticut, USA).

Dry block heating steps (for PCR tubes or small vials) involved in this research were performed by IKA-Werke GmbH (Staufen, Germany), while a dry oven was purchased from Binder (Tuttlingen, Germany). Also, a water bath was obtained from Benchmark Scientific (New Jersey, USA).

The microcentrifuge that was utilized in all cycles of SELEX and other process was obtained from Eppendorf (Hamburg, Germany).

The thermal cycler for PCR amplifications and the polyacrylamide gel electrophoresis system have been obtained from Bio-Rad (California, USA).

The steps of freeze drying were performed by lab vacuum freeze dryer from LabsNova (Zhengzhou, China).

A UV transilluminator (312 nm wavelength) from Thistle Scientific Ltd (Warwickshire, UK) was utilized for visualization of polyacrylamide gels.

A Nano UV-Vis Spectrophotometer (to determine the concentration of DNA) and Nano Fluorospectrometer (for the analysis of fluorescein-labelled aptamers) were obtained from Thermo Scientific (Delaware, USA).

Shaking incubator (5 °C – 80 °C) was obtained from Corning Life Sciences (Massachusetts, USA). The dissociation constant (Kd) for each aptamer was measured by a Monolith System (depending on the microscale thermophoresis principle), purchased from NanoTemper Technologies (Munich, Germany).

2.3 Methodology

2.3.1 Preparation of Drug-Coupled Sepharose Beads

NHS-activated Sepharose (i.e. crosslinked, beaded-form of agarose) beads are applied to selectively isolate proteins, nucleic acids, or other biomolecules from complex mixtures. They are serving as a pre-activated matrix (i.e. already functionalized and ready for use without needing an additional activation step, simplifying the immobilization process) for covalent immobilization, where the carbonyl carbon of the NHS ester links with primary amines on a ligand to form a stable amide bond. This process covalently attaches the ligand to the bead, making it suitable for affinity separation and purification of specific substances from complex mixtures, which can enhance the stability of the immobilized target molecule and their tolerance to sever pH levels and high temperatures (Hermanson, 2013).

The target analyte was conjugated with NHS activated sepharose beads according to the manufacturer's protocol. In brief, 2 ml of NHS activated sepharose beads were washed with 5 ml of 1 mM HCl by centrifuging at 250 rpm for three minutes. This washing process had repeated five more times. Concurrently, around 30 mg of the drug reference material (i.e., Lenalidomide, 6-Mercaptopurine, Dabrafenib and Venetoclax) was dissolved in 100 µl of DMSO. This stock solution is called 'Drug solution'. Only 2 ml of coupling buffer (0.2 M $NaHCO_3$ + 0.5 M NaCl) were mixed with the washed beads, then the drug solution was added to the beads. The obtained new stock solution was a mixture of washed beads and target analyte in a coupling buffer. This new stock mixture was left for 24-48 hours on shaker at room temperature. After 24 hours of shaking the mixture, the clear 'upper layer' was discarded and 3 ml of 0.1 M Tris HCl (pH 8.5) was added to the stock mixture and left for 1-2 hours on the shaker. After 1 hour on shaker, the stock mixture was washed with alkaline buffer, pH 8.5 (3 ml of 0.1 M Tris HCl + 0.5 M NaCl, centrifuged at 250 rpm for three minutes) and another with acidic buffer, pH 4.5 (3 ml 0.1 M Sod. Acetate + 0.5 M NaCl, centrifuged at 250 rpm for three minutes). This washing step was repeated six times. After the last wash, the stock mixture was washed only once with 3 ml of TE buffer by centrifuging at 250 rpm for three minutes, then an equal volume of beads was added from the TE buffer. The obtained mixture was stored at 5 °C to be the stock for the SELEX cycles.

A total of 100 µl of stock solution that stored in a refrigerator was transferred to the Spin-x filter tube and 300 µl of binding buffer was added to the Spin-x filter as well and washed by centrifuging at 0.7 rpm for three minutes. This step was repeated three times and the obtained solution was called 'M Solution', referring to solution that contains medicine. Meanwhile,

around 400 µl of binding buffer was mixed with around 15-20 µl of DNA library and the mixture was heated at 95 °C in the oven for five minutes, then cooled directly in an ice bath for 5-10 minutes, then maintained at room temperature for 10 minutes. The obtained mixture in this step was called 'L Solution', which refers to solution that contains the library of DNA.

All the amount of L solution was transferred to M solution, mixed gently by micropipette and left on the rotator 'right & left movement' for 2 hours.

After 2 hours on the rotator, the mixture of 'L and M' solution in the Spin-x filter was centrifuged at 0.6 - 0.8 rpm for five minutes, then the clear solution was collected and stored at –20 °C (positive control). After collecting the clear layer in the Spin-x filter, the beads were washed five times with 400 µl of binding buffer by centrifuging at 0.6 rpm for two minutes. in parallel, the 7M of elution buffer was prepared by dissolving 21 gm of urea powder in 50 ml of binding buffer. Around 400 µl of heated elution buffer 'heated at 90 °C in water bath' was added to the beads in the Spin-x filter and then incubated in dry heater for 10 minutes at 80-90 °C, then centrifuged at 1 rpm for two minutes. This step was repeated 7-9 times and the flow-through was collected each time in a dark tube with the fluorescence measured by nano fluorospectrometric. After collecting and measuring the fluorescence of flow-through of the beads, the obtained solutions was stored in dark tubes in 5 °C.

The obtained solution in each time was transferred to Amicon Ultra Centrifugal Filter 3 kDa (starting from the last wash), centrifuged at 13 rpm for 10 minutes, discarding the flow-through each time. In the final wash, the solution was centrifuged until below 1k in the filter tube (remaining of ~ 50 – 70 µl of the solution), then the filter was washed five times, each time with 500 µl of free nuclease water by centrifuging at 13 rpm for five minutes at 18-20 °C. The filtrate was discarded each time, except in the last wash, the filter was centrifuged for 15 minutes (until the volume in filter had reached approximately 50 µl). Then the filter was turned upside down in a new dark tube and centrifuged at 3 rpm for two minutes. The obtained solution called 'DNA Cycle #1', which means that it contains the desired (i.e., eluted) DNA sequence that conjugated with the target analyte in the first cycle of SELEX, will be amplified by PCR.

Before amplifying the eluted solution, the concentration of DNA had been measured by Nano UV-Vis Spectrophotometer.

2.3.2 PCR Amplification and Separation of the ssDNA from the Gel

To prepare the step of amplifying the DNA by PCR, 625 µl of master mix ready solution was mixed with 50 µl of forward primer, 50 µl of reversed primer and 430 µl PCR water. This

mixture was prepared in a dark tube and ice bath, stored in –20 °C and called 'PCR Master Mixture'. After that, three main tubes were prepared and labelled as following: positive tube, negative tube and target DNA tube.

The positive tube contains 25 µl of PCR Master Mixture + 5 µl of 'positive control solution' + 20 µl of PCR water, so the total is 50 µl, while the negative tube contains only 25 µl of PCR Master Mixture + 25 µl of PCR water, so the total is 50 µl.

The target DNA tube contains 1155 µl + the volume of DNA Cycle # 1 + up to 1255 µl with PCR water, so the total volume is 1255 µl, which was divided into 24 PCR tubes, each one containing around 50 µl. All these PCR tubes (i.e., 1 positive, 1 negative and 24 target DNA) were prepared and kept on ice in a dark place.

The PCR protocol that was applied on samples is summarized in Table 2.1.

Table 2.1: PCR protocol for amplification step in SELEX cycle

Temperature	94 °C	94 °C	47 °C	72 °C	72 °C
Time	5 minutes	1 minute	1 minute	1 minute	10 minutes
Cycle(s)	1 X	26 X			1 X

After finishing the PCR run, all tubes except positive and negative tubes had transferred to –80 °C directly for 10 minutes, then all samples were lyophilized by vacuum freeze dryer at –70 °C. After drying with lyophilization, the dried powder was resuspended by adding a mixture of water and formamide (50:50) to each tube, then heated at 90 °C for five minutes in a water bath.

The step of separation of flu-relevant DNA from poly-A strand by Polyacrylamide gel electrophoresis (PAGE) was subsequently applied by preparing 10% gel (mixing 8 gm of urea + 6 ml of acrylamide + 4 ml of TBE buffer + 3.5 ml of PCR water and heating the mixture at 45 °C for 15 minutes). After that, 8.5 µl of Tetramethylethylenediamine (TEMED) solution and 110 µl of 10% ammonium persulfate (APS) were added to the mixture at room temperature. Then that mixture was poured directly in the cassette of electrophoresis cells containing TBE 1X buffer, and the samples were prepared as described in Table 2.2

Table 2.2: Components of mixture that loaded on PAGE

Cell	DNA Ladder + DNA dye	Positive control	Negative control	Sample	Sample
Amount	10 µl ladder + 2 µl Dye	45 – 50 µl	45 – 50 µl	45 – 50 µl	45 – 50 µl

After loading ladder, positive control, negative control and samples in the acrylamide gel, the electric current operated at 160 Volt for 45 minutes. The PAGE gel was then exposed to a UV transilluminator to take the image of PAGE gel under UV transilluminator.

The elution of fluorescent ssDNA step was carried out by cutting and slicing the bands of the fluorescent ssDNA directly, transferring them to a syringe and squeezing them out with 3 ml of TE buffer. The lyophilizing step was then performed by the 'freeze-thaw' protocol as follows: 10 minutes in –80 °C freezer then five minutes in 50 °C dry heat, then five minutes in 90 °C dry heat, then the mixture of squeezed gel and 3 ml TE buffer left on a rotator overnight in the incubator at 37 °C.

The mixture, after rotating overnight in an incubator at 37 °C, was transferred into spin filter to separate the eluted DNA from the gel matrix by centrifuging it at 3 rpm for one minute. The filtrate was collected in a dark tube and then transferred to an Amicon filter tube to concentrate and wash the eluted DNA by adding 450 µl of nuclease free water and centrifuging at 13 rpm for 10 minutes. This concentrating and washing step was repeated at least five times and in the last one, the filter was turned upside down in a new dark tube and centrifuged at 3 rpm for two minutes, with the obtained solution stored at –20 °C. This solution contains the DNA that will be used in next cycle instead of the DNA from the library. By the end of this step, a whole cycle of SELEX has been completed.

2.3.3 Cloning and Sequencing of the Selected DNA Aptamers

Selection (SELEX) cycles were stopped at the tenth round (the number of total cycles and counter selection was determined based on the protocol followed in the laboratory with previous researchers and students with my supervisors) and the ssDNA that resulted from the last round after collecting and desalting was amplified by the PCR for ligation with the unlabelled primers (see Table 2.3).

Table 2.3: PCR protocol for ligation in cloning step

Temperature	94 °C	94 °C	47 °C	72 °C	72 °C
Time	5 minutes	1 minute	1 minute	1 minute	10 minutes
Cycle(s)	1 X	26 X			1 X

After finishing the PCR run, 2 µl of the fresh ligated product was mixed with the following: 1 µl of salt solution in the cloning kit (stored at –20 °C), 2 µl PCR water and 1 µl vector in the cloning kit (stored at –20 °C). This mixture was kept at room temperature for 40 minutes. Promptly, E. coli competent cells (stored at –80 °C) were removed from the freezer and left in room temperature for a few seconds to let the cells thaw. Immediately thereafter, 2 µl of the mixture in the previous step was added.

The mixture of E. coli cells and ligated PCR product was placed directly in ice for 40 minutes and then placed at 42 ℃ for 40 seconds (i.e., heat-shock treatment), then placed on ice for three minutes, then 250 µl of SOC media was added to the mixture and kept on rotation at 37 ℃ in an incubator for one hour. Consequently, three different volumes of the cells mixture solution (25 µl, 50 µl and 75 µl) were spread on Luria-Bertani (LB) broth agar medium, which was supplemented in advance with 250 µl of kanamycin (50 µg/mL) and 40 µl of X-Gal on each plate and left upside down in the incubator at 37 °C overnight. Thereafter, the positive colonies (white ones) which had grown and were identified on the medium plate were picked and grown in liquid LB medium for 12 hours with mild shaking at 37 °C.

Meanwhile, a mixture for PCR was prepared as following: 50 µl of TBE 10X buffer + 50 µl (10 µM) of MgCl2 + 40 µl of dNTP + 25 µl of M13 forward primer + 25 µl of M13 reverse primer + 5 µl of DNA polymerase + 320 µl PCR water. Around 25 µl of that mixture was transferred into 20 PCR tubes. Two µl of medium colonies were added to each PCR tube and then run in the following protocol (Table 2.4) in thermal PCR.

Table 2.4: PCR protocol for cloning with M13 primers

Temperature	94 °C	94 °C	55 °C	72 °C	72 °C
Time	10 minutes	1 minute	1 minute	1 minute	10 minutes
Cycle(s)	1 X	26 X			1 X

The obtained products from the previous step were sequenced and aligned utilizing the Clustal-Omega programme (Version 1.2.2).

2.3.4 Determination of Dissociation Constant (Kd)

The selected aptamer sequences were chemically synthesized with Cy5 in Metabion International AG (Planegg, Germany) for the determination of the dissociation constant (Kd) by microscale thermophoresis (MST). Around 10 µL (of 50 nM working stock) of the Cy5 aptamer was transferred into 2 PCR tubes. Then, 10 µL of the MST buffer was transferred into each tube, mixed by a micropipette. The mixture in each PCR tube was incubated for five minutes at room temperature in a dark place before loading the solution into the MST capillaries. 20 µL of a 3.2 µM Lenalidomide solution of compound was transferred into tube 1 followed by a transfer 10 µL of dilution (i.e., MST buffer) into PCR tubes from 2 to 16.

A serial dilution (1:1) was prepared by transferring 10 µL from tube to tube (from tube 1 to tube 16) and mixed by pipetting up and down. 10 µL from tube 16 was discarded to obtain equal volume of 10 µL for all samples. Ten microliters of Cy5 aptamer (50 nM) were added to

each tube from 16 to 1 and mixed by the pipette. The mixture in each PCR tube was incubated for five minutes at room temperature in a dark place before loading the solution into the MST capillaries.

The experiment was repeated in triplicate (three independent triplicates) and the results analysed by MO-Affinity Analysis software (version 2.1.3, Nano Temper Technologies) to calculate the binding affinities of the aptamers to the compound (i.e., Lenalidomide, 6-Mercaptopurine, Dabrafenib and Venetoclax) expressed in Kd values.

The principle of MO-Affinity Analysis software is to measure the binding strength (i.e. affinity) between molecules by measuring changes in a molecule's movement in response to a temperature gradient. This approach is based on Micro Scale Thermophoresis (MST), which works by monitoring a molecule's thermal diffusion behaviour (the motion of the molecule within a temperature gradient) as it binds to another molecule. Changes in a molecule's size, charge upon binding, or hydration alter its thermophoretic mobility, allowing for the calculation of binding parameters like the dissociation constant (K_d).

In addition to the dissociation constant (Kd), there are some important parameters for aptamer specificity and affinity include binding kinetics, specifically the association rate (ka) and dissociation rate (kd), and thermodynamic parameters such as entropy (ΔS) and enthalpy (Δ H). These parameters provide a more complete insight of how and why an aptamer binds, which is critical for practical applications, as different aptamers with similar (Kd) values can have very different binding dynamics (Thevendran and Marimuthu, 2022).

Chapter Three: Selection of Aptamer for Lenalidomide

Chapter Three: Selection of Aptamer for Lenalidomide

3.1 Immobilization of Lenalidomide on NHS-Activated Sepharose Beads

Lenalidomide, a small molecule with a molecular weight of 259.26 g/mol, is more soluble in organic solvents and low pH solutions; however, it is soluble in organic solvent/water mixtures, and buffered aqueous solvents (Celgene, 2008).

Selection of high-affinity small-molecule-binding aptamers is often complicated and requires a specific design and consideration of all experimental conditions. Amongst the important steps for a successful SELEX protocol is the stable immobilization of the molecule analyte on a solid matrix. This attachment enables the partitioning of analyte bound from unbound DNA during the selection cycles. Since the Lenalidomide chemical structure contains amino radical, the commercial NHS activated sepharose beads have been chosen as a solid matrix for target immobilization, as shown in Figure 3.1.

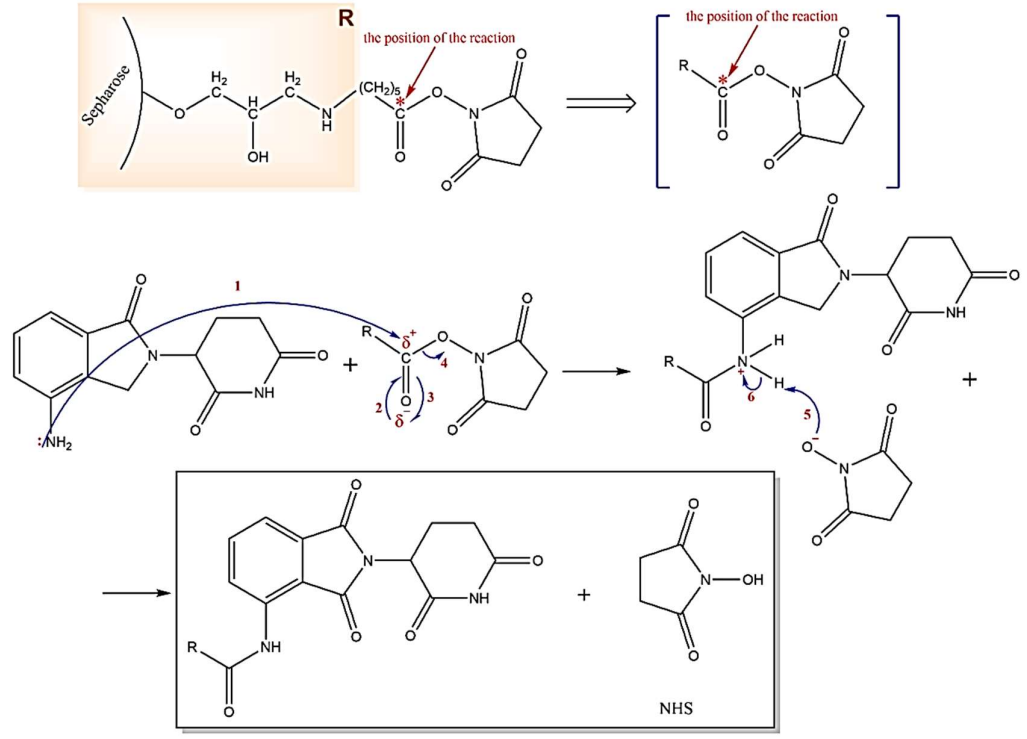

Figure 3.1: Mechanism of immobilization of Lenalidomide molecules on NHS-activated sepharose beads

3.2 Selection of Lenalidomide Aptamers using SELEX

After the immobilization of Lenalidomide on the sepharose beads, they were used for SELEX rounds. Each round of selection was performed by incubating Lenalidomide beads with an ssDNA library containing around 10^{15} random sequences, removal of unbound DNA by washing steps, elution of Lenalidomide beads bound to DNA, desalting and PCR amplification of the eluted DNA and finally, purification of the dsDNA PCR product to separate ssDNA sequences. By performing this selection cycle, a DNA pool was obtained with higher-affinity sequences to the target than the initial library used afterwards to start the subsequent SELEX cycle. This process was repeated for 10 rounds as shown in the recovery graph (Figure 3.2)

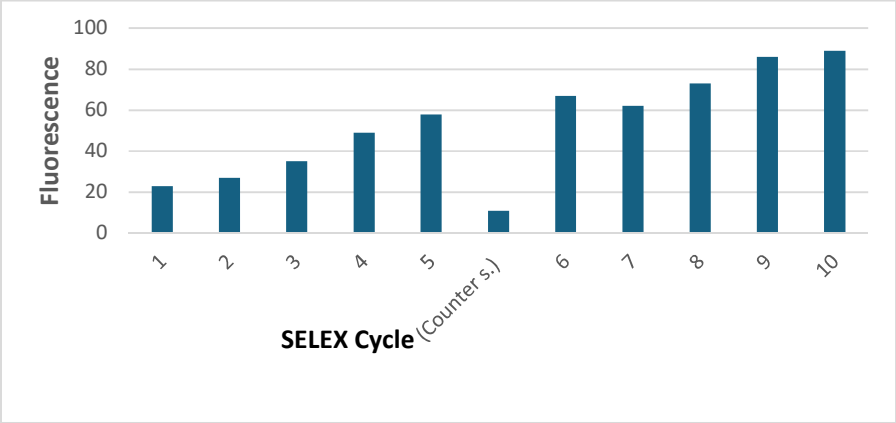

Figure 3.2: Fluorescence of Lenalidomide per cycle

(Fluorescence recovery graph of the bound ssDNA eluted from Lenalidomide conjugated sepharose beads in each SELEX cycle: cycle number versus the fluorescence intensity of the eluted DNA)

A significant increase of the DNA recovery with each progressive cycle of the selection was indicative of the enrichment of Lenalidomide binding ssDNA. The counter selection step (CS) was performed after the sixth round to eliminate the non-specifically bound ssDNA to the sepharose beads; a drop in the fluorescence intensity was noted (see Figure. 3.2). After counter selection, five more cycles of SELEX were undertaken to reach the fluorescence intensity plateau. The constant fluorescence recovery after 10 cycles indicates that the target binding sites are saturated and no more sites are available for binding. Once the binding amount reached a plateau between consecutive cycles, the pool is considered 'enriched' for Lenalidomide, the selection cycles were stopped and the DNA was eluted and cloned. Amplification of DNA eluted during SELEX rounds was preceded by running PCR, then 10% denaturing PAGE was performed to separate two DNA strands (see Figures 3.3-3.12) and there are clear and well-defined bands at 100 bp that correspond to ssDNA. The ssDNA was extracted from the resulting

gel bands which were processed and quantified by UV and used for the subsequent SELEX round. In the third cycle, which was at the beginning of the research, the obtained volume was insufficient to load samples from 7 to 10. Regarding the low intensity in the sample 2 and its appearance in the previous cycle, this is simply related to how the sample was loaded on the gel. All 10 samples that had loaded, collected from one vial and they will cut and collect again together from the gel.

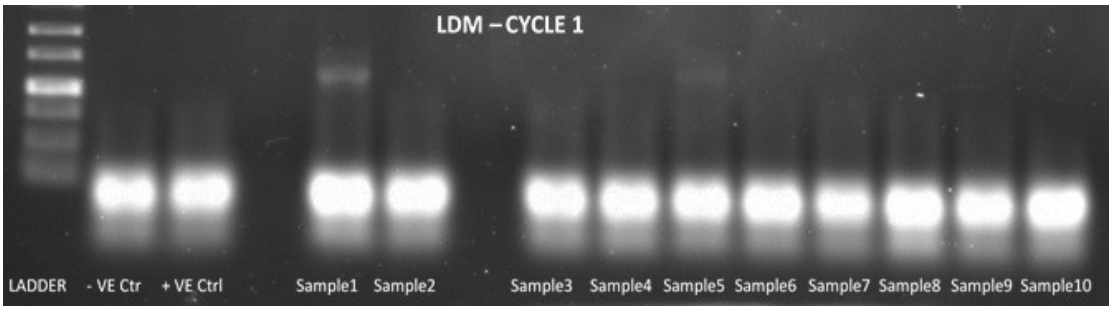

Figure 3.3: SDS-PAGE gel with - ve control, + ve control and different lots of Lenalidomide (LDM) sample obtained from SELEX cycle 1

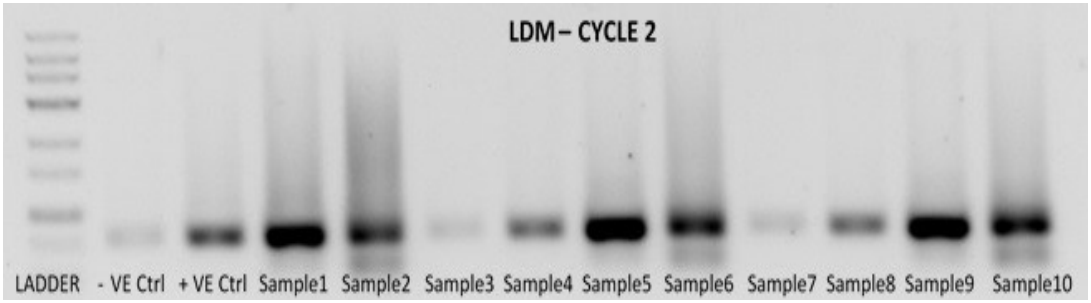

Figure 3.4: SDS-PAGE gel with -ve control, +ve control and different lots of Lenalidomide (LDM) sample obtained from SELEX cycle 2

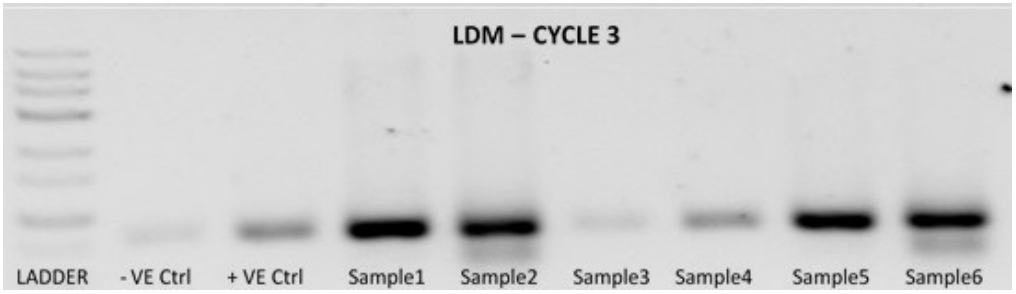

Figure 3.5: SDS-PAGE gel with -ve control, +ve control and different lots of Lenalidomide (LDM) sample obtained from SELEX cycle 3

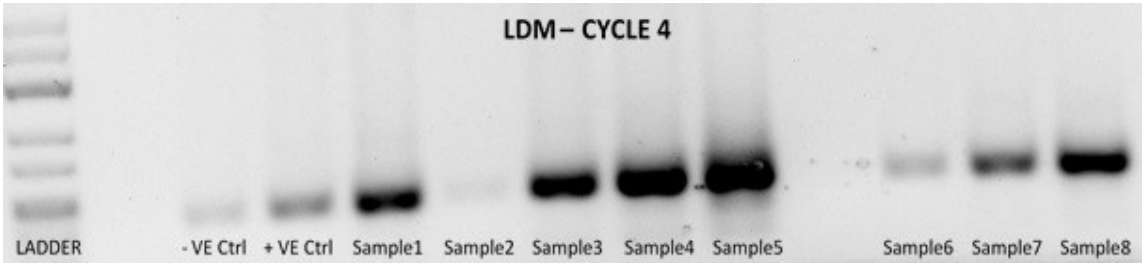

Figure 3.6: SDS-PAGE gel with -ve control, +ve control and different lots of Lenalidomide (LDM) sample obtained from SELEX cycle 4

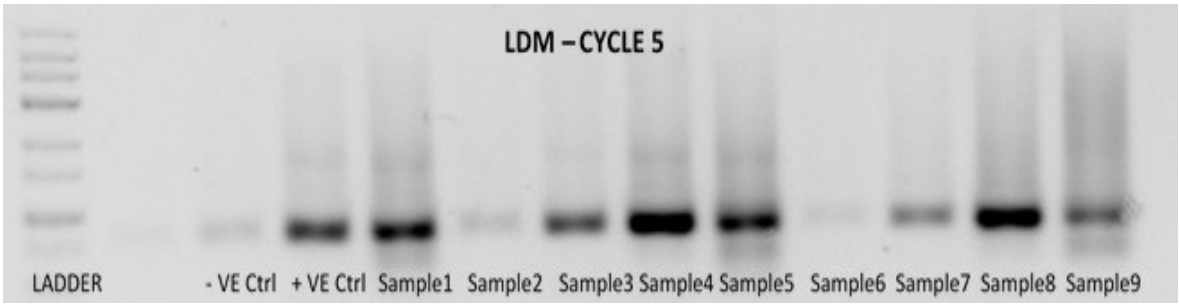

Figure 3.7: SDS-PAGE gel with -ve control, +ve control and different lots of Lenalidomide (LDM) sample obtained from SELEX cycle 5

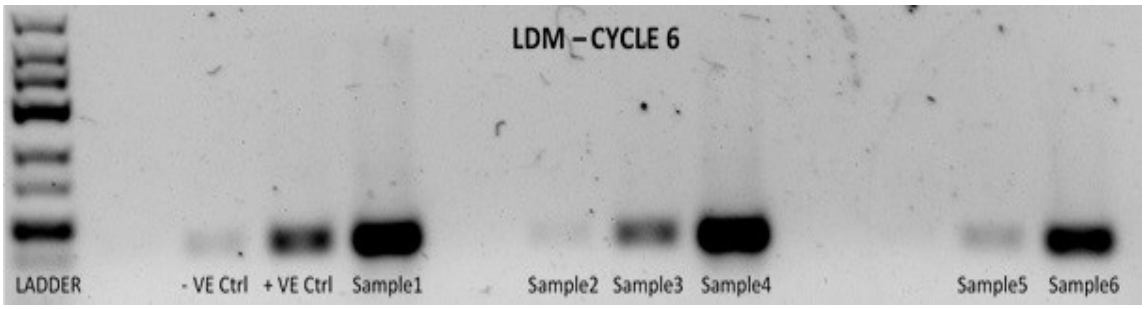

Figure 3.8: SDS-PAGE gel with -ve control, +ve control and different lots of Lenalidomide (LDM) sample obtained from SELEX cycle 6

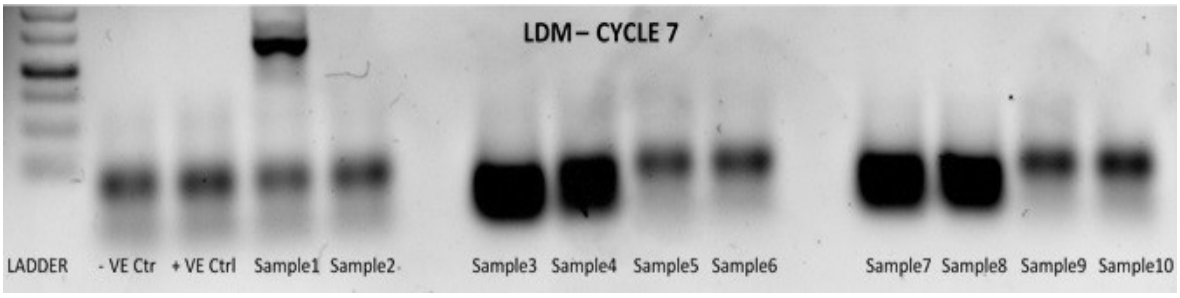

Figure 3.9: SDS-PAGE gel with -ve control, +ve control and different lots of Lenalidomide (LDM) sample obtained from SELEX cycle 7.

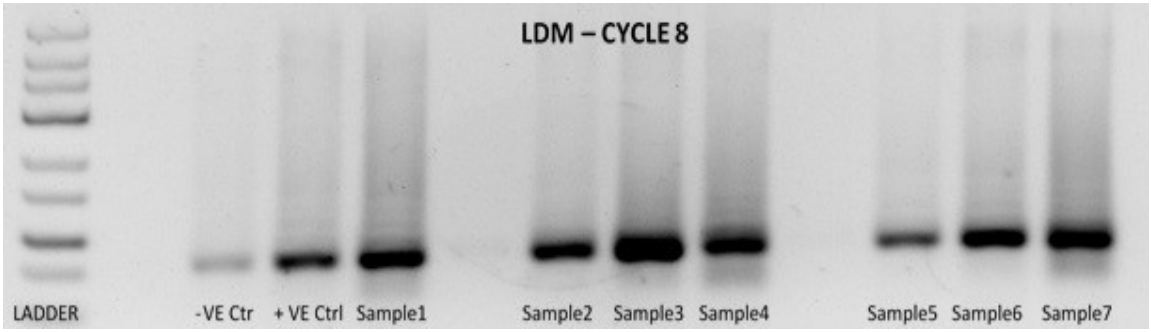

Figure 3.10: SDS-PAGE gel with -ve control, +ve control and different lots of Lenalidomide (LDM) sample obtained from SELEX cycle 8

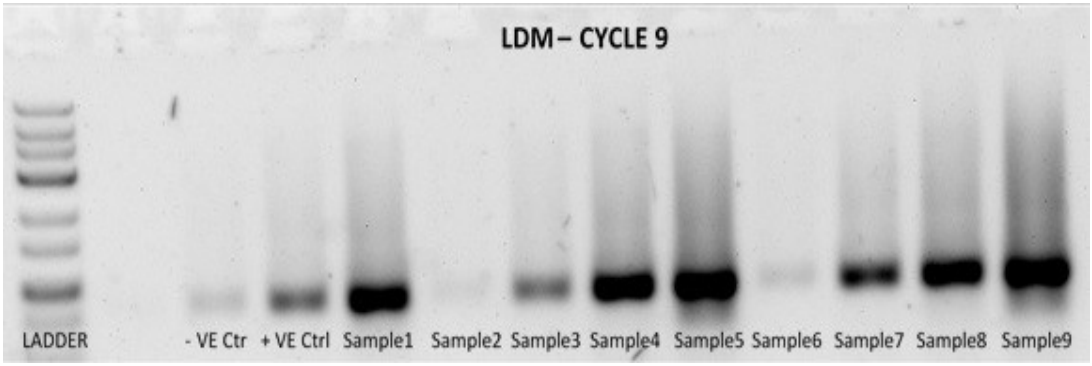

Figure 3.11: SDS-PAGE gel with -ve control, +ve control and different lots of Lenalidomide (LDM) sample obtained from SELEX cycle 9

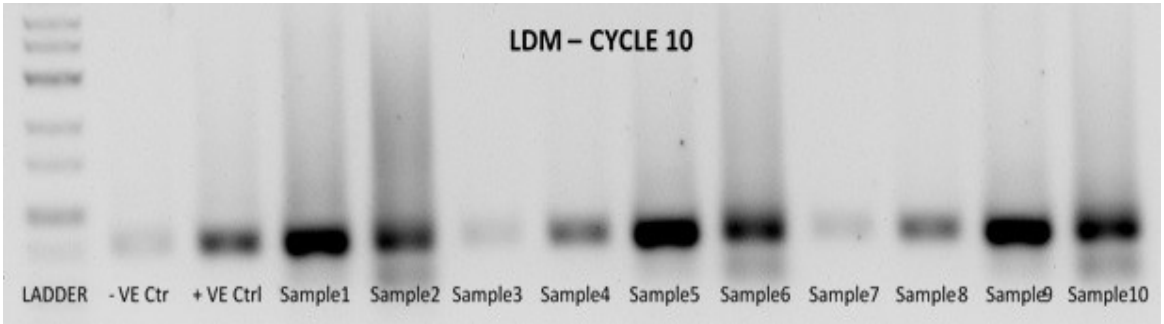

Figure 3.12: SDS-PAGE gel with -ve control, +ve control and different lots of Lenalidomide (LDM) sample obtained from SELEX cycle 10

The SELEX cycle for selection aptamer for the Lenalidomide molecule is summarized and demonstrated in Figure 3.13.

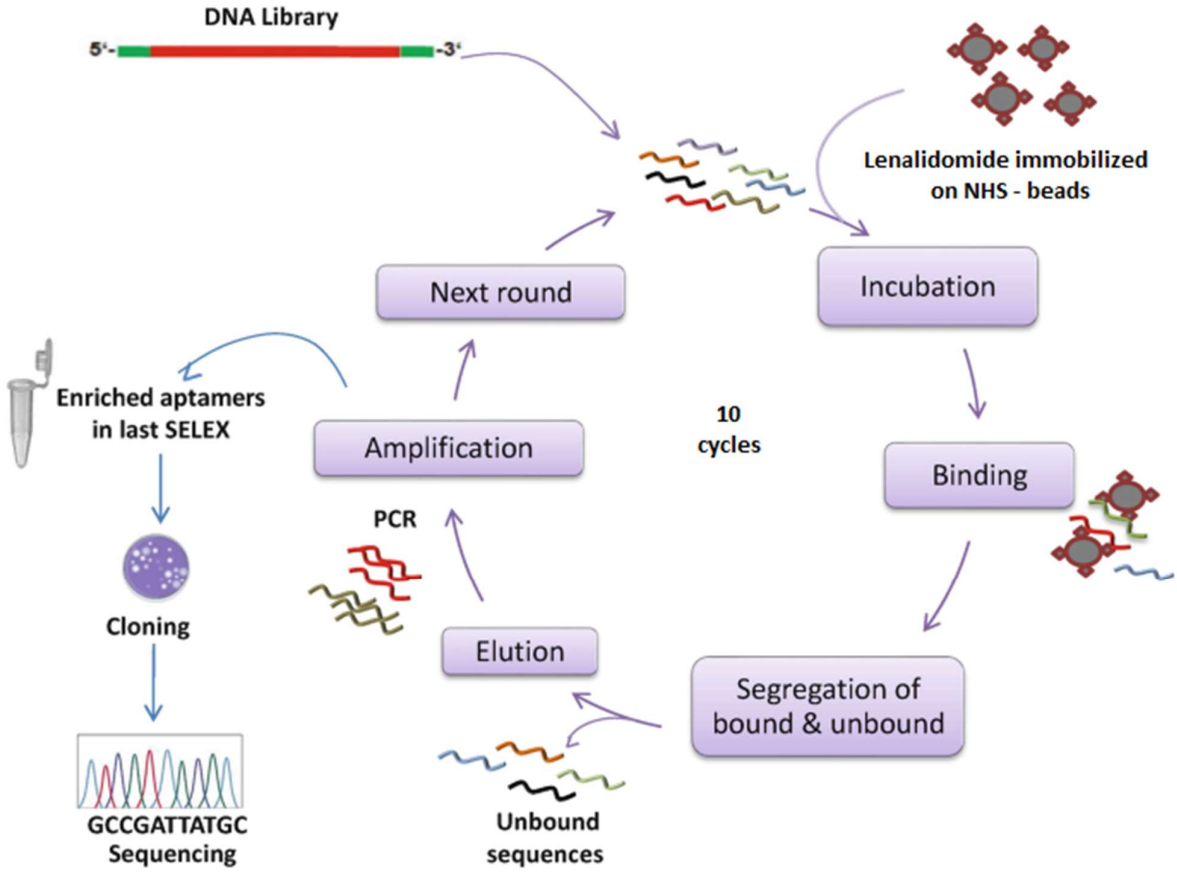

Figure 3.13: SELEX cycle for selection aptamer for the Lenalidomide

3.3 Cloning and Sequencing of Lenalidomide Aptamers

DNA cloning was performed by ligation into a cloning vector and then transformed into DH5α-T1 competent cells. After growing the cells for 24 hours, 30 colonies containing the DNA inserts were collected individually (see Figure 3.14).

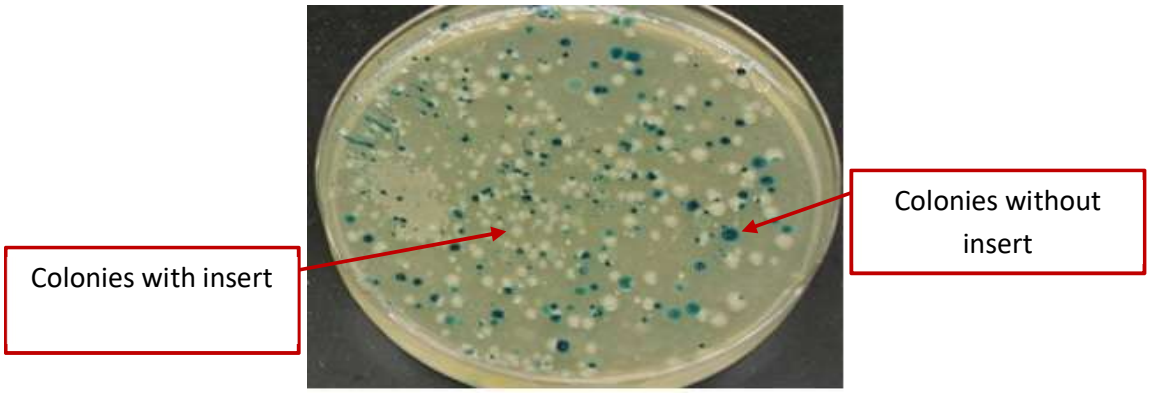

Figure 3.14: Transformed E. coli DH5α with and without ssDNA inserts: white colonies are with ssDNA while blue colonies are without

Thereafter, PCR amplification was performed to check the size, using 2% agarose gel electrophoresis. Of these colonies, 19 were confirmed at the correct size (300 bp) and were Sanger-sequenced, as shown in Figure 3.15 below.

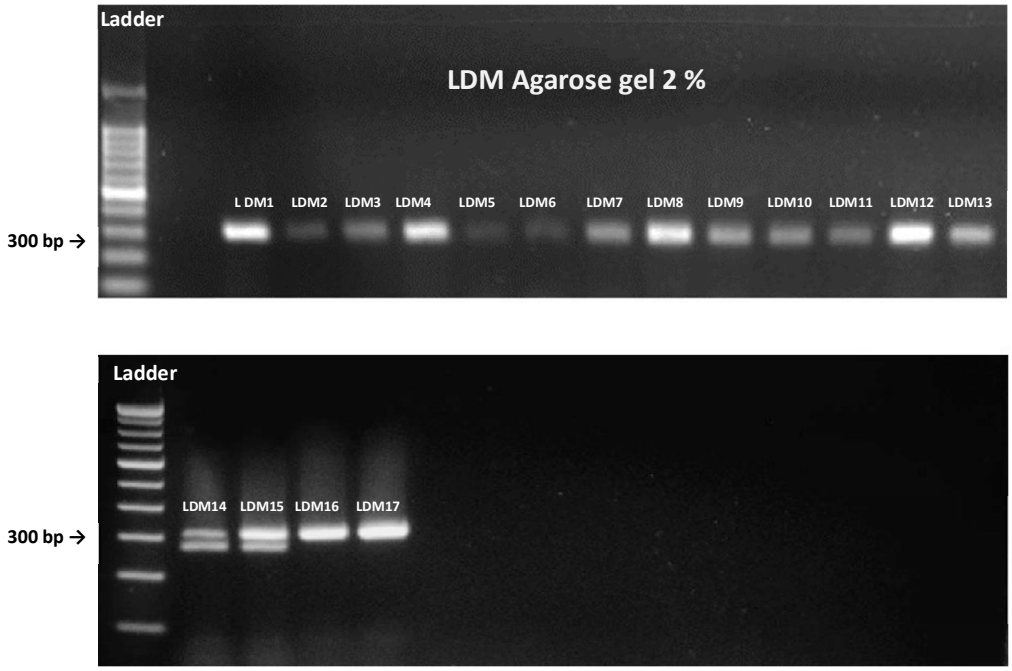

Figure 3.15: Gel electrophoresis (2% agarose) of PCR (white colonies) using M13 forward and reverse primers

The identified sequences revealed some identical sequences, indicating the enrichment of the DNA pool. The obtained DNA sequences were imported into the Geneious software for

analysis. The software was used to pair and merge the sequences amplified by the forward and reverse primers to form dsDNA. The sequences that showed non-complementary forward and reverse sequences were discarded and considered background noise. The complementary DNA strands were extracted based on the length of the library pool used during SELEX. The forward primer sequence was used as a reference when the merged sequences were blasted to identify aptamers with similar sequences. The sequences with the correct nucleotide sequences at the 5' end were isolated from the sequences that lacked the correct nucleotide sequence at the 3' end. Sequences were then truncated, to select only the regions of the aptamers that appeared enriched to the target during SELEX. Aptamers, as shown in Table 3.1, were then tested for binding to the Lenalidomide molecule.

Table 3.1: List of isolated ssDNA aptamers of Lenalidomide

Aptamer name	Sequence	E - value
LDM - 1	TCCCTACGGCGCCGCTAACGGCGCGCGCGCGCGCGCGGGGTTACGCGCGCGCGC GCGGTTGTAGCACGGTGGC	1.6e-28
LDM - 2	TCCCTACGGCGCCGCTAACGGCGCGCGCGCGCGCGCGGTTGAACGCGCGCGCGC GCGGTTGTAGCACGGTGGC	6.7e-28
LDM - 3	TCCCTACGGCGCCGCTAACGGCGCGCGCGCGCGCGCGTGGTGTCGCGCGCGCGCG CGGTTGTAGCACGGTGGC	1.7e-27
LDM - 4	TCCCTTCGGCGCCGCTAAACGCGCGCGCGCGCGCGCAATTACGCGCCGCGCGCAA GCGTTGTAGCACGGTTAG	6.29e-25
LDM - 5	TGGCTAAGGCGGCGATAACGCGCGCGCGCGCCCGCGATTTCGCGCGCGCGCG CGTTGTAGCACGGTGGC	2.42e-24
LDM - 6	TTCCTACGCGACGCTAACGGCGCGCGTTCGCGCGCGGAAAATCGCGCGCGCGCGC GGTTGTAGCACGGTAGC	1.58e-24
LDM - 7	TGCCTAAGGCGCCGCTAACGGCACGCGCGCAAGCGCGGCAATCCGCGCGCTTGC GCGGTTGTAGCACGGTGAC	1.36e-23
LDM - 8	TCCTTACGGCGCCGCTAACGGCGCGCGCGCGCGCGCGGTACCACGCGCGCAAGC GCGGTTGTAGCACGGTGGC	1.40e-23
LDM - 9	TGACTACGGCGCCGCTAACGGCGCGCGCGCGCATGCGGGGGTACGCGCGCGCGC GCCGTTGTAGCACGGTGCT	5.04e-25
LDM - 10	ACTACGGCGCTAACGGCGCGCGCGCGCGCGGTTGCGCGCGAGCGCGCGCGGT TGTAGCACGGTGGC	4.12e-25
LDM - 11	GGCCTACGGAACCGCTAACGGCGCGCGCGAAAGCGGTGGCACGCGCGCATGCGC GGTTGTAGCACGGTGGT	1.58e-24
LDM - 12	CTTCCACGGCGCCGCTAACGGCGCGCGCGCGCGCGCGGTGGCGCGCGCGCGCGC GCGGTTGTGGGACGGTGGC	1.09e-24
LDM - 13	AGAGTACGGCGCCGCTAACGGCGCGCGCGCGCTAGCGGTGGTGCGCGCGCGCGC GCGGTTGTAGCACGGTGGC	3.00e-24
LDM - 14	ACTATACGGCGCCGCTAACGGCGCGAAAGCGCCGGGTGTGGCGCGCGCGCGCGC GGTTGTAGCACGGTGGA	3.34e-25
LDM - 15	TCGTTACGGCGCCGCTAACGGCGCGCGCGCGAACGCGGTTCTGCGCGCGTGCGCG CGGTTGTAGCACGGTGCT	1.92e-24
LDM - 16	GGCTTACGGCGCCGCTAACGGCGCGCGCGCGCTCGCGTAGTTTCGCGCGCGCGCG CGGTTGTAGCAAGGGCGT	7.00e-26
LDM - 17	TGACTACGGCGCCGCTAACGGCGCAGGCGCGCGCGTGGGCGCGCGCGCGCCGGT TGTAGCACGGTGCA	7.99e-24

3.4 Determination of Dissociation Constant

A total of 17 aptamers were isolated and identified, as shown in Table 3.1. Three have been selected and synthesized with Cy5 in Metabion International AG (Planegg, Germany) for the determination of dissociation constant (Kd) by microscale thermophoresis (MST). Around 10 µL (of 50 nM working stock) of the Cy5 aptamer was transferred into 2 PCR tubes. Afterward, 10 µL of MST buffer was transferred into each tube, mixed by a micropipette. The obtained mixture in each PCR tube was incubated for five minutes at room temperature in the dark place before loading the solution into the MST capillaries. Afterward, 20 µL of a 3.2 µM Lenalidomide solution of compound was transferred into tube 1 then 10 µL of dilution (i.e., MST buffer) was transferred into PCR tubes from 2 to 16.

A serial dilution (1:1) was prepared by transferring 10 µl from tube to tube (from tube 1 to tube 16) and mix by pipetting up and down. 10 µL from tube 16 was discarded to obtain equal volume of 10 µL for all samples.

Afterwards, 10 µl of Cy5 aptamer (50 nM) was added to each tube from 16 to 1 and mixed by pipette; the mixture in each PCR tube was incubated for five minutes at room temperature in a dark place before loading the solution into the MST capillaries. The experiment was repeated in triplicate (three independent triplicates) with results analysed by MO-Affinity Analysis software (version 2.1.3, Nano Temper Technologies) to calculate the binding affinities of the aptamers to the compound (i.e., Lenalidomide) expressed in K_D values.

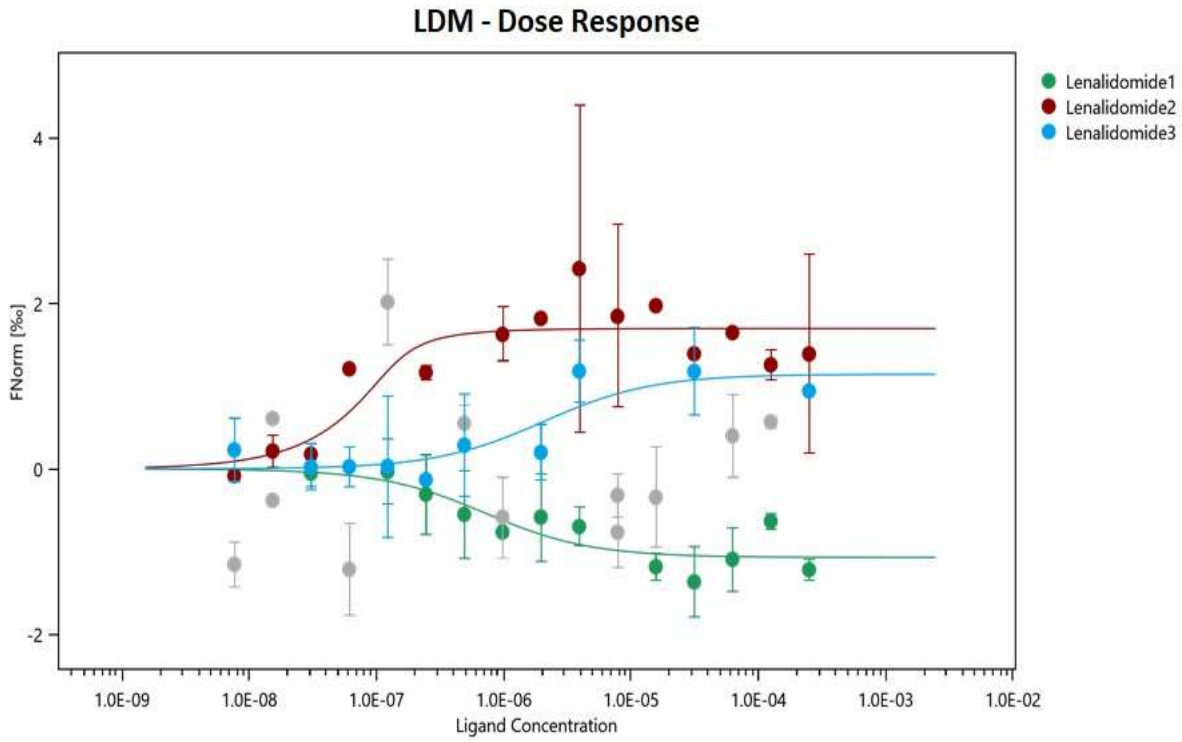

Figure 3.16: Affinity of binding of three aptamers to Lenalidomide molecule

The Lenalidomide 1 aptamer (green) induces a change (reduction) of fluorescence when it binds with the Lenalidomide molecule, while Lenalidomide 2 aptamer (red) and Lenalidomide 3 aptamer (blue) induce an increase in fluorescence when they bind to the Lenalidomide molecule. All three candidate aptamers bind in nM range, where aptamer Lenalidomide 3 binds the strongest (Kd:7.75 ± 0.09 nM), followed by aptamer Lenalidomide 2 (Kd:15.18 ± 0.37 nM) and then aptamer Lenalidomide 1 (Kd:653.46 ± 0.23 nM).

Chapter Four: Selection of Aptamer for 6-Mercaptopurine

Chapter Four: Selection of Aptamer for 6-Mercaptopurine

4.1 Immobilization of 6-Mercaptopurine on NHS-Activated Sepharose Beads

6-Mercaptopurine, a small molecule with a molecular weight of 170.20 g/mol, has poor aqueous solubility and is very soluble in organic solvents such as DMSO (Sletten et al., 1969).

The selection of high-affinity small-molecule-binding aptamers is often complicated and requires a specific design and consideration of all experimental conditions. Amongst the important steps for a successful SELEX protocol is the stable immobilization of the molecule analyte on a solid matrix. This attachment enables the partitioning of analytes bound from unbound DNA during the selection cycles. Since the 6-Mercaptopurine chemical structure contains amino radical, the commercial NHS activated sepharose beads have been chosen as a solid matrix for target immobilization (see Figure 4.1).

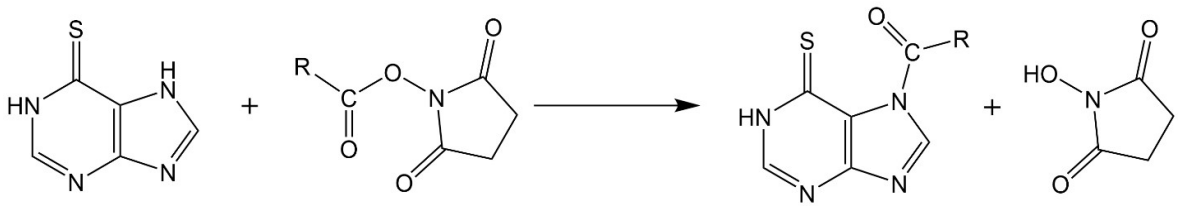

Figure 4.1: Mechanism of chemical reaction/binding between 6-Mercaptopurine and NHS-activated beads

4.2 Selection of 6-Mercaptopurine Aptamers using SELEX

After the immobilization of 6-Mercaptopurine on the sepharose beads, they were used for SELEX rounds. Each round of selection was performed by incubating 6-Mercaptopurine beads with an ssDNA library containing around 10^{15} random sequences, removal of unbound DNA by washing steps, elution of 6-Mercaptopurine beads bound to DNA, desalting and PCR amplification of the eluted DNA, and finally, purification of the dsDNA PCR product to separate ssDNA sequences. By performing this selection cycle, a DNA pool obtained higher-affinity sequences to the target than the initial library used afterwards to start the subsequent SELEX cycle. This process was repeated for 10 rounds, as shown in the recovery graph (Figure 4.2).

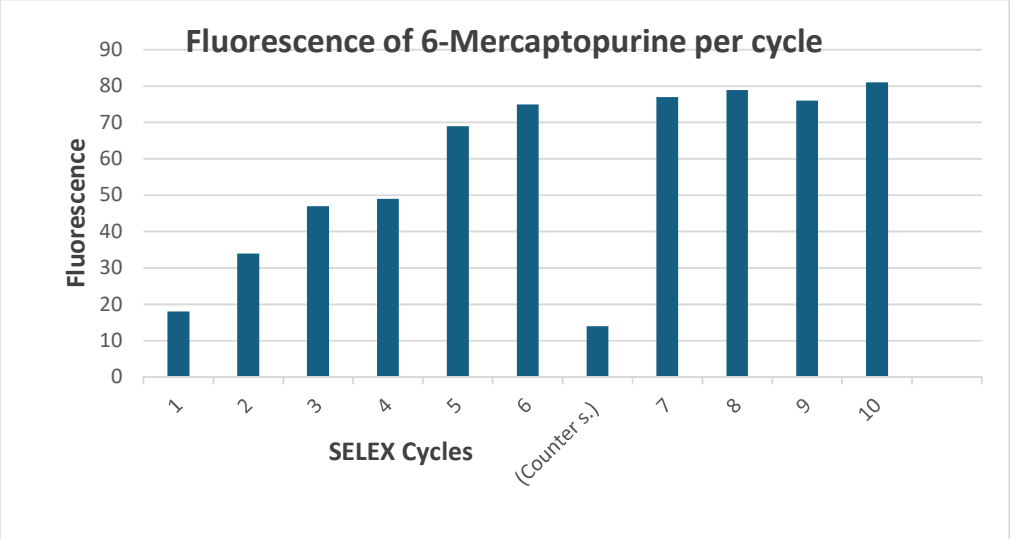

Figure 4.2: Fluorescence of 6-Mercaptopurine per cycle

(Fluorescence recovery graph of the bound ssDNA eluted from 6-Mercaptopurine conjugated sepharose beads in each SELEX cycle: cycle number versus the fluorescence intensity of the eluted DNA)

A significant increase of the DNA recovery with each progressive cycle of the selection was indicative of the enrichment of 6-Mercaptopurine binding ssDNA. The counter selection step (CS) was performed after the sixth round to eliminate the non-specifically bound ssDNA to the sepharose beads. A drop in fluorescence intensity was noted (see Figure. 4.2). After counter selection, four more cycles of SELEX were undertaken to reach the fluorescence intensity plateau. The constant fluorescence recovery after 10 cycles indicates that the target binding sites are saturated and no more sites are available for binding. Once the binding amount reaches a plateau between consecutive cycles, the pool is considered 'enriched' for 6-Mercaptopurine, the selection cycles were stopped, and the DNA was eluted and cloned.

Amplification of DNA eluted during SELEX rounds was preceded by running PCR and then 10% denaturing PAGE was performed to separate two DNA strands (see Figures 4.3-4.12). There are clear and well-defined bands at 100 bp that correspond to ssDNA.

The ssDNA was extracted from the resulting gel bands which were processed and quantified by UV and used for the subsequent SELEX round.

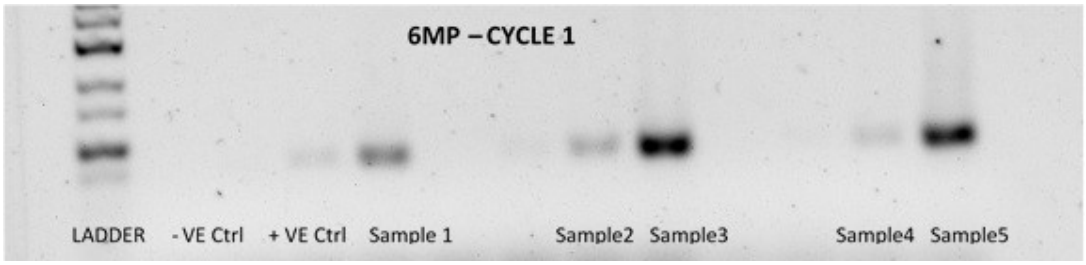

Figure 4.3: SDS-PAGE gel with -ve control, +ve control and different lots of 6-Mercaptopurine (6-MP) sample obtained from SELEX cycle 1

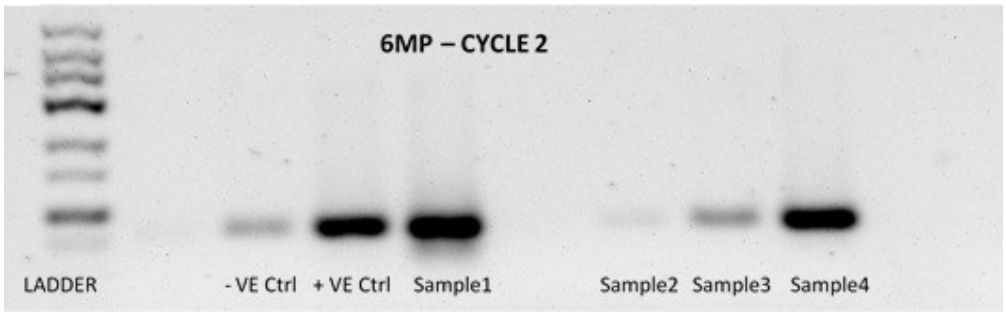

Figure 4.4: SDS-PAGE gel with -ve control, +ve control and different lots of 6-Mercaptopurine (6-MP) sample obtained from SELEX cycle 2

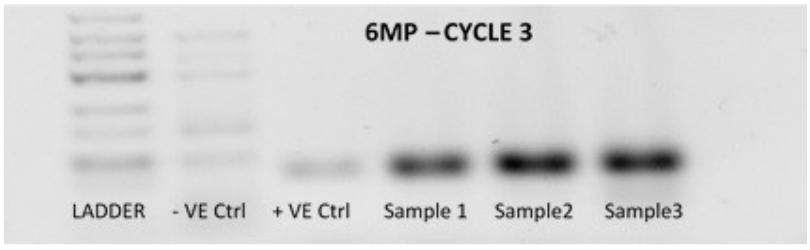

Figure 4.5: SDS-PAGE gel with -ve control, +ve control and different lots of 6-Mercaptopurine (6-MP) sample obtained from SELEX cycle 3

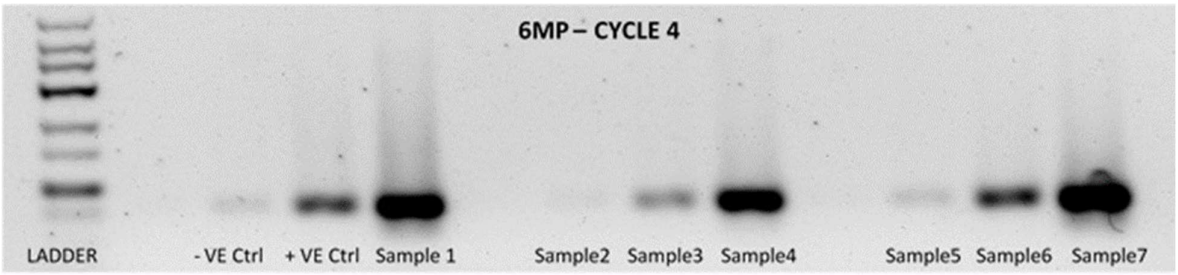

Figure 4.6: SDS-PAGE gel with -ve control, +ve control and different lots of 6-Mercaptopurine (6-MP) sample obtained from SELEX cycle 4

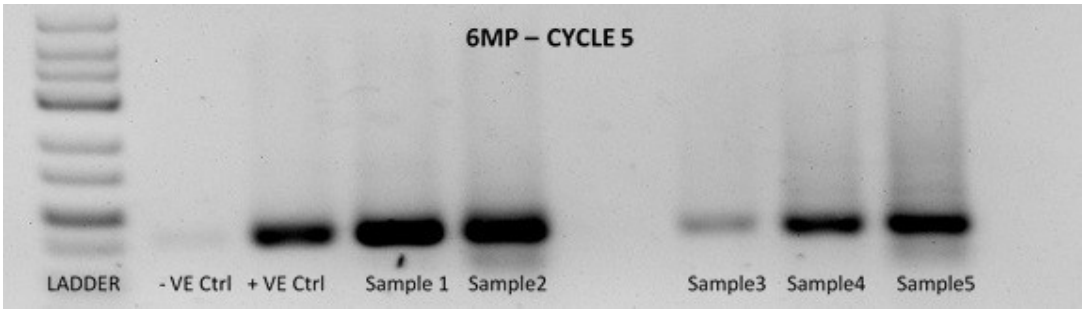

Figure 4.7: SDS-PAGE gel with -ve control, +ve control and different lots of 6-Mercaptopurine (6-MP) sample obtained from SELEX cycle 5

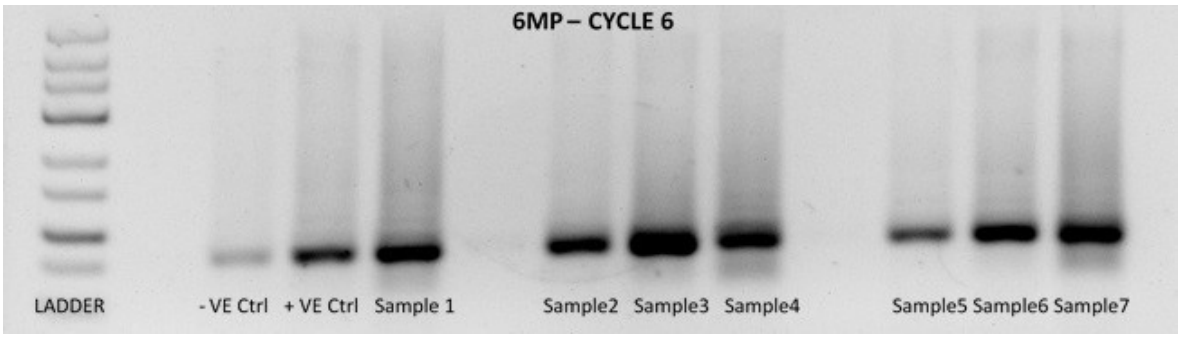

Figure 4.8: SDS-PAGE gel with -ve control, +ve control and different lots of 6-Mercaptopurine (6-MP) sample obtained from SELEX cycle 6

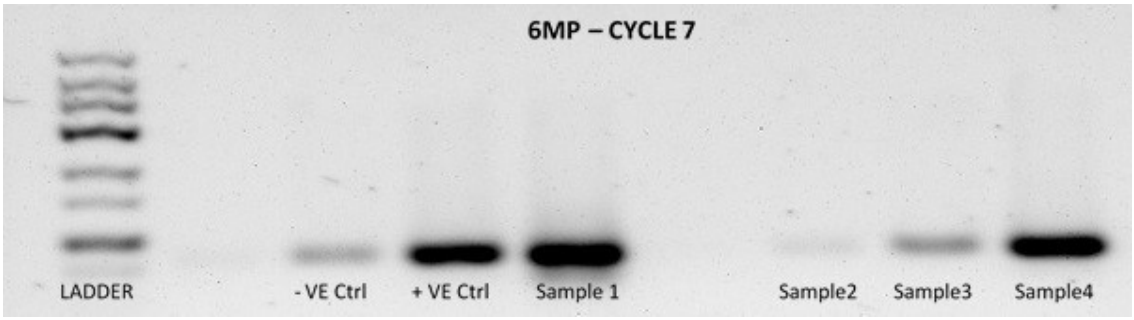

Figure 4.9: SDS-PAGE gel with -ve control, +ve control and different lots of 6-Mercaptopurine (6-MP) sample obtained from SELEX cycle 7

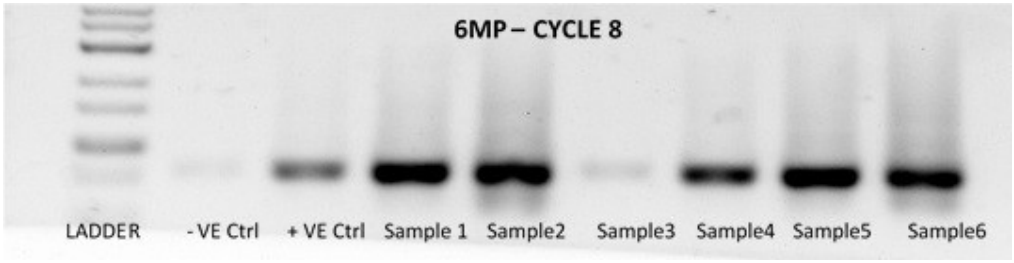

Figure 4.10: SDS-PAGE gel with -ve control, +ve control and different lots of 6-Mercaptopurine (6-MP) sample obtained from SELEX cycle 8

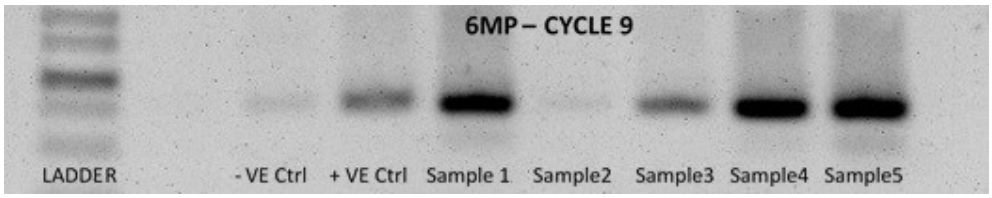

Figure 4.11: SDS-PAGE gel with -ve control, +ve control and different lots of 6-Mercaptopurine (6-MP) sample obtained from SELEX cycle 9

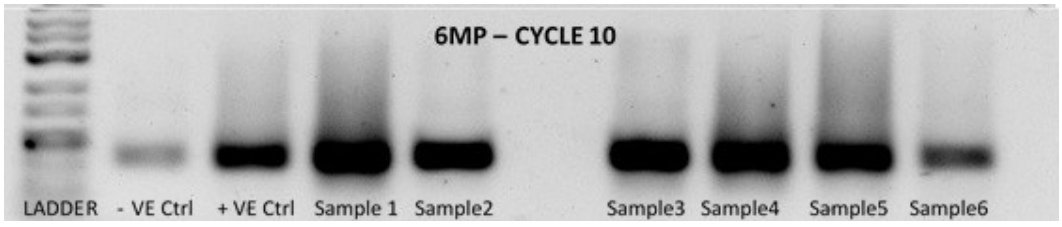

Figure 4.12: SDS-PAGE gel with -ve control, +ve control and different lots of 6-Mercaptopurine (6-MP) sample obtained from SELEX cycle 10

The SELEX cycle for selection aptamer for the 6-Mercaptopurine molecule is summarized and demonstrated below in Figure 4.13.

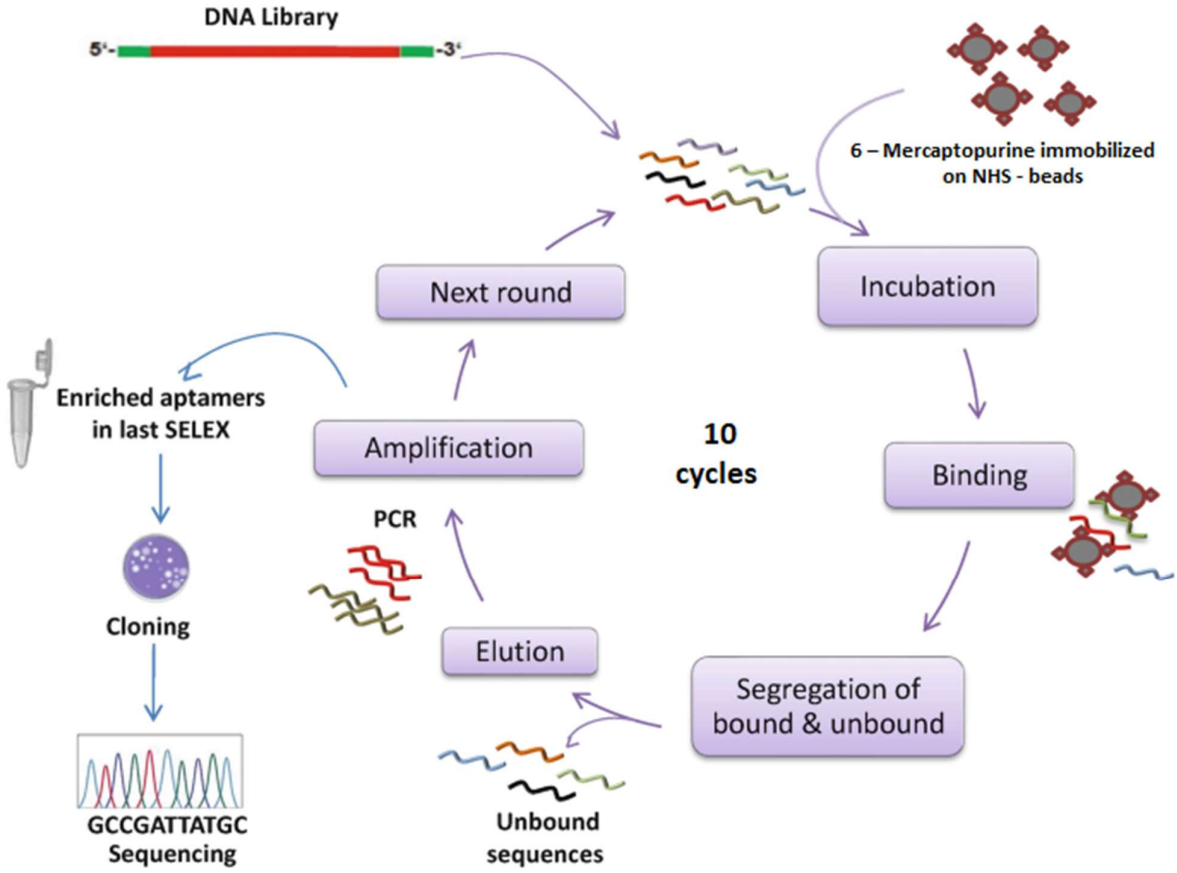

Figure 4.13: SELEX steps for 6-Mercaptopurine

4.3 Cloning and Sequencing of 6-Mercaptopurine Aptamers

DNA cloning was performed by ligation into a cloning vector and then transformed into DH5α-T1 competent cells. After growing the cells for 24 hours, 26 colonies containing the DNA inserts were collected individually, as shown in Figure 4.14.

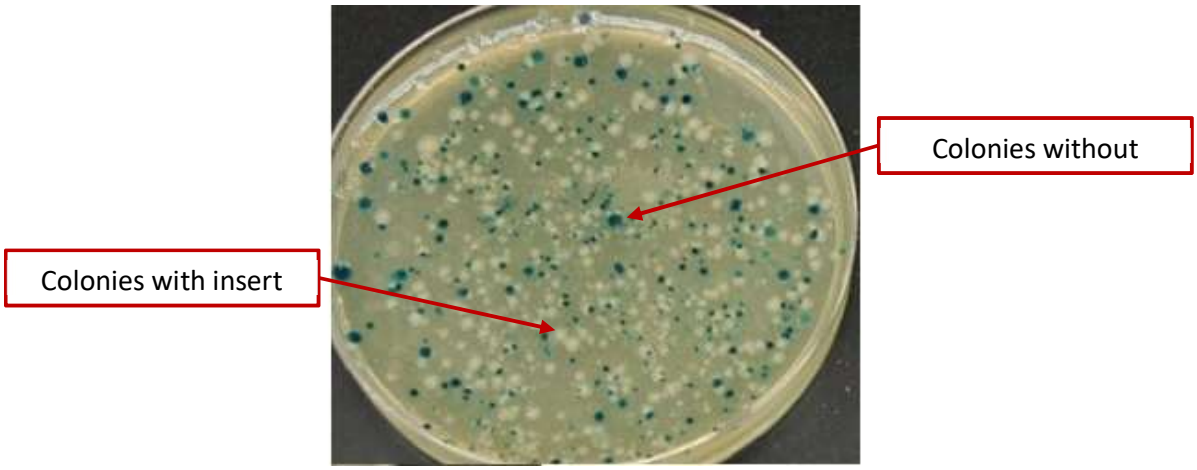

Figure 4.14: Transformed E. coli DH5α with and without ssDNA inserts: white colonies are with ssDNA while blue colonies are without

Thereafter, PCR amplification was performed to check the size, using 2% agarose gel electrophoresis. Of these colonies, 10 were confirmed as the correct size (300 bp) and were Sanger-sequenced, as shown in Figure 4.15 below.

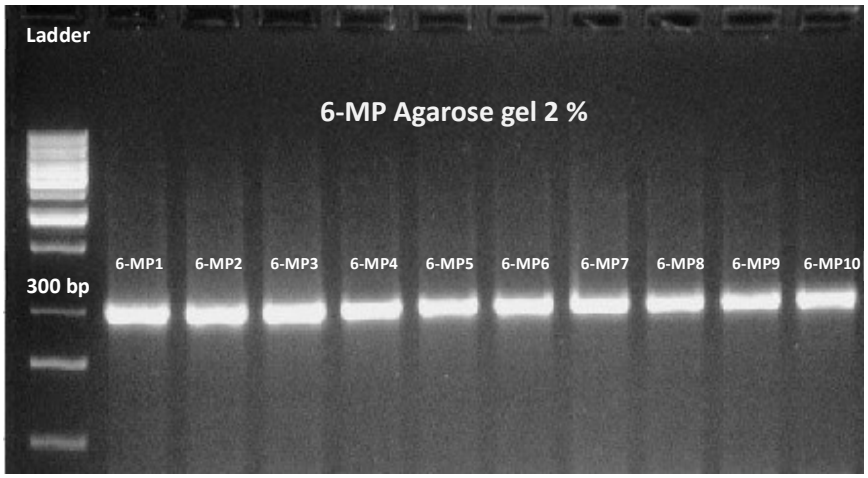

Figure 4.15: Gel electrophoresis (2% agarose) of PCR (white colonies) using M13 forward and reverse primers

The identified sequences showed some identical sequences indicating the enrichment of the DNA pool. The DNA sequences obtained were imported into the Geneious software for analysis. The software was used to pair and merge the sequences amplified by the forward and reverse primers to form dsDNA. The sequences that showed non-complementary forward and reverse sequences were discarded and considered background noise. The complementary DNA

strands were extracted based on the length of the library pool used during SELEX. The forward primer sequence was used as a reference when the merged sequences were blasted to identify aptamers with similar sequences. The sequences with the correct nucleotide sequences at the 5' end were isolated from the sequences that lacked the correct nucleotide sequence at the 3' end. Sequences were then truncated, to select only the regions of the aptamers that appeared enriched to the target during SELEX.

Aptamers shown in Table 4.1 were then tested for binding to a 6-Mercaptopurine molecule.

Table 4.1: List of isolated ssDNA aptamers to 6-Mercaptopurine

Aptamer name	Sequence	E - value
6-MP - 1	GCCCTACGGCAACGCTAACCGCGCTCGCGCGCGCGATTCGACGCGCCGCGCGTGC GCGTTGTAGCACGGTGTC	2.0e-33
6-MP - 2	TCCCTACGGCGCCGCTAACCGCGAATGCGCGCGCGCTTTTACGCGCCGCGCGCGC GCGTTGTAGCACGGTGGC	3.3e-34
6-MP - 3	TCCGTACGGCGCCGCTAACCGCGCGCGCGCGCGCGGTGAAACGCGCCGCGCGCG CGCGTTGTAGCACGGTTAC	1.7e-33
6-MP - 4	TCCCTTCGGCGCCGCTAAACGCGCGCGCGCGCGCGCAATTACGCGCCGCGCGCAA GCGTTGTAGCACGGTTAG	3.79e-26
6-MP - 5	TGGCTAAGGCGGATAACGCGCGCGCGCGCGCCCGCGATTTCGCGCGCGCGCGCG TTGTAGCACGGTGGC	2.57e-28
6-MP - 6	TTCCTACGCGACGCTAACGGCGCGCGTTCGCGCGCGGAAAATCGCGCGCGCGCGC GGTTGTAGCACGGTAGC	1.50e-26
6-MP - 7	TGCCTAAGGCGCCGCTAACGGCACGCGCGCAAGCGCGGCAATCCGCGCGCTTGC GCGGTTGTAGCACGGTGAC	2.32e-26
6-MP - 8	TCCTTACGGCGCCGCTAACGGCGCGCGCGCGCGCGCGGTACCACGCGCGCAAGC GCGGTTGTAGCACGGTGGC	1.85e-27
6-MP - 9	TGACTACGGCGCCGCTAACGCGCGCGCGCATGCGGGGGTACGCGCGCGCGCGCC GTTGTAGCACGGTGCT	2.32e-26
6-MP - 10	ACTACGGCGCTAACGGCGCGCGCGCGCGGTTGCGCGCGAGCGCGCGCGGTTG TAGCACGGTGGC	5.70e-28

4.4 Determination of Dissociation Constant

A total of 10 aptamers were isolated and identified (see Table 4.1). Three have been selected and synthesized with Cy5 in Metabion International AG (Planegg, Germany) for the determination of a dissociation constant (Kd) by microscale thermophoresis (MST). Around 10 µL (of 50 nM working stock) of the Cy5 aptamer was transferred into 2 PCR tubes. Afterward, 10 µL of MST buffer was transferred into each tube, mixed by micropipette. The obtained mixture in each PCR tube was incubated for five minutes at room temperature in the dark place before loading the solution into the MST capillaries.

Afterward, 20 µl of a 3.2 µM 6-Mercaptopurine solution of compound was transferred into tube 1 then 10 µl of dilution (i.e., MST buffer) was transferred into PCR tubes from 2 to 16.

A serial dilution (1:1) was prepared by transferring 10 µl from tube to tube (from tube 1 to tube 16) and mixed by pipetting up and down. 10 µL from tube 16 was discarded to obtain an equal volume of 10 µl for all samples.

Afterwards, 10 µl of Cy5 aptamer (50 nM) was added to each tube from 16 to 1 and mixed by pipette. The mixture in each PCR tube was incubated for five minutes at room temperature in a dark place before loading the solution into the MST capillaries.

The experiment was repeated in triplicate (three independent triplicates) and the results analysed by MO-Affinity Analysis software (version 2.1.3, Nano Temper Technologies) to calculate the binding affinities of the aptamers to the compound (i.e., 6-Mercaptopurine), expressed in Kd values.

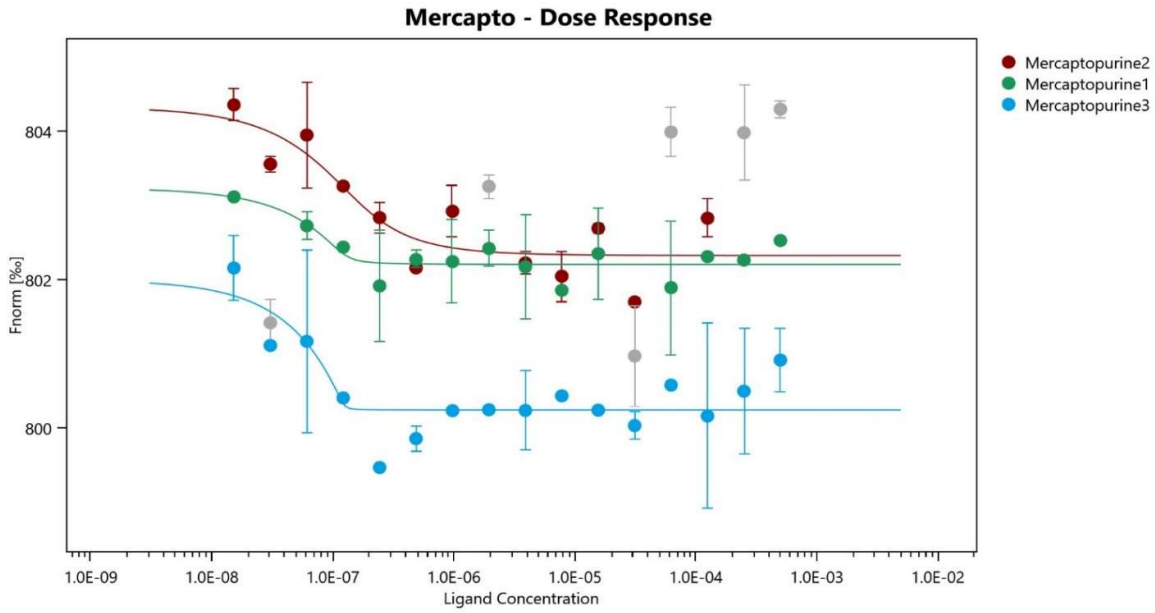

Figure 4.16: Affinity of binding of three aptamers to 6-Mercaptopurine molecule

The Mercaptopurine 3 aptamer (blue) induces a change (reduction) of fluorescence when it binds with the 6-Mercaptopurine molecule, while Mercaptopurine 2 aptamer (red) and Mercaptopurine 1 aptamer (green) induce an increase in fluorescence when bound to the 6-Mercaptopurine molecule.

All the three candidate aptamers bind in nM range, where aptamer 6-Mercaptopurine 3 (Kd:0.1552 ± 0.37 nM) binds the strongest, followed by aptamer 6-Mercaptopurine 1 (Kd: 2.30 ± 0.22 nM) and then aptamer 6-Mercaptopurine 2 (Kd: 46.8 ± 0.23 nM).

Chapter Five: Selection of Aptamer for Dabrafenib

Chapter Five: Selection of Aptamer for Dabrafenib

5.1 Immobilization of Dabrafenib on NHS-Activated Sepharose Beads

Dabrafenib, a small molecule with a molecular weight of 519.6 g/mol, is sparingly soluble in water. However, it is very soluble in organic solvents such as dimethyl formamide and dimethyl sulfoxide (DMSO) (Sunil et al., 2020).

Selection of high-affinity small-molecule-binding aptamers is often complicated, requiring a specific design and consideration of all experimental conditions. Amongst the important steps for a successful SELEX protocol is the stable immobilization of the molecule analyte on a solid matrix. This attachment enables the partitioning of analyte bound from unbound DNA during the selection cycles. Since the Dabrafenib chemical structure contains amino radical, the commercial NHS-activated sepharose beads have been chosen as a solid matrix for target immobilization, as shown in Figure 5.1.

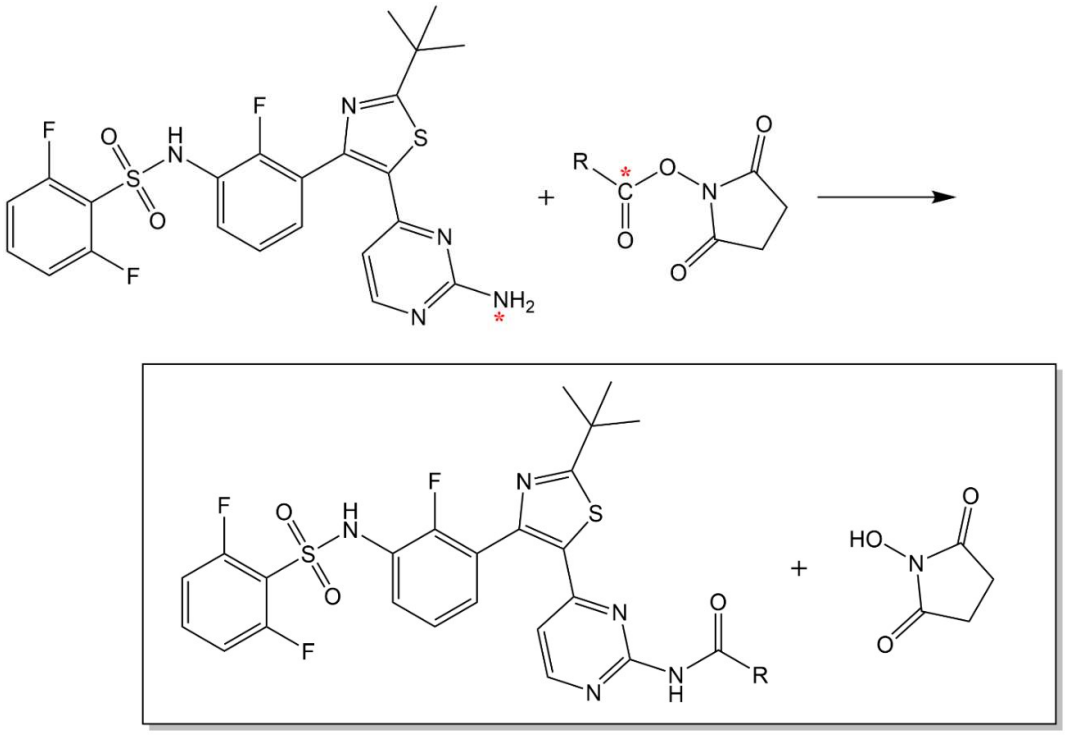

Figure 5.1: Mechanism of chemical reaction/binding between Dabrafenib and NHS-activated bead

5.2 Selection of Dabrafenib Aptamers using SELEX

After the immobilization of Dabrafenib on the sepharose beads, they were used for SELEX rounds. Each round of selection was performed by incubating Dabrafenib beads with an ssDNA library containing around 10^{15} random sequences, removal of unbound DNA by washing steps, elution of Dabrafenib beads bound DNA, desalting and PCR amplification of the eluted DNA and finally, purification of the dsDNA PCR product to separate ssDNA sequences. By performing this selection cycle, a DNA pool obtained higher-affinity sequences to the target than the initial library used afterwards to initiate the subsequent SELEX cycle. This process was repeated for 10 rounds, as shown in the recovery graph (Figure 5.2).

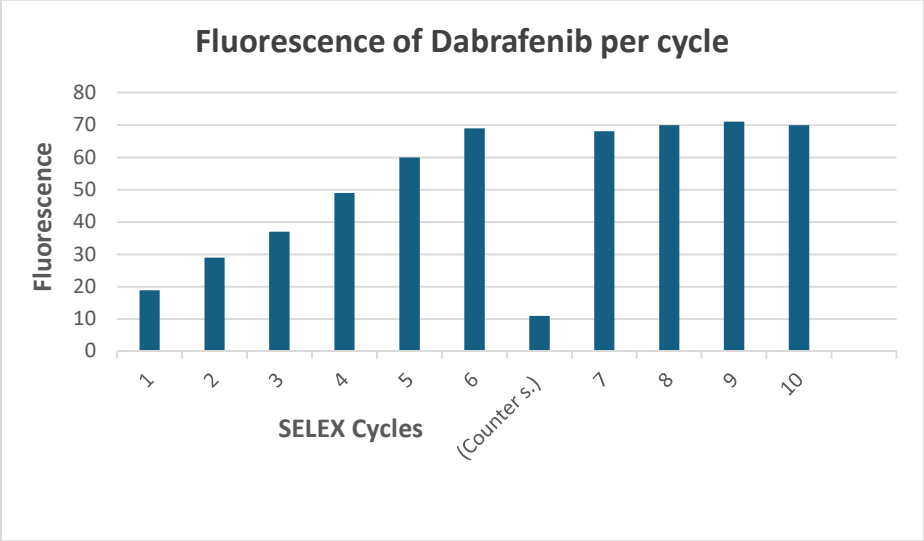

Figure 5.2: Fluorescence of Dabrafenib per cycle

(Fluorescence recovery graph of the bound ssDNA eluted from Dabrafenib conjugated sepharose beads in each SELEX cycle: cycle number versus the fluorescence intensity of the eluted DNA)

A significant increase of DNA recovery with each progressive cycle of the selection was indicative of the enrichment of Dabrafenib binding ssDNA. The counter selection step (CS) was performed after the sixth round to eliminate the non-specifically bound ssDNA to the sepharose beads; a drop in fluorescence intensity was observed, as shown in Figure 5.2. After counter selection, four more cycles of SELEX were undertaken to reach the fluorescence intensity plateau. The constant fluorescence recovery after 10 cycles indicates that the target binding sites are saturated and no more sites are available for binding. Once the binding amount

reached a plateau between consecutive cycles, the pool is considered 'enriched' for Dabrafenib, the selection cycles were stopped, and the DNA was eluted and cloned.

Amplification of DNA eluted during SELEX rounds was preceded by running PCR and then 10% denaturing PAGE was performed to separate two DNA strands (see Figures 5.3-5.12). Clear and well-defined bands are evident at 100 bp that correspond to ssDNA.

The ssDNA was extracted from the resulting gel bands which were processed and quantified by UV and used for the subsequent SELEX round.

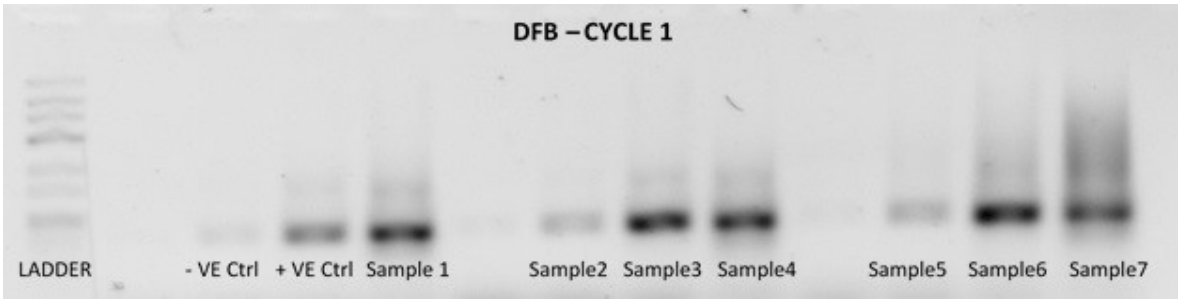

Figure 5.3: SDS-PAGE gel with -ve control, +ve control and different lots of Dabrafenib (DFB) sample obtained from SELEX cycle 1

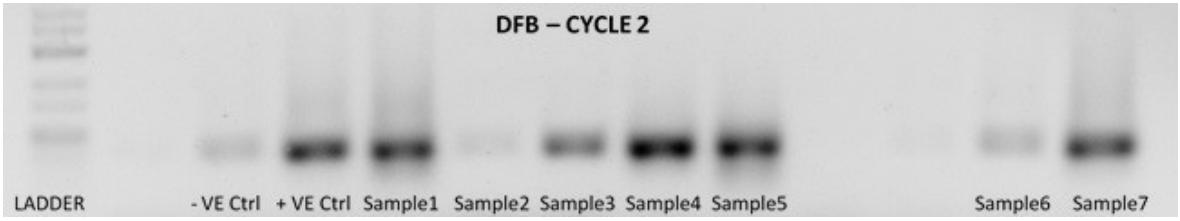

Figure 5.4: SDS-PAGE gel with -ve control, +ve control and different lots of Dabrafenib (DFB) sample obtained from SELEX cycle 2

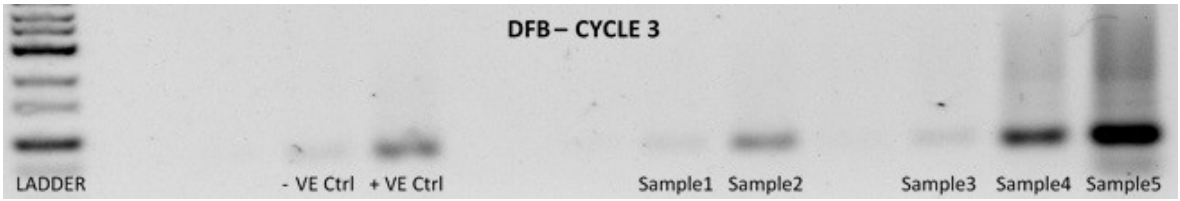

Figure 5.5: SDS-PAGE gel with -ve control, +ve control and different lots of Dabrafenib (DFB) sample obtained from SELEX cycle 3

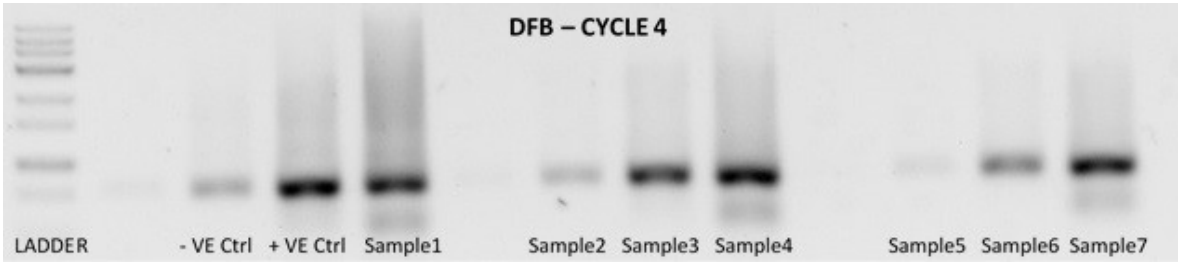

Figure 5.6: SDS-PAGE gel with -ve control, +ve control and different lots of Dabrafenib (DFB) sample obtained from SELEX cycle 4

Figure 5.7: SDS-PAGE gel with -ve control, +ve control and different lots of Dabrafenib (DFB) sample obtained from SELEX cycle 5

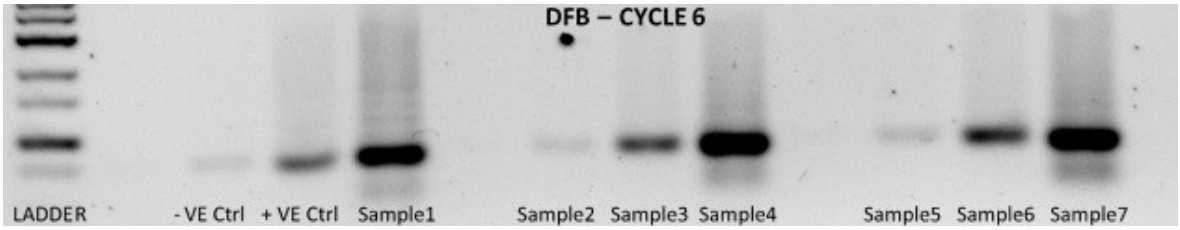

Figure 5.8: SDS-PAGE gel with -ve control, +ve control and different lots of Dabrafenib (DFB) sample obtained from SELEX cycle 6

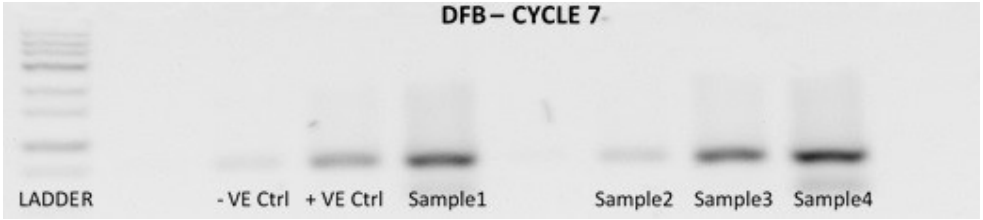

Figure 5.9: SDS-PAGE gel with -ve control, +ve control and different lots of Dabrafenib (DFB) sample obtained from SELEX cycle 7

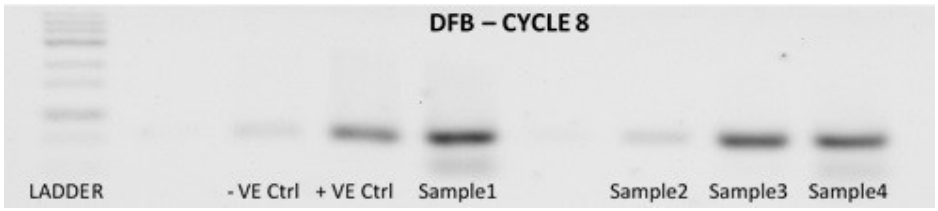

Figure 5.10: SDS-PAGE gel with -ve control, +ve control and different lots of Dabrafenib (DFB) sample obtained from SELEX cycle 8

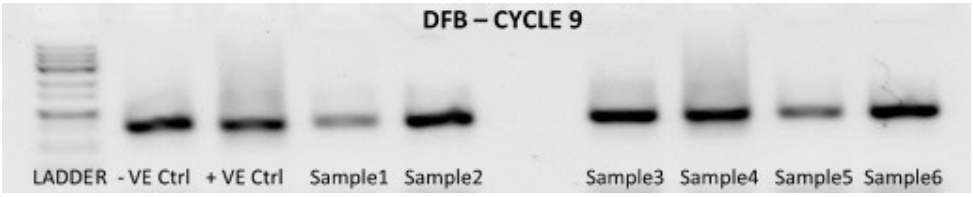

Figure 5.11: SDS-PAGE gel with -ve control, +ve control and different lots of Dabrafenib (DFB) sample obtained from SELEX cycle 9

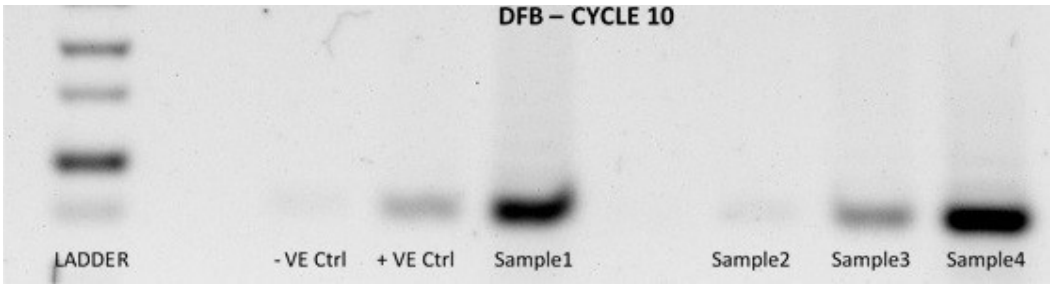

Figure 5.12: SDS-PAGE gel with -ve control, +ve control and different lots of Dabrafenib (DFB) sample obtained from SELEX cycle 10

The SELEX cycle for selection aptamer for the Dabrafenib molecule is summarized and demonstrated below in Figure 5.13.

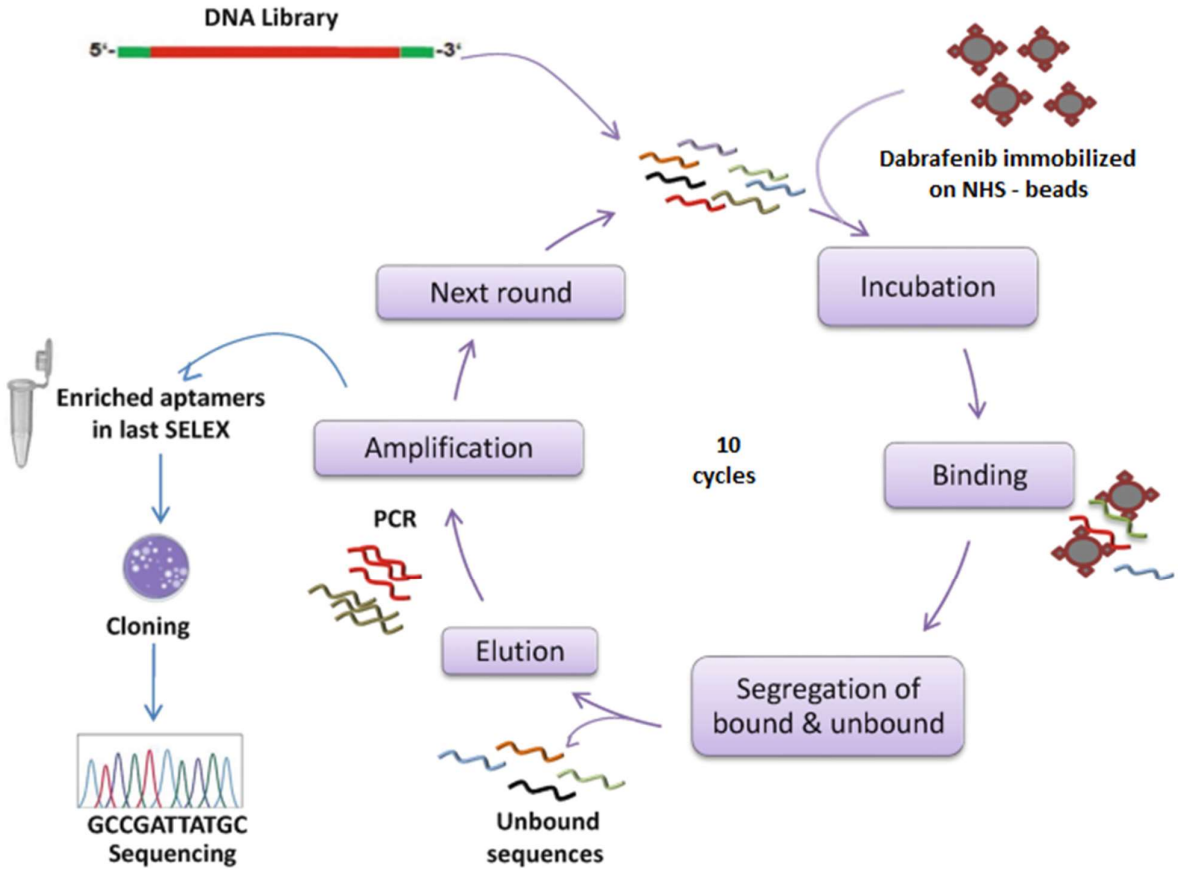

Figure 5.13: SELEX steps for Dabrafenib

5.3 Cloning and Sequencing of Dabrafenib Aptamers

DNA cloning was performed by ligation into a cloning vector and then transformation into DH5α-T1 competent cells. After growing the cells for 24 hours, 42 colonies containing the DNA inserts were collected individually (see Figure 5.14).

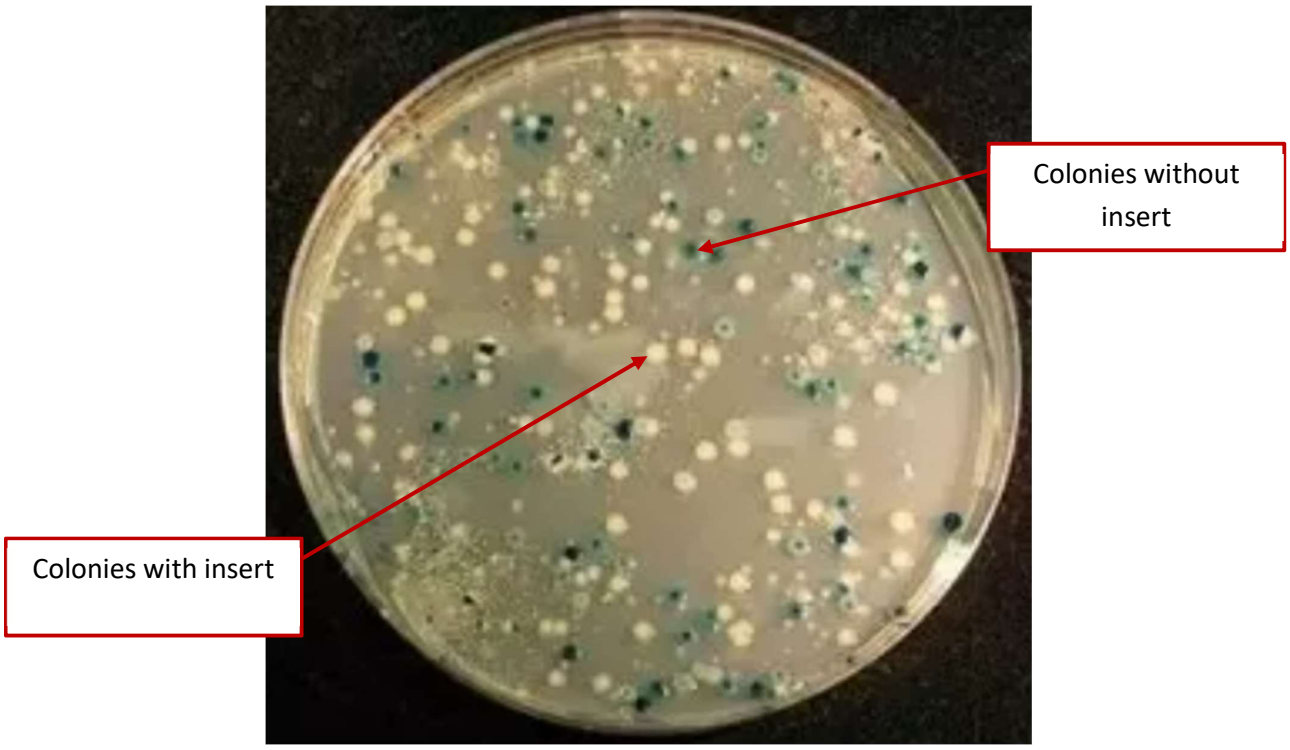

Figure 5.14: Transformed E- coli DH5α with and without ssDNA inserts: white colonies are with ssDNA while blue colonies are without

Thereafter, PCR amplification was performed to check the size using 2% agarose gel electrophoresis. Of these colonies, 28 confirmed the correct size (300 bp) and were Sanger-sequenced, as shown in Figure 5.15 below.

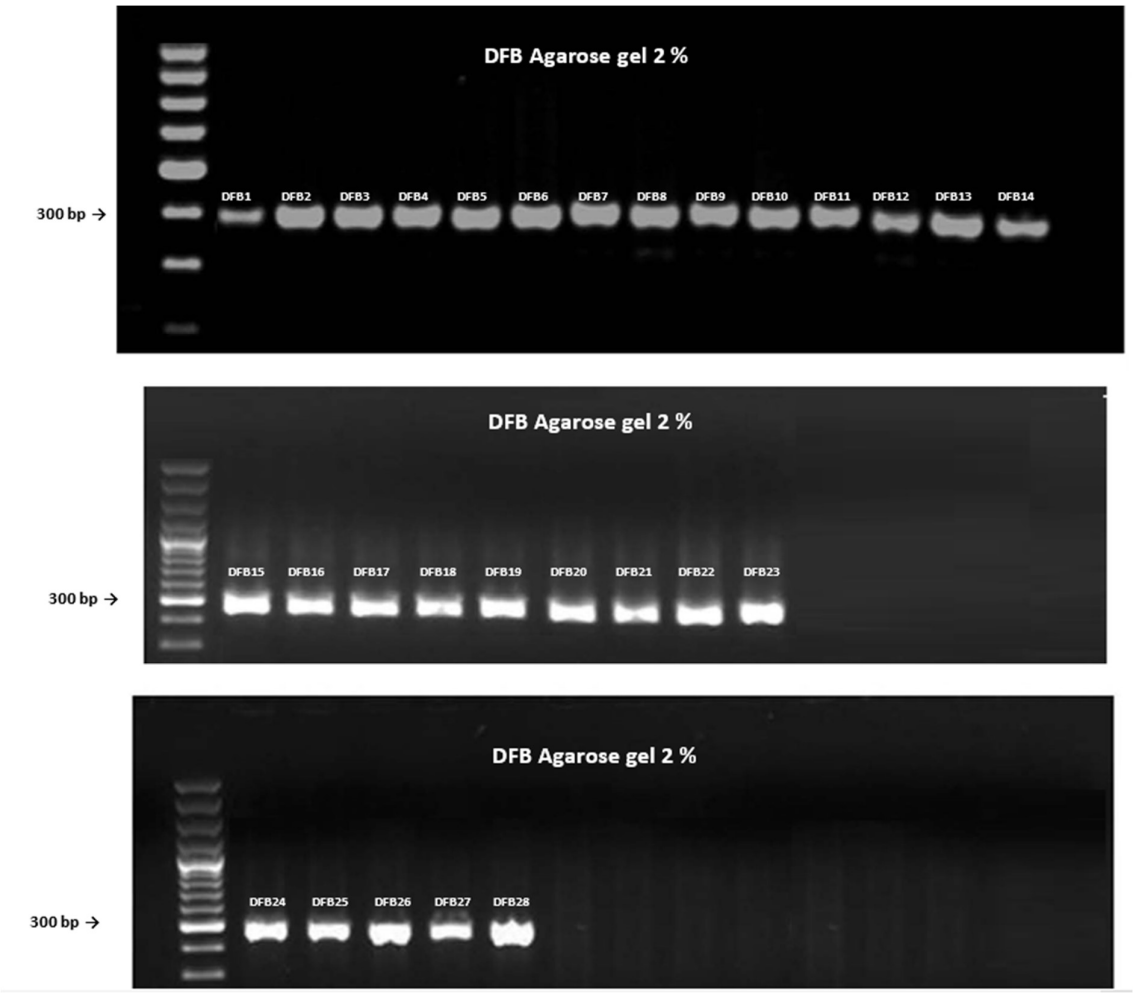

Figure 5.15: Gel electrophoresis (2% agarose) of PCR (white colonies) using M13 forward and reverse primers

The identified sequences showed some identical sequences, indicating the enrichment of the DNA pool. The DNA sequences obtained were imported into the Geneious software for analysis. The software was used to pair and merge the sequences amplified by the forward and reverse primers to form dsDNA. The sequences that showed non-complementary forward and reverse sequences were discarded and considered background noise. The complementary DNA strands were extracted based on the length of the library pool used during SELEX. The forward primer sequence was used as a reference when the merged sequences were blasted to identify aptamers with similar sequences. The sequences with the correct nucleotide sequences at the 5' end were isolated from the sequences that lacked the correct nucleotide sequence at the 3' end. Sequences were then truncated to select only the regions of the aptamers that appeared enriched to the target during SELEX. Aptamers were then tested for binding to a Dabrafenib molecule (Table 5.1).

Table 5.1: List of isolated ssDNA aptamers to Dabrafenib

Aptamer name	Sequence	E - value
DFB - 1	TCTCTACGGCGCCGCATACCGAAACGCGCGCTGCGCGATGCTCCGCGAACGCGCG CGCGTTGTAGCACGGT	2.3e-32
DFB - 2	TCCGTACGGCGCCGCAATCCGCGAATGCGCGCGCGCTTTTACGCGCCGCGCGCGC GTTGTAGCACGGTGGC	2e-33
DFB - 3	TGCGTACGGAACCGCTATCCGCGCGCGCGGCGTGAAACGCGCTCGCGCGCGCGC GTTGTAGCACGGTTAC	2.7e-32
DFB - 4	ACGCTTAGGCGCCGCTAACGCGCGCGCGCGCGCAATTACGCGCCGCGCGCAAGC GTTGTAGCACGGTTAG	3.3e-33
DFB - 5	TGGCTAAGGCGGCGATAACGCGCGCGCGCGGCCCGCGATTTCGCGCGCGCGCGC GTTGTAGCACGGTGGC	4.4e-33
DFB - 6	TTCCTACGCGACGCTAACGGCGCGCGTTCGCGCGCGGAAAATCGCGCGCGCGCGC GGTTGTAGCACGGTAGC	4.4e-33
DFB - 7	AGCCTAAGGCGCCGCTAACGGCACGCGCGCAAGCGGGCAATCCGCGCGCTTGCG CGGTTGTAGCACGGTGA	5.8e-33
DFB - 8	TCCTTACGGCGCCGCTAACGGCGCGCGCGCGCGCCGGTACCACGCGCGCAAGCG CGGTTGTAGCACGGTGGC	7.3e-33
DFB - 9	GAGCTACGGAGGGCGCTAAGGCCGCGCGCGCATGGGGGGGTAAGCGCGCGCGCGC CGTTGTAGCACGGCAGT	1.4e-33
DFB - 10	AGAGCTAACCGCGCGCGCGCGCGCGGATTCACGCGCCGCGCGCGCGTTGTAGCA CGGTTCACTACGGCGCC	8.8e-33
DFB - 11	GCACGCGCGCGCGGTCGATCGCGCCGGCGCGCGCGTTGTATCCGCGCCGCTAACC GCGCACGGTGGCCTATA	7.7e-33
DFB - 12	ACAAATTCAGAGTAATTGAATAATAGCGCCGGCGAAGTAACAATGATCATCTGA AAAGCGCTACGGTCAGG	4.4e-32
DFB - 13	TAGAGACACTCCGGGCCTTAGGTAGATGCTTCATCTCGTCCGTAACGATAATCAA CAAATCGCGCGTGTACC	4.3e-32
DFB - 14	TTGTAGCACGGTGAATCCTAAGGCGCCGCTAACGGCACGCAAGGGGCAATCCGC GCGCTTGCGCGGTTGTA	5e-32
DFB - 15	ATCGCGCGTGTACCAGTCAGGTATATGAAGTGATAACAAATCGTATGGATGACAC AGCAGGTTGCTACGGCG	3.4e-32
DFB - 16	CATCAGCCTACGTGGATACACCACATACAAACCGCGCGCGCGCTCCATAACCCCG TGTCATGTGTCGTGCG	8.8e-33
DFB - 17	GACCTTAAGGGGACACCACAGATGAATGTAACCGCGCGCGCGCGTACAGTACCA TGTTACGACCATATGG	2.4e-32
DFB - 18	TGTCACCAACAACAGGGAGCGGCGCGCCTACGCGAGGGTCAATGTAACGTCATG CGGATGTGTGGAATCG	7.1e-33
DFB - 19	CACCAACACACAAGTGGACCCCCGCGCGCGCGCGCGCGGTGACGATGGATGGTG ACGGTATACGCGCATGG	9.5e-33
DFB - 20	GTCACCACCCTATTCCTCTGCCGTTGTAACCGCGCGCGCGCGCGCGTAACTCTCAC GAGAGAGCGATGTGGC	2.4e-32
DFB - 21	TTCCTCTGCCGTTGGCGAGAGCGCCCCCCCTAACCGCGCGCGCGCGCGCGTCTCA CCACAGCCGTCACACCCT	3.3e-32
DFB - 22	ACGTCTCGACATACTAACCGCGCGCGCGCGCGCGTCTCTCCGCGCTGACGCATGG AGCGCGCGACACTATTG	2.6e-32
DFB - 23	CGGGCAGAGGGATAGGTTGTTGACGGGCTAACCGCGCGCGCGCGCGCGTCTCTCC GCGCACTATGTTGTCCA	5.1e-32
DFB - 24	AGACAATCGAAAAGTAAAGGAATCTAACCGCGCGCGCGCGCGCGTCTCTCCGCG CATAGAAGTAACC	1.9e-32
DFB - 25	AGCTGACACAGAGGTTGGTGCTAACCGCGCGCGCGAACGCGTCCTCCGCGCTCTC TCCGCGCCCATATGG	3.5e-32
DFB - 26	TGACACAGCAGGTTGGTGCTAACCGCGCGCGCGCGCCGCGCGCGCGCGTCTCTTA TGACCCCTATGAACCC	2.6e-33
DFB - 27	CCCAAGCTTAATACGACTCACTATAGGGAGCTCCAGGCGCGCGGAGTAACGGTAT CCTAGTTGAATTGAAT	6.4e-32
DFB - 28	AGCTGACACAGCAGGTTGCAACCTGCTGTGGCGCGCGCGCGGAGTAACGCGCGA ACGGTATACGTCATGGA	7.3e-33

5.4 Determination of Dissociation Constant

A total of 28 aptamers were identified and isolated, as shown in Table 5.1. Three have been selected and synthesized with Cy5 in Metabion International AG (Planegg, Germany) for the determination of the dissociation constant (Kd) by microscale thermophoresis (MST). Around 10 µl (of 50 nM working stock) of the Cy5 aptamer was transferred into 2 PCR tubes. Afterward, 10 µl of MST buffer was transferred into each tube, mixed by micropipette. The obtained mixture in each PCR tube was incubated for five minutes at room temperature in a dark place before loading the solution into the MST capillaries. Afterward, 20 µl of a 3.2 µM Dabrafenib solution of compound was transferred into tube 1 then 10 µl of dilution (i.e., MST buffer) transferred into PCR tubes from 2 to 16.

A serial dilution (1:1) was prepared by transferring 10 µl from tube to tube (from tube 1 to tube 16) and mixed by pipetting up and down. 10 µl from tube 16 was discarded to obtain equal volume of 10 µl for all samples.

Afterwards, 10 µl of Cy5 aptamer (50 nM) was added to each tube from 16 to 1 and mixed by pipette; then the mixture in each PCR tube was incubated for five minutes at room temperature in a dark place before loading the solution into the MST capillaries.

The experiment was repeated in triplicate (three independent triplicates) and the results analysed by MO-Affinity Analysis software (version 2.1.3, Nano Temper Technologies) to calculate the binding affinities of the aptamers to the compound (i.e., Dabrafenib) expressed in Kd values.

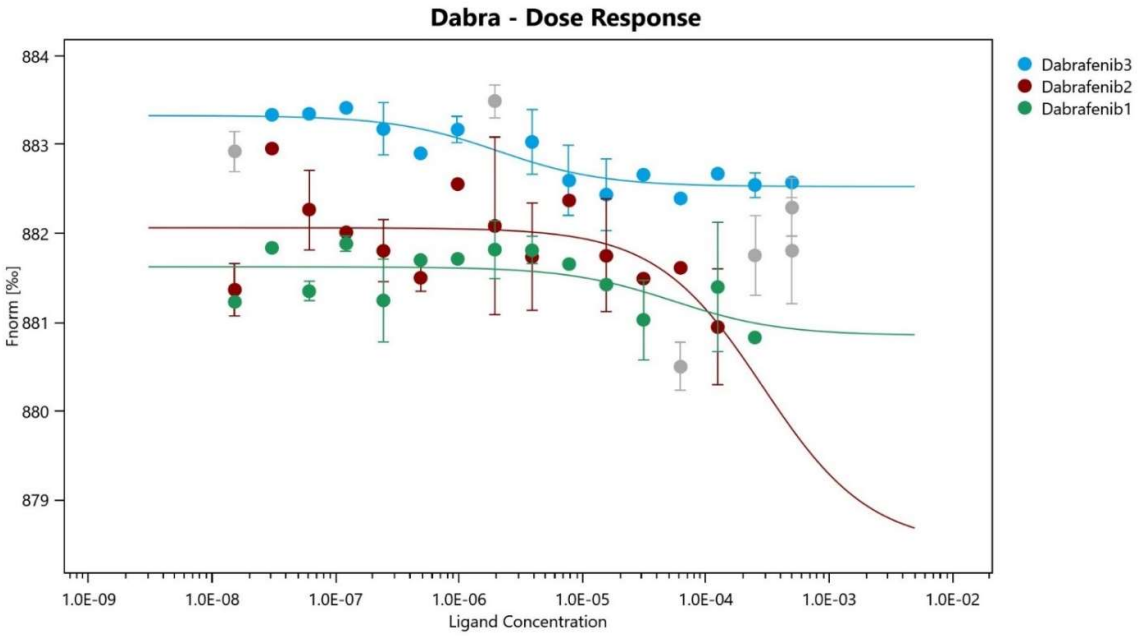

Figure 5.16: Affinity of binding of three aptamers to Dabrafenib molecule

The Dabrafenib 2 aptamer (red) induces a change (reduction) of fluorescence when it binds with the Dabrafenib molecule, while Dabrafenib 3 aptamer (blue) and Dabrafenib 1 aptamer (green) induce an increase in fluorescence when they bind to the Dabrafenib molecule. In conclusion, only aptamer Dabrafenib 1 (Kd: 0.324 ± 0.23 nM) and aptamer Dabrafenib 2 (Kd: 0.153 ± 0.23 nM) bind in nM range, while aptamer Dabrafenib 3 (Kd: 2.016 ± 0.23 uM) binds in uM, so aptamer Dabrafenib 2 binds the strongest, followed by aptamer Dabrafenib 1.

Chapter Six: Selection of Aptamer for Venetoclax

Chapter Six: Selection of Aptamer for Venetoclax

6.1 Immobilization of Venetoclaxon NHS-Activated Sepharose Beads

Venetoclax, a small molecule with a molecular weight of 868.4 g/mol, is insoluble in ethanol and water. However, it is soluble in organic solvents such as DMSO. Selection of high-affinity small-molecule-binding aptamers is often complicated and requires a specific design and consideration of all experimental conditions. Amongst the important steps for a successful SELEX protocol is the stable immobilization of the molecule analyte on a solid matrix. This attachment enables the partitioning of analyte bound from unbound DNA during the selection cycles. Since the Venetoclax chemical structure contains amino radical, the commercial NHS activated sepharose beads have been chosen as a solid matrix for target immobilization (Figure 6.1).

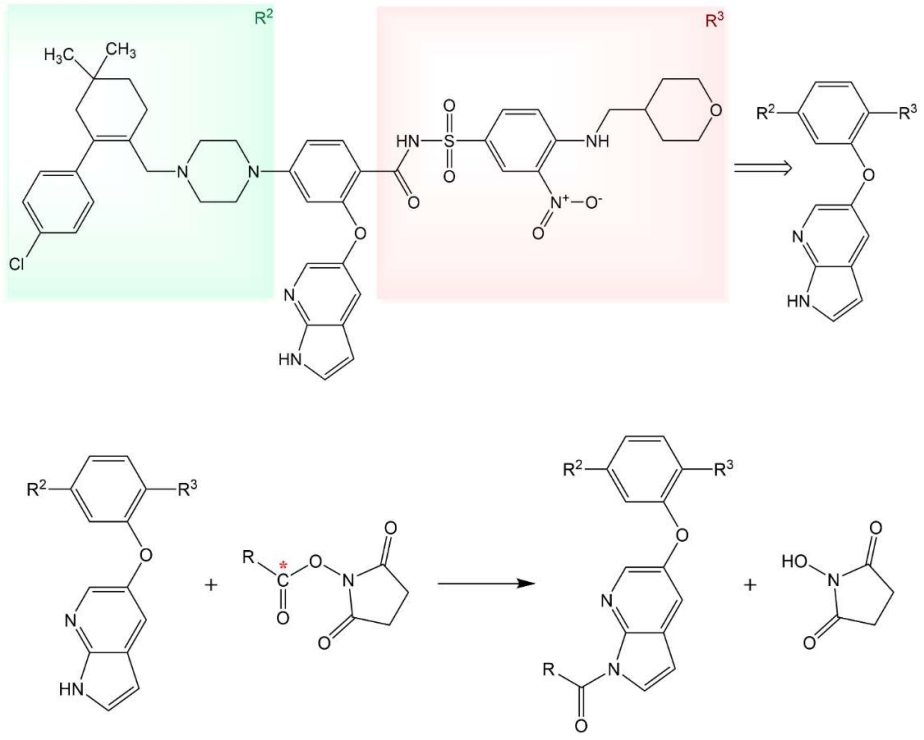

Figure 6.1: Mechanism of chemical reaction/binding between Venetoclax and NHS-activated beads

6.2 Selection of Venetoclax Aptamers using SELEX

After the immobilization of Venetoclax on the sepharose beads, they were used for SELEX rounds. Each round of selection was performed by incubating Venetoclax beads with an ssDNA library containing around 10^{15} random sequences, removal of unbound DNA by washing steps, elution of Venetoclax beads bound DNA, desalting and PCR amplification of the eluted DNA and finally, purification of the dsDNA PCR product to separate ssDNA sequences. By performing this selection cycle, a DNA pool obtained higher-affinity sequences to the target than the initial library used afterwards to start the subsequent SELEX cycle. This process was repeated for 10 rounds, as presented in the recovery graph (Figure 6.2)

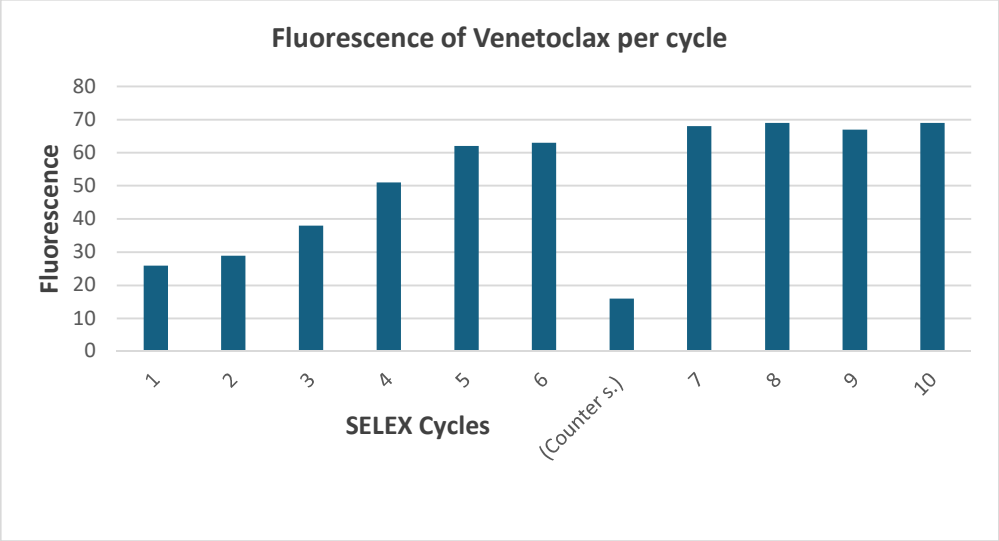

Figure 6.2: Fluorescence of Venetoclax per cycle

(Fluorescence recovery graph of the bound ssDNA eluted from Venetoclax conjugated sepharose beads in each SELEX cycle: cycle number versus the fluorescence intensity of the eluted DNA)

A significant increase of the DNA recovery with each progressive cycle of the selection was indicative of the enrichment of Venetoclax binding ssDNA. The counter selection step (CS) was performed after the sixth round to eliminate the non-specifically bound ssDNA to the sepharose beads; a drop in the fluorescence intensity was noted, as shown in Figure 6.2. After counter selection, four more cycles of SELEX were undertaken to reach the fluorescence intensity plateau. The constant fluorescence recovery after 10 cycles indicates that the target binding sites are saturated and no more sites are available for binding. Once the binding amount reaches a plateau between consecutive cycles, the pool is considered 'enriched' for Venetoclax; then, the selection cycles were stopped and the DNA was eluted and cloned.

Amplification of DNA eluted during SELEX rounds was preceded by running PCR, then 10% denaturing PAGE was performed to separate two DNA strands (Figures 6.3-6.12). Clear and well-defined bands are evident at 100 bp that correspond to ssDNA.

The ssDNA was extracted from the resulting gel bands which were processed and quantified by UV and used for the subsequent SELEX round.

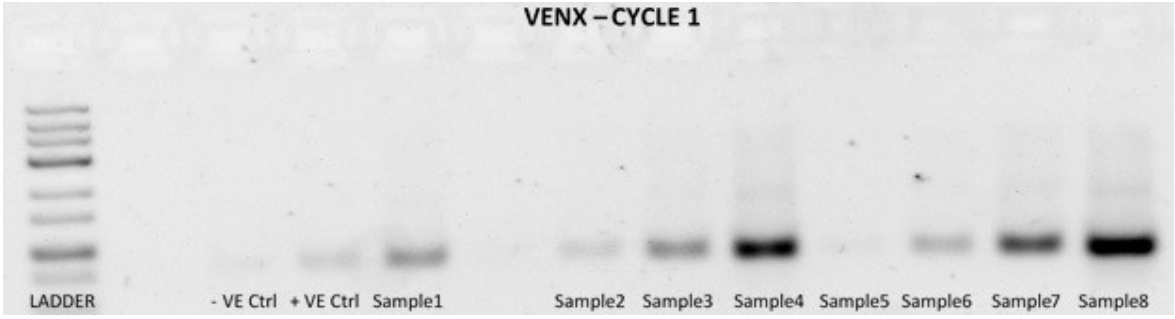

Figure 6.3: SDS-PAGE gel with -ve control, +ve control and different lots of Venetoclax (VENX) sample obtained from SELEX cycle 1

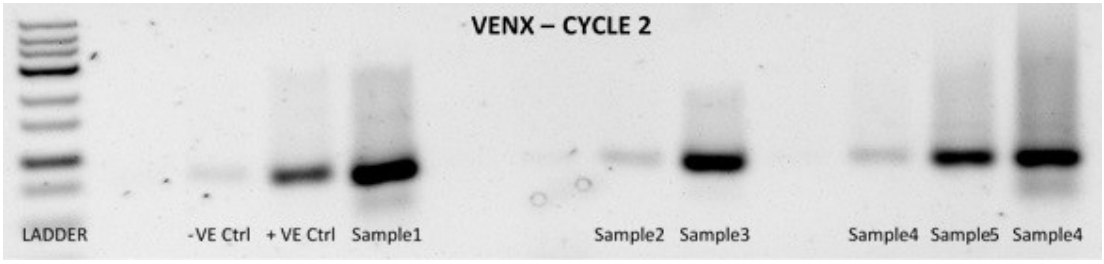

Figure 6.4: SDS-PAGE gel with -ve control, +ve control and different lots of Venetoclax (VENX) sample obtained from SELEX cycle 2

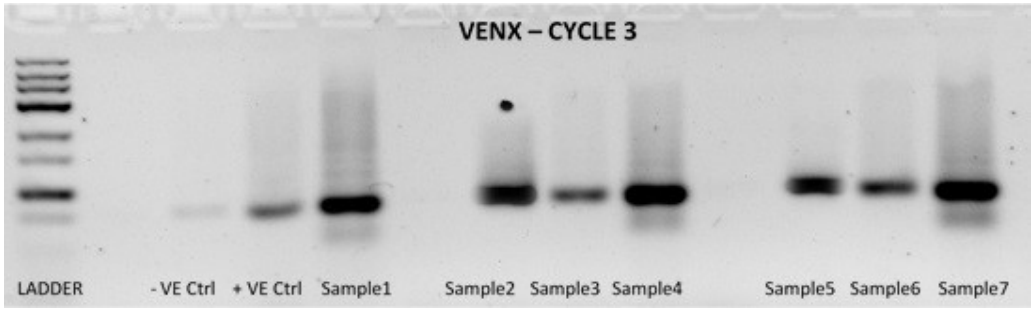

Figure 6.5: SDS-PAGE gel with -ve control, +ve control and different lots of Venetoclax (VENX) sample obtained from SELEX cycle 3

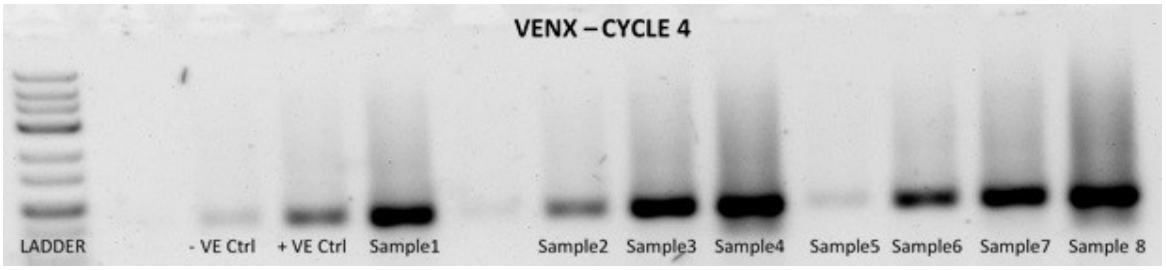

Figure 6.6: SDS-PAGE gel with -ve control, +ve control and different lots of Venetoclax (VENX) sample obtained from SELEX cycle 4

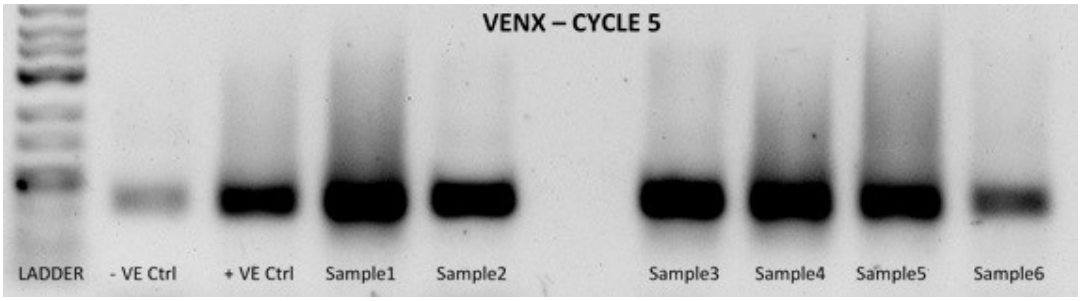

Figure 6.7: SDS-PAGE gel with -ve control, +ve control and different lots of Venetoclax (VENX) sample obtained from SELEX cycle 5

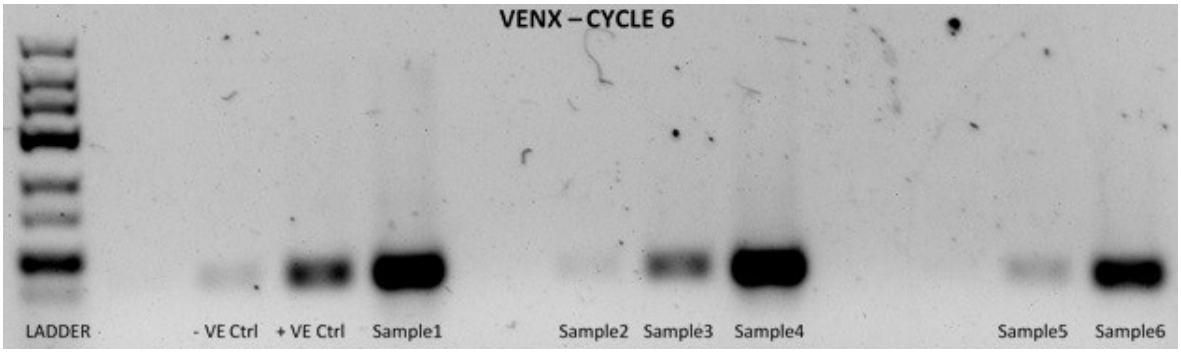

Figure 6.8: SDS-PAGE gel with -ve control, +ve control and different lots of Venetoclax (VENX) sample obtained from SELEX cycle 6

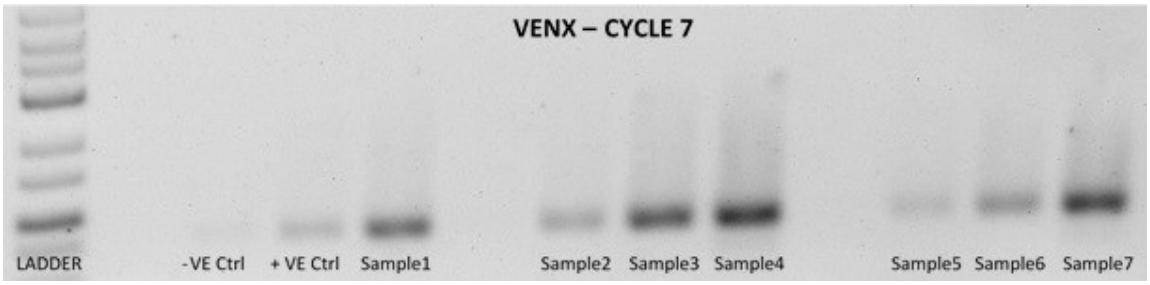

Figure 6.9: SDS-PAGE gel with -ve control, +ve control and different lots of Venetoclax (VENX) sample obtained from SELEX cycle 7

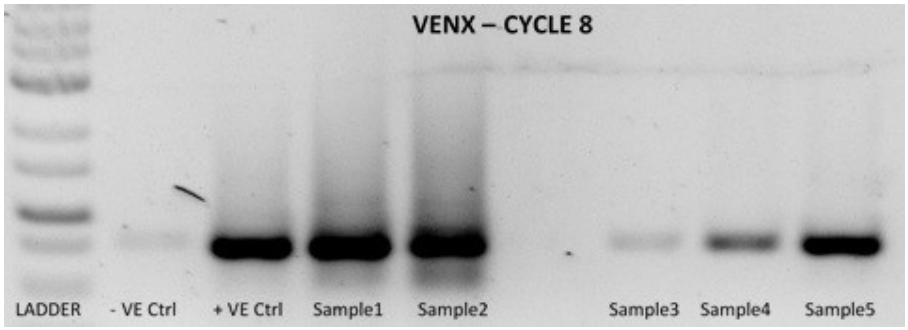

Figure 6.10: SDS-PAGE gel with -ve control, +ve control and different lots of Venetoclax (VENX) sample obtained from SELEX cycle 8

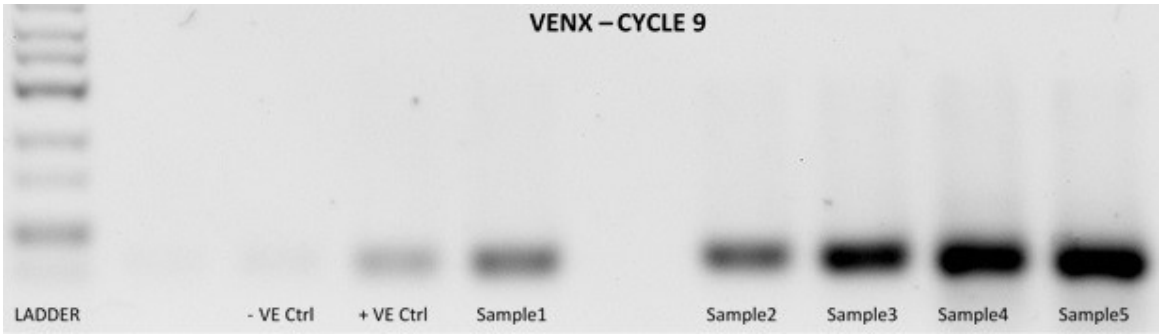

Figure 6.11: SDS-PAGE gel with -ve control, +ve control and different lots of Venetoclax (VENX) sample obtained from SELEX cycle 9

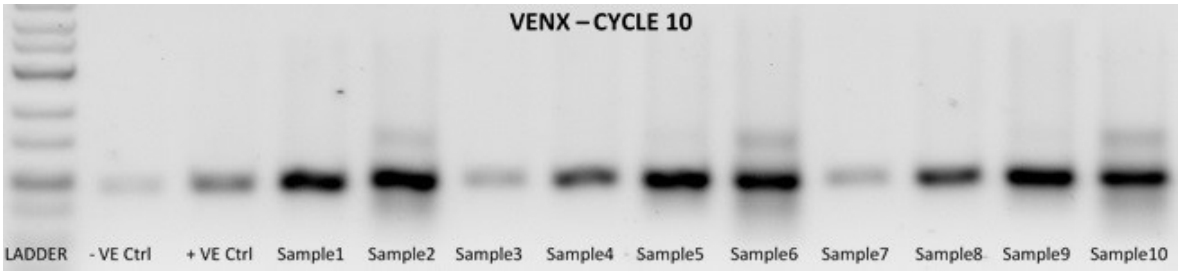

Figure 6.12: SDS-PAGE gel with -ve control, +ve control and different lots of Venetoclax (VENX) sample obtained from SELEX cycle 10.

The SELEX cycle for selection aptamer for the Venetoclax molecule is summarized and demonstrated below in Figure 6.13.

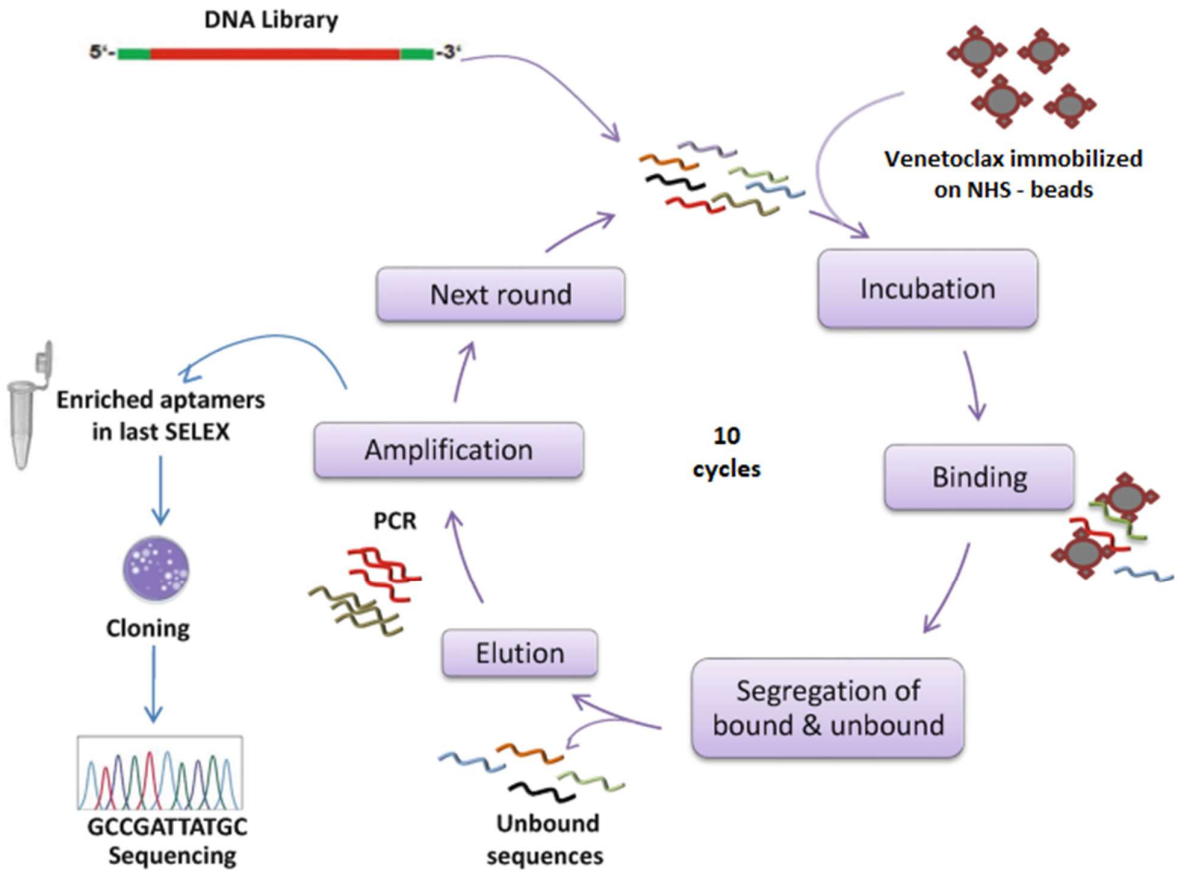

Figure 6.13: SELEX steps for Venetoclax

6.3 Cloning and Sequencing of Venetoclax Aptamers

DNA cloning was performed by ligation into a cloning vector and then transformed into DH5α-T1 competent cells. After growing the cells for 24 hours, 22 colonies containing the DNA inserts were collected individually (see Figure 6.14).

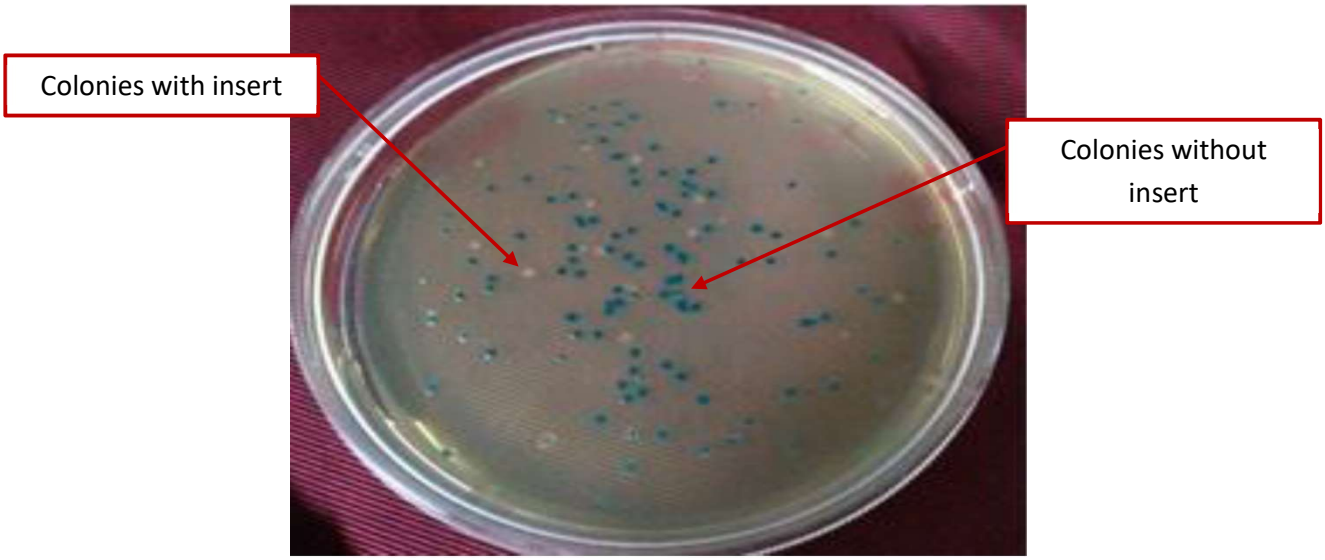

Figure 6.14: Transformed E. coli DH5α with and without ssDNA inserts: white colonies are with ssDNA while blue colonies are without

Thereafter, PCR amplification was performed to check the size using 2% agarose gel electrophoresis. Of these colonies, eight confirmed the correct size (300 bp) and were Sanger-sequenced, as shown in Figure 6.15 below.

Figure 6.15: Gel electrophoresis (2% agarose) of PCR (white colonies) using M13 forward and reverse primers

The identified sequences showed some identical sequences, indicating enrichment of the DNA pool. The DNA sequences that were obtained were imported into the Geneious software for analysis. The software was used to pair and merge the sequences amplified by the forward and reverse primers to form dsDNA. The sequences that showed non-complementary forward and reverse sequences were discarded and considered background noise. The complementary DNA strands were extracted based on the length of the library pool used during SELEX. The forward primer sequence was used as a reference when the merged sequences were blasted to identify aptamers with similar sequences. The sequences with the correct nucleotide sequences at the 5' end were isolated from the sequences that lacked the correct nucleotide sequence at the 3' end. Sequences were then truncated to select only the regions of the aptamers that appeared enriched to the target during SELEX. Aptamers shown in Table 6.1 were then tested for binding to Venetoclax molecule.

Table 6.1: List of isolated ssDNA aptamers to Venetoclax

Aptamer name	Sequence	E - value
VENX - 1	TTGTAGCACGGTGGCTCCCTACGGCGCCGCTAACCGCGCGCGCGGTGTGGCGCGC GCGCAAGCGCGT	1.3e-41
VENX - 2	TAACGCGCTTCGCGCGCGCGCGCGCGCGCGCGCGCGTCCCTACGGCGCCGCTA ACTTGTAGCACGG	2.0e-41
VENX - 3	GTTGTAGCACGGTGGCCGCGCGCGCGGGGTGACGCGCCGCGGCGCGCGCTCCCT ACGGCGCCGCTAAC	1.4e-41
VENX - 4	GCCTGTTGTGAGCCTCCTAACGGGGGCAATGGGTCAACGATTCAATGGTGTCGCT TATTCTTGTCTCCC	9.2e-42
VENX - 5	ACTCTGATTTGTAGAGAAGGGGCAATGGGTCAACGATTCAATGGTGTCACTCTGA TTTGTAGAGAACAT	3.7e-42
VENX - 6	CATGCTTATTCTTGTCTCCCGCCTGTTGTGAGCCTCCTAACGGGGGCAATGGGTCA ACGATTCAATGGC	1.8e-42
VENX - 7	ATTCAATGGTGTCACTCTGATTTGTAGAGAAGGGGGCAATGTCAACGGCCTGTTG TGAGCCTCCTAAC	1.6e-41
VENX - 8	CGCAAAGAAGCAAGACAGTAAGGTATGCACACGATATAGGGCCAGGAAGATATA GGGCCATATAG	5.2e-41

6.4 Determination of Dissociation Constant

A total of eight aptamers were isolated and identified as shown in Table 6.1. Three have been selected and synthesized with Cy5 in Metabion International AG (Planegg, Germany) for the determination of dissociation constant (Kd) by microscale thermophoresis (MST). Around 10 µl (of 50 nM working stock) of the Cy5 aptamer was transferred into 2 PCR tubes. Afterward, 10 µl of MST buffer was transferred into each tube, mixed by micropipette. The obtained mixture in each PCR tube was incubated for five minutes at room temperature in a dark place before loading the solution into the MST capillaries. Afterward, 20 µl of a 3.2 µM Venetoclax solution of compound was transferred into tube 1 then 10 µl of dilution (i.e., MST buffer) transferred into PCR tubes 2 to 16.

A serial dilution (1:1) was prepared by transferring 10 µl from tube to tube (from tube 1 to tube 16) and mixed by pipetting up and down. 10 µl from tube 16 was discarded to obtain an equal volume of 10 µl for all samples.

Afterwards, 10 µl of Cy5 aptamer (50 nM) was added to each tube from 16 to 1 and mixed by pipette, then the mixture in each PCR tube was incubated for five minutes at room temperature in a dark place before loading the solution into the MST capillaries.

The experiment was repeated in triplicate (three independent triplicates) and the results analysed using MO-Affinity Analysis software (version 2.1.3, Nano Temper Technologies) to calculate the binding affinities of the aptamers to the compound (i.e., Venetoclax) expressed in Kd values.

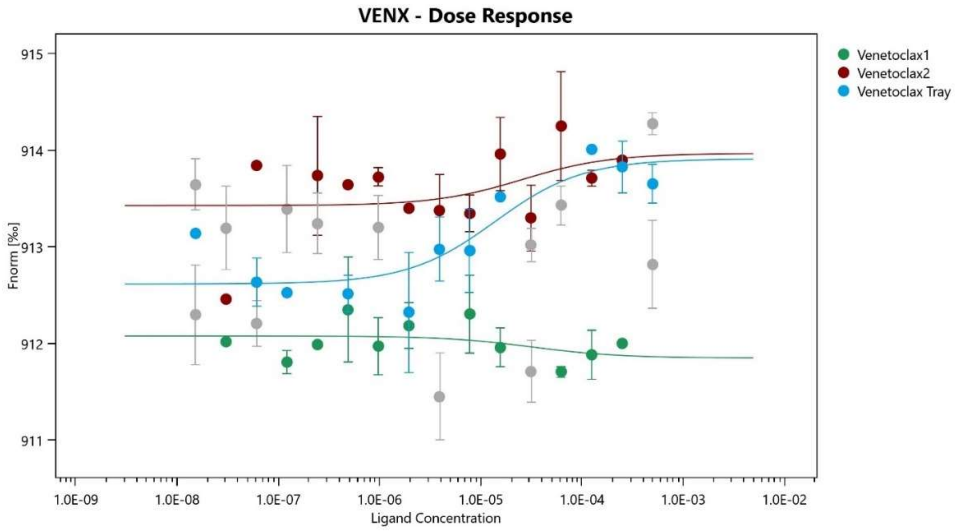

Figure 6.16: Affinity of binding of three aptamers to Venetoclax molecule

The Venetoclax 1 aptamer (green) induces a change (reduction) of fluorescence when it binds with the Venetoclax molecule, while Venetoclax 2 aptamer (red) and Venetoclax 3 aptamer (blue) induce an increase in fluorescence when they bind to the Venetoclax molecule. In conclusion, only aptamer Venetoclax 1 (Kd: 29.06 ± 0.28 nM) and aptamer Venetoclax 2 (Kd: 11.66 ± 0.24 nM) bind in nM range, while aptamer Venetoclax 3 (Kd: 13.87 ± 0.29 uM) binds in uM. Aptamer Venetoclax 2 binds the strongest, followed by aptamer Venetoclax 1.

Chapter Seven: Discussion, Conclusion and Future Work

Chapter Seven: Discussion, Conclusion and Future Work

7.1 Discussions

7.1.1 Aptamers as Recognition Receptors in Small Molecule Biosensors

It is a general perception that nucleic acids are the source of storage for genetic code information and are thought to be less complex than proteins. Nonetheless, like proteins, nucleic acids have the potential to perform multiple functions such as gene regulations, bio-catalysis and molecular interactions by secondary and tertiary folding conformations. These types of nucleic acids are called functional nucleic acids. For example, the non-coding ribonucleic acids (RNAs) exhibits a catalytic or binding properties. Many researchers revolutionized the molecular recognition from the synthetic nucleic acid motifs that bind to the target molecules specifically. These functional nucleic acids are called aptamers, which are selected from SELEX. Synthetic aptamers bind to their target with very specific and high sensitivity. However, invitro selection of an aptamer against small molecules is difficult and tedious due to the immobilization of molecules on the solid surfaces and the inactivation of molecular functionality after immobilization.

7.1.2 Challenges in Aptamer Selection Against Small Molecules

Selection of target-specific aptamers for small molecule targets is challenging. The isolation of high-affinity aptamers from the non-specific large quantities of ssDNA library pool of oligonucleotide sequences is crucial in SELEX processes. In the case of protein targets, the separation of bound aptamers from the unbound aptamers can be achieved easily. For example, nitrocellulose filters retain protein on the surface due to their hydrophobicity and the nature of nucleic acid permeability allows to separate the bound aptamers from the target. However, this kind of partitioning is not possible for small molecules. Therefore, a primary complication occurs in immobilizing the small molecule targets in a solid matrix such as sepharose beads, magnetic beads and acrylic beads for an efficient separation of specific aptamers from non-specific sequences. A variety of commercially available functional beads are available for the immobilization of small molecule targets by multiple bioconjugation methods.

Another dispute in the bioconjugation process depends on the presence of functional groups in the targets for coupling reactions. If the target has no desired functional group for coupling, it will complicate the SELEX processes. In addition, the aptamers selected against the target molecule, in which the bioactive functional group was used for the bioconjugation, lead to a

reduction in the binding affinity or non-specific to the targets. In other words, the aptamer selected against the bioconjugate targets may not be specific and sensitive to the unconjugated targets. Therefore, validation of the selected aptamer with the real sample is important for field applications. Finally, the design and fabrication of aptamer-based biosensors for the detection of small molecules will be an important part for the application point of view. In most cases, signal strength depends on the change in the conformation of the aptamer upon binding the target. Unlike large targets (proteins, lipids, exosomes and whole cells), the magnitude of a small molecule inducing conformation changes is less. Thus, additional signal amplification materials such as nanomaterials will be necessary for efficient aptasensors for small molecule detection. Four different antitumour drugs (small molecules) were used as a target for the selection of aptamers.

7.1.3 Immobilization of Drugs on NHS-Activated Sepharose Beads

Antitumour drugs such as Lenalidomide, 6-Mercaptopurine, Dabrafenib and Venetoclax are important drugs for treating various cancer cells. In vitro selection of highly specific and sensitive aptamers against these small molecule drugs will be adopted to construct a low-cost, rapid, user-friendly biosensor for point-of-care treatment (POCT). As the first step of the SELEX process, we immobilize the drugs on the sepharose beads which act as a solid supporting matrix for partitioning the bound ssDNA aptamers from unbound sequences. All four drugs have functional groups that can undergo coupling reactions with the N-Hydroxy succinimide (NHS) activated beads by EDC-NHS chemistry. In general, an EDC-NHS coupling reaction occurs between the carboxylic acid and amine functional groups in an aqueous medium at an optimal pH without affecting the other functional groups in the reactants. The drugs are not freely soluble in aqueous media; therefore, we used a mixture of organic solvent and water or buffer (DMSO/water). The functional group in the drugs reacts with NHS-activated beads in slightly basic pH in an amine-free coupling buffer to avoid any coupling reaction between the NHS and the buffer. Most reactions are carried out at 4 °C to retain the activity of the drug as is. The primary amine in Lenalidomide and Dabrafenib was involved in the coupling reaction with the activated NHS group on the sepharose beads, whereas the secondary amine in the five-membered ring of 6-Mercaptopurine and Venetoclax are involved in the coupling reaction with the activated NHS group on the sepharose beads. After completion of the coupling reaction, the unreacted NHS active sites are quenched by reaction with the ethanolamine. The NHS deactivation step significantly reduces the non-specific adsorption of ssDNA oligonucleotides in the sepharose beads.

7.1.4 In vitro Selection of ssDNA Aptamers Against Drugs by SELEX Processes

In vitro selection of drug-specific aptamers by SELEX processes was achieved by multiple steps as illustrated in the schematic diagram. In the first step, a pool of 10^{15} oligonucleotide sequences were incubated with the drug-conjugated beads. The ssDNA oligonucleotide sequences consist of 40 random sequences in the middle and 16 fixed primer binding sites at both 3' and 5' ends. The forward and reverse primers are modified with FITC and HEGL-polyA20, respectively. The FITC is used for the quantification of DNA recovery and HEGL-polyA_{20} prevents PCR elongation. The second step is the removal of non-specific or unbound sequences by washing with wash buffer. In the third step, the high affinity target bound aptamers are separated using an elution buffer under a slightly harsh condition. The excess salt in the elution buffer will be desalted, followed by PCR amplification of the eluted ssDNA. The final step is the separation of ssDNA aptamer from the complementary sequences by denatured PAGE purification. Two strands of DNA from the PCR product were separated based on the difference in molecular weight.

The eluted and purified ssDNA from the previous cycle was used as a PCR amplification template. Fluorescein-labelled forward primer and HEGL-polyA20-labelled reverse primers were used for the amplification to generate a library pool for the next cycle of SELEX. The amplified PCR duplex has a fluorescein-labelled strand and a complementary strand with -HEGL-A_{20}. The DNA strand with fluorescein-labelled is the desired aptamer, which must be separated from the complementary strand. The PCR product was denatured using 50% formamide water mixture at 95 °C for 10 minutes before loading the denatured polyacrylamide gel electrophoresis. The molecular weight of the complementary sequence is much larger compared to the aptamer sequence, which leads to different mobility rates, and both bands are separated in the gel. After completion of the electrophoresis, the aptamer band was sliced under the UV-light and the ssDNA was extracted from the gel. The quantity of the ssDNA collected from the gel was quantified from the UV-visible absorption at 260 nm. In each cycle of SELEX, a constant amount of ssDNA pool was incubated with the conjugated target. After completion of the cycle, the eluted DNA was measured using the fluorescence intensity of fluorescein at 520 nm. The fluorescent ssDNA recovery of each cycle was plotted as presented in the figures. The enrichment of ssDNA with an increasing number of SELEX cycles was observed. This is the sign of an increased amount of high-affinity aptamer against the drug molecules. On the other hand, the weakly bound low-affinity aptamer sequences were washed out over the

increasing number of cycles. After five rounds of SELEX, counter SELEX was undertaken using blank beads to remove the nonspecific ssDNA that binds to the sepharose beads, the spacer between the beads and the target molecule. The major exposure areas for the ssDNA pool in the drug-conjugated beads are blank bead surface and spacer between the beads and the target. Therefore, a major quantity of the non-specific sequences is removed, and hence the fluorescence intensity after counter-selection was significantly decreased. After few rounds of SELEX, the fluorescence intensity increased and attained a plateau, indicating the saturation of binding sites in the beads. After 10 rounds, the elected ssDNA was amplified with unlabelled forward and reverse primers. The PCR-amplified product was used for cloning.

7.1.5 Cloning and Sequencing

The purified ssDNA collected from the last rounds of SELEX was amplified with unmodified forward and reverse primers. 2μL of the PCR product was used for the ligation with the TOPO cloning vector (according to the manufacturer protocol). After completion of the ligation reaction, the ligated product was transformed into an E. coli DH5α competent cell by heat shock method using a water bath at 42 °C. The product was incubated overnight on LB agar plates containing X-GAL. Depending upon the PCR product inserted in the plasmid, the colour of the colonies appeared either white or blue. White colonies are with insert and blue colonies are without insert, as illustrated in the figures. The LacZ gene in the plasmid produces β-galactosidase during the bacterial culture. Restriction enzymes, used to cut the gene, act as a ligation site for the last round SELEX PCR products. The PCR product was inserted between the LacZ gene, the β-galactosidase enzyme production was inhibited, and the colonies with inserts are colourless. However, the plasmid without inserting (self-ligated) is blue in colour.

The mechanism of blue colony formation has been explained as follows: β-galactosidase produced from LacZ gene cleave -Gal (5-bromo-4-chloro-3-indolyl-β-d-galactopyranoside) and produce 5-bromo-4-chloro-3-hydroxyindol, which undergo a dimerization reaction in the presence of oxygen and produce a blue coloured (5,5'-Dibromo-4,4' dichloroindigo) product. More than 25 white colonies were picked up and subject to colony PCR using M13 forward and reverse primers. The products are sequenced and the extracted ssDNA sequences were aligned using Clustal-Omega programme (Version 1.2.2). software to classify the various groups of sequences.

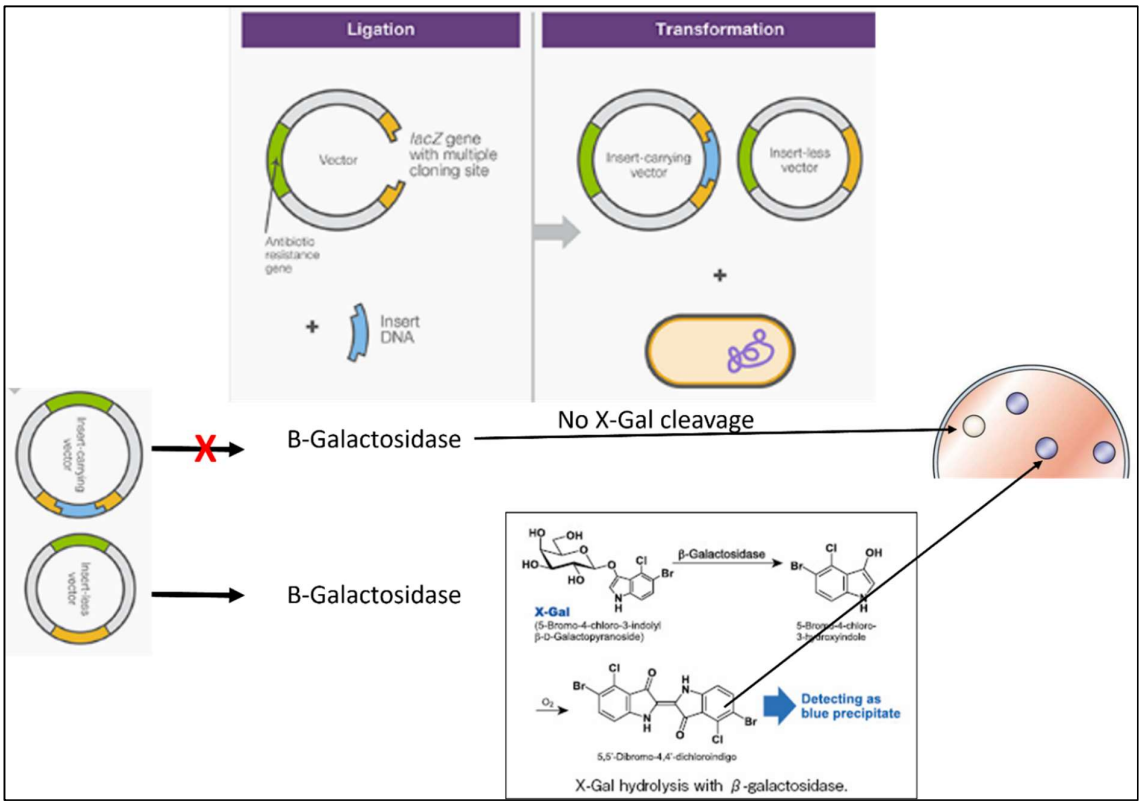

Figure 7.1: Principles and mechanism of cloning and β-galactosidase activity on X-Gal

7.1.6 Dissociation Constant (Kds)

The affinity of the selected aptamer for the target molecule is a curtailed parameter as a recognition element for the development of biosensors. Therefore, the determination of affinity or the dissociation equilibrium constant is important. The dissociation constant (Kd) is a kinetic parameter used to measurement of binding affinity between a single biomolecule (e.g., DNA) to its binding partner (e.g., a drug) driven by biophysical attractions (Jarmoskaite et al., 2020). The strength of the binding affinity is typically measured by the equilibrium dissociation constant (Kd), which is used to evaluate and rank order strengths of bimolecular interactions. A low Kd value indicates that two molecules are highly attracted to each other, while a high Kd value indicates that attraction is weak (Stangherlin et al., 2025).

Understanding binding affinity is key to appreciating the intermolecular interactions driving biological processes, structural biology and structure-function relationships.

Whenever characterizing ssDNA is the first step in developing the new aptamers, understanding their binding affinity to the drug molecule is key to appreciating their

intermolecular interactions, which will help to design aptamers that bind their targets selectively and specifically (Krylov, 2024).

There are several methods available for the determination of the dissociation constant. The microscale thermophoresis (MST) method has been used for the calculation of Kd. The selection of the three aptamers for each molecule was based the best value in Kd and on the financial budget for the research.

Three different aptamer candidates selected against Lenalidomide were used for the calculation of Kds. The calculated Kd values for aptamers, Lenalidomide 1, Lenalidomide 2 and Lenalidomide 3 are 653.46 ± 0.23 nM, 15.18 ± 0.37 nM and 7.75 ± 0.09 nM, respectively. Lower values of Kd represent the high affinity of the aptamer for the target. Among the three ssDNA Lenalidomide aptamers, Lenalidomide 3 showed a high affinity of 7.75 ± 0.09 nM, indicating that Lenalidomide 3 affinity constant in the nanomolar range is excellent at binding with the Lenalidomide drug. This sequence can be used for the construction of aptamer-based biosensors.

There are three aptamers selected for the determination of dissociation constant for 6-Mercaptopurine namely Mercaptopurine 1, Mercaptopurine 2 and Mercaptopurine 3. The Kd values calculated from the Microscale thermophoresis (MST) Mercaptopurine 1, Mercaptopurine 2 and Mercaptopurine 3 are 2.30 ± 0.22 nM, 46.8 ± 0.23 nM and 0.1552 ± 0.37 nM, respectively. The aptamer Mercaptopurine 3 has an outstanding affinity for 6-Mercaptopurine. This would be an ideal sequence for the development of aptamer-based sensors for the sensitive detection of 6-Mercaptopurine.

Similar to the other two drugs, three different aptamers of Dabrafenib were tested for Kd values. Two aptamers, Dabrafenib 1 and Dabrafenib 2, have 0.324 ± 0.23 nM and 0.153 ± 0.23 nM, respectively. However, Dabrafenib 3 has a low affinity of 2.016 ± 0.23 µM.

Finally, the Kd values of Venetoclax aptamers were determined to be 29.06 ± 0.28 nM, 11.66 ± 0.24 nM and 13.87 ± 0.29 µM for Venetoclax 1, Venetoclax 2 and Venetoclax 3, respectively. Despite a few aptamers with a low affinity in the micromolar range, there are other sequences with extraordinary affinities in the sub-nanomolar range. These candidates would be used for the construction of highly specific and sensitive aptamer-based biosensors for the detection of target drugs.

Table 7.1: Summary of affinity constants for the aptamers selected against Lenalidomide, 6-Mercaptopurine, Dabrafenib and Venetoclax drugs

Aptamer name	Kd (nM)
Lenalidomide 1	653.46 ± 0.23
Lenalidomide 2	15.18 ± 0.37
Lenalidomide 3	7.75 ± 0.09
6-Mercaptopurine 1	2.30 ± 0.22
6-Mercaptopurine 2	46.8 ± 0.23
6-Mercaptopurine 3	0.1552 ± 0.37
Dabrafenib 1	0.324 ± 0.23
Dabrafenib 2	0.153 ± 0.23
Dabrafenib 3	2016 ± 230
Venetoclax 1	29.06 ± 0.28
Venetoclax 2	11.66 ± 0.24
Venetoclax 3	13870 ± 290

There are still several parameters and factors that need to be investigated or applied, starting with the utilizing more than one DNA library with specific features to ensure high purity and yield of amplified libraries. Among other factors, immobilizing the drug molecules via carboxyl groups or epoxy modified beads to see whether the orientation of immobilized drug molecule can affect the selection of aptamers.

In addition, the type of partitioning, method for generation of ssDNA (e.g. lambda exonuclease digestion and magnetic separation), change more than one binding buffer used in selection process and the effect of changes in temperature or pH for some steps of the selection on the yield ssDNA

7.2 Conclusion

Lenalidomide is one of the medicines approved to treat adults with multiple myeloma (MM). 6-Mercaptopurine has been approved to treat acute lymphocytic leukaemia (ALL). Dabrafenib is a cancer growth blockers used to treat melanoma. Venetoclax is one of the targeted cancer medicines approved to treatment of chronic lymphocytic leukaemia (CLL) and acute myeloid leukaemia (AML). All four anti-tumours are commonly used today in Saudi Arabia and worldwide for treatment specific cancer cases, but they cause several adverse effects such as blood clots, heart failure, white blood cell drop, shortness of breath, high blood sugar and changes in liver function; therefore, therapeutic drug monitoring is recommended for patients who are treated with Lenalidomide, 6-Mercaptopurine, Dabrafenib or Venetoclax.

Conventional methods such as HPLC, mass spectroscopy, ELISA, radioimmunoassay, immunobinding, fluorescence polarization immunoassay (FPIA) and enzyme immunoassay (EMIT) are used for the therapeutic drug monitoring (TDM). Despite the high accuracy and

specificity of HPLC and mass spectrometry, they have certain limitations such as excessive cost and bulky instruments associated with laboratory-based analysis. This is inconvenient for the point of care testing of patients in limited resource settings. In addition, because of the high cost of this testing, developing and underdeveloped nations cannot offer these methods. The other techniques such as ELISA, EMIT and FPIA are associated with antibodies. Antibodies are produced from animals and the sensitivity and specificity of the antibodies varies batch to batch, potentially causing variation in a sample analysis report. Moreover, antibodies are thermally unstable, and storage and transportation are complicated. However, aptamer-based assay overcomes all these limitations. Therefore, aptamer-based therapeutic drug monitoring (TDM) would be more accurate and more specific. Based on these points, we have selected highly sensitive and specific aptamers against these drugs.

This research focussed on selecting and characterizing DNA aptamers for the monitoring of Lenalidomide, 6-Mercaptopurine, Dabrafenib and Venetoclax by systematic evolution of ligands through an exponential enrichment (SELEX) approach. Several aptamer candidates that exhibited the ability to bind to Lenalidomide, 6-Mercaptopurine, Dabrafenib and Venetoclax were identified. Three ssDNA aptamers have been selected for each medicine and their binding affinity (i.e., the dissociation constant [Kd]) was measured and evaluated by microscale thermophoresis (MST). This work reports the first oligonucleotide aptamers selected for Lenalidomide, 6-Mercaptopurine, Dabrafenib and Venetoclax with Kd in the nanomolar range. These aptamers can be used for both basic research and clinical purposes. The sub-nanomolar range of Kds indicate that these aptamers have very high affinity for their respective drugs. These aptamers could be an emerging molecular recognition receptor for the construction of highly specific and very sensitive aptamer-based biosensors for therapeutic drug monitoring applications.

7.3 Future Work

The high affinity aptamer from each drug will be further studied for the development of either optical or electrochemical biosensing applications. Aptamers are chemical antibodies that replace the antibodies produced from animal immunization. Constriction of aptamer-based biosensors is uncomplicated compared to antibody-based biosensors.

Customized functional group conjugated aptamers can be synthesized and purchased from many suppliers in the markets depending upon the requirements. Initially, we will be focused on developing aptamers-based electrochemical biosensors and testing their ability to measure Lenalidomide, 6-Mercaptopurine, Dabrafenib and Venetoclax individually in vitro and vivo condition. The construction of the aptasensor should be followed by electrochemical measurements of the square wave voltammetry (SWV). Selection of the highest affinity (lowest Kd) to Lenalidomide, 6-Mercaptopurine, Dabrafenib and Venetoclax to develop a competitive aptasensor should also constitute future research. For electrochemical aptasensor construction, a thiolated high-affinity aptamer will be immobilized on the gold electrode surface. The immobilization of the aptamer on the electrode surface will be monitored for electrochemical signal changes compared to the bare electrode. After optimization of the electrode, a variable concentration of target drugs will be added. The variation in the electrochemical signal in the presence of the drugs will be proportional to the concentration of the analytes present in the sample. The change in the electrochemical signal will be plotted against the quantity of drugs added into the measuring solution. A linear plot will be obtained, indicating the linear relationship between the drug concentration and the electrochemical signal intensity. The limit of detection (LOD) of the developed biosensor will be calculated from the given formula:

$$LOD = \frac{3.3\sigma}{S}$$

Where σ = standard deviation of the electrochemical signal in the absence of analyte; and S = slope of the linear plot.

The specificity of the developed sensor against the target analyte will be tested using similar functional or structured molecules. Electrochemical signal changes in the biosensor due to the presence of nonspecific molecules indicates the cross reactivity of the developed aptasensors. The least cross-reactivity with the non-specific targets will indicate the best performance of the biosensor. Finally, the newly developed sensor will be validated with real samples. A number of patient samples treated with these drugs will be collected and quantified from these biosensors. The real sample analysis report from this method will be compared to the standard method for the accuracy of this method.

In the end, we will apply a paper-based point of care testing (POCT) approach for testing the patient at home. A gold nanoparticle conjugated aptamer will be used for developing the control line and test line. Partial complementary DNA will be immobilized on the test line and a

complete complementary sequence will be immobilized on the control line. In the presence of a target-positive sample, the aptamer binds to the target tightly and will not hybridize with the partial complementary DNA. Thus, there is no colour change on the test line. However, in the absence of a target, the gold nanoparticle conjugated aptamer hybridizes with the particle complementary on the test line and turn its from colourless to red. This rapid, low-cost, highly sensitive, more specific miniaturized point of care testing tool will be an ideal device for TDM, specifically for patients located in remote areas with limited access to laboratory-based analysis.

References

6-mercaptopurine future-proof strategies: Trends, Competitor Dynamics, and opportunities 2025-2033. Comprehensive Market Research & Forecast Analysis. http://www.datainsightsmarket.com/reports/6-mercaptopurine-1050001.

Abraham, J., Allegra, C.J. 2001. Bethesda handbook of clinical oncology. Lippincott Williams & Wilkins: Philadelphia.

Aghai, F. et al. 2021 'Development and validation of a sensitive liquid chromatography tandem mass spectrometry assay for the simultaneous determination of ten kinase inhibitors in human serum and plasma.' Anal. Bioanal. Chem., 413, 599–611.

Albertioni, F., Pettersson, B., Ohlman, S., Peterson, C. 1995 Analysis of azathioprine and 6-mercaptopurine in plasma in renal transplant recipients after administration with oral azathioprine. J. Liq. Chromatogr. Relat. Technol., 18, 3991–4004.

Al-Ghobashy, M.A. et al. 2016 Development and validation of LCMS/MS assay for the simultaneous determination of methotrexate, 6-mercaptopurine and its active metabolite 6-thioguanine in plasma of children with acute lymphoblastic leukemia: correlation with genetic polymorphism. J. Chromatogr. B, 1038, 88–93.

Alhabbab, R.Y. In: Basic serological testing 2018 'Radioimmunoassay (RIA)': 77–80.

Ardolino, M., Hsu, J., Raulet, D.H. 2015 Cytokine treatment in cancer immunotherapy. Oncotarget, 6, 19346–19347.

Bailey, D.G., Wilson, T.W., Johnson, G.E. 1975 A gas-chromatographic method for measuring 6-mercaptopurine in serum. J. Chromatogr., 111, 305–310.

Baktır, G. 2017 'Therapeutic drug monitoring (TDM).' Lectio Sci., 1, 54–65.

Balakirouchenane, D. et al. 2021 'Simultaneous quantification of dabrafenib, hydroxy-dabrafenib and trametinib in human plasma by liquid chromatography-tandem mass spectrometry.' J. Pharm. Biomed. Anal., 193, 113718.

Balch, C.M., et al 2009 Final version of 2009 AJCC melanoma staging and classification. J. Clin. Oncol., 27, 6199–6205.

Bavi, Rohit, et al. "In silico designed RNA aptamer against epithelial cell adhesion molecule for cancer cell imaging." *Biochemical and biophysical research communications* 509.4 (2019): 937-942.

Beechinor, Ryan J., et al. "The story of the development of generic lenalidomide: How one company thwarted the Hatch-Waxman Act to generate billions of dollars in revenue." *Journal of Cancer Policy* 38 (2023): 100446.

Belaiche, J., Desager, J.P., Horsmans, Y., Louis, E. 2001 Therapeutic drug monitoring of azathioprine and 6-mercaptopurine metabolites in Crohn's disease. Scand. J. Gastroenterol., 36, 71–76.

Bergveld, P. 1970 Development of an ion-sensitive solid-state device for neurophysiological measurements. IEEE Trans. Bio Med. Eng., 17, 70–71.

Bershas, D.A. et al. 2013 'Metabolism and Disposition of Oral Dabrafenib in Cancer Patients: proposed Participation of Aryl nitrogen in carbon-carbon Bond Cleavage via Decarboxylation following Enzymatic Oxidation.' Drug Metab. Dispos., 41, 2215–2223.

Bhatnagar, S. et al. 2021 'Dose adjustment of venetoclax when co-administered with posaconazole: clinical drug–drug interaction predictions using a PBPK approach.' Cancer Chemother. Pharmacol., 87, 465–474.

Birkett, D.J. 1997 Pharmacokinetics made easy: Therapeutic drug monitoring. Aust. Prescr., 20, 9–11.

Bociek, R.G., Armitage, J.O. 1996 Hematopoietic growth factors. CA Cancer J. Clin., 46, 165–184.

Borowitz, M., Bene, M.C., Harris, N.L., et al. In: Swerdlow S, Campo E, Harris NL, et al., eds. WHO classification of tumours of haematopoietic and lymphoid tissues, 4th ed. IARC: Lyon, France 2008: 149–154.

Bostrom, B., Erdmann, G. 1993 Cellular pharmacology of 6-mercaptopurine in acute lymphoblastic leukaemia. Am. J. Pediatr. Hematol. Oncol., 15, 80–86.

Brown, Alex, et al. Development of better aptamers: structured library approaches, selection methods, and chemical modifications. *Angewandte Chemie International Edition*, 2024, 63.16.

Brown, J.M. 2001 Therapeutic targets in radiotherapy. Int. J. Radiat. Oncol. Biol. Phys., 49, 319–325.

Burton, N.K., Aherne, G.W., Marks, V. 1984 A novel method for the quantitation of 6-mercaptopurine in human plasma using high performance liquid chromatography with f1uoreseenee detection. J. Chromatogr. Biomed. Appl., 309, 409–414.

Cao, Q. et al. 2023 'Mechanisms of action of the BCL-2 inhibitor venetoclax in multiple myeloma: a literature review.' Front. Pharmacol., 14, 1291920.

Cappi, G., Spiga, F.M., Moncada, Y., Ferretti, A., Beyeler, M., Guiducci, C. et al. (2015). Label-Free Detection of Tobramycin in Serum by Transmission-Localized Surface Plasmon Resonance. *Anal. Chem*. 87,5278–5285.

Cardoso, E. et al. 2018 'Quantification of the next-generation oral anti-tumor drugs dabrafenib, trametinib, vemurafenib, cobimetinib, pazopanib, regorafenib and two metabolites in

human plasma by liquid chromatography-tandem mass spectrometry.' J. Chromatogr. B Analyt. Technol. Biomed. Life Sci., 1083, 124–135.

Carelle, N. et al. 2002 Changing patient perceptions of the side effects of cancer chemotherapy. Cancer, 95, 155–162.

Celgene Inc 17 January 2008. REVLIMID® product monograph. Oakville, Ontario.

Chalmers, A.H. A spectrophotometric method for the estimation of urinary azathioprine.

Chalmers, A.H. Six-mercaptopurine, and 6-thiouric acid 1975. Biochem. Med., 12, 234–240.

Chen, C., et al. 2013 'Lenalidomide in multiple myeloma—a practice guideline.' Curr. Oncol., 20, e136–e149.

Chen, C.M., Ho, Y.H., Wu, S.M., Chang, G.L., Lin, C.H. of mercaptopurine (MP) in a PMMA biochip with on-chip gold nanoelectrode ensemble (GNEE) working and decouple electrodes 2009. J. Nanosci. Nanotechnol., 9, 718–721.

Chen, Long, et al. "In Silico discovery of aptamers with an enhanced library design strategy." *Computational and Structural Biotechnology Journal* 21 (2023): 1005-1013.

Cheung, T.S. et al. 2017 'Pharmacokinetics of the BCL-2 inhibitor Venetoclax in healthy Chinese subjects.' Clin. Pharmacol. Drug Dev., 7, 435–440.

Chow, C.S., Liu, J.P. 1999. Design and analysis of bioavailability and bioequivalence studies. (2nd ed., pp. 1-600). CRC Press: United States.

Chrzanowska, M., Sloderbach, A. 1997 Spectrophotometric determination of 6-mercaptopurine and 6-thiouric acid by means of induced iodine-azidereaction. Chim. Anal., 42, 381–385.

Chung, Saeromi, *et al*. Electrochemical carbamazepine aptasensor for therapeutic drug monitoring at the point of care. *ACS omega*, 2022, 7.43: 39097-39106.

Clark, L.C., Lyons, C. 1962 'Electrode systems for continuous monitoring in cardiovascular surgery.' Ann. N. Y. Acad. Sci., 102, 29–44.

Clarke, W. 2004 'Immunoassays for therapeutic drug monitoring and clinical toxicology.' Drug Monit. Clin. Chem., 5, 95–111.

Cremer, M. 1906 'Über die Ursache der elektromotorischen Eigenschaften der Gewebe, zugleich ein Beitrag zur Lehre von den polyphasischen Elektrolytketten. Z. Biol., 47, 562–607.

Dabrafenib 2025-2033 overview: Trends, dynamics, and Growth Opportunities. Comprehensive Market Research & Forecast Analysis. Available at: http://www.datainsightsmarket.com/reports/dabrafenib-318999.

Danesh, N. M., Ramezani, M., Sarreshtehdar Emrani, A., Abnous, K., and Taghdisi, S. M. (2016). A novel electrochemical aptasensor based on arch-Shape structure of aptamer-

complimentary strand conjugate and exonuclease I for sensitive detection of streptomycin. *Biosens. Bioelectron*. 75,123–128.

Dasgupta, A. 2016. 'Limitations of immunoassays used for therapeutic drug monitoring of immunosuppressants.' Personalized immunosuppression in transplantation. Elsevier: 29–55.

Dauphin-Ducharme, P., et al. 2019 'Electrochemical aptamer-based sensors for improved therapeutic drug monitoring and high-precision, feedback-controlled drug delivery.' ACS Sens., 4, 2832–2837.

De Nicolò, A. et al. UPLC–MS/MS method for quantification of the azathioprine metabolites 6-mercaptoguanosine and 6 - methyl mercaptopurine riboside in peripheral blood mononuclear cells 2014. J. Pharm. Biomed. Anal., 98, 271–278.

De Nicolo, A., Agnesod, D., Simiele, M., Rigan, D., Adriani, A. et al. 2016 'Venetoclax: first global approval.' Drugs, 76, 979–986.

Déglon, J., Thomas, A., Mangin, P., Staub, C. 2012 Direct analysis of dried blood spots coupled with mass spectrometry: concepts and biomedical applications. Anal. Bioanal. Chem., 402, 2485–2497.

Delaney, G., Jacob, S., Featherstone, C., Barton, M. 2005 The role of radiotherapy in cancer treatment: estimating optimal utilization from a review of evidence-based clinical guidelines. Cancer, 104, 1129–1136.

Dervieux, T. et al. 2005 Liquid chromatography-tandem mass spectrometry analysis of erythrocyte thiopurine nucleotides and effect of thiopurine methyltransferase gene variants on these metabolites in patients receiving azathioprine/6-mercaptopurine therapy. Clin. Chem., 51, 2074–2083.

DeVita, V.T. Jr, Chu, E. 2008 A history of cancer chemotherapy. Cancer Res., 68, 8643–8651.

Dolgin, E. 2016 Using DNA, radiation therapy gets personal. Science, 353, 1348–1349.

Dougherty, T.J., et al 1998 Photodynamic therapy. J. Natl Cancer Inst., 90, 889–905.

Eklind, J., Tartler, U., Maschke, J., Lidbrink, P., Hengge, U.R. 2003 August Imiquimod to treat different cancers of the epidermis. Dermatol. Surg., 29, 890–896; discussion 896.

Ellington, A.D., Szostak, J.W. 1990 In vitro selection of RNA molecules that bind specific ligands. Nature, 346, 818–822.

EMEA: European Medicines Agency Revlimid: http://www.emea.europa.eu/humandocs/PDFs/EPAR/revlimid/H-717-en6.pdf.

Emrani, A.S., Danesh, N. M., Lavaee, P., Ramezani, M., Abnous, K., And Taghdisi, S. M. (2016). Colorimetric and fluorescence quenching Aptasensors for detection of streptomycin

in blood serum and milk based on double-stranded DNA and gold nanoparticles. *Food Chem*. 190,115–121.

Ensafi, A.A., Karimi-Maleh, H. 2012 Determination of 6- mercaptopurine in the presence of uric acid using modifed multiwall carbon nanotubes-TiO2 as a voltammetric sensor. Drug Test. Anal., 4, 970–976.

Eriksson, D., Stigbrand, T. 2010 Radiation-induced cell death mechanisms. Tumour Biol., 31, 363–371.

Eshhar, Z., Waks, T., Gross, G. 2014 The emergence of T-bodies/CAR T cells. Cancer J., 20, 123–126.

Esteve-Romero, J., Albiol-Chiva, J., Peris-Vicente, J. 2016 A review on development of analytical methods to determine monitorable drugs in serum and urine by micellar liquid chromatography using direct injection. Anal. Chim. Acta, 926, 1–16.

European Medicines Agency (EMEA). Committee for Medicinal Products for Human Use (CHMP): Guideline on Bioanalytical Method Validation 2011. European Medicines Agency: London, UK.

Falchook, G.S. et al. 2014 'Dose Selection, Pharmacokinetics, and pharmacodynamics of BRAF inhibitor Dabrafenib (GSK2118436).' Clin. Cancer Res., 20, 4449–4457.

Fang, Zhihui, et al. "Aptamer screening: current methods and future trend towards Non-SELEX approach." *Biosensors* 14.7 (2024): 350.

Fay, F., Scott, C.J. 2011 Antibody-targeted nanoparticles for cancer therapy. Immunotherapy, 3, 381–393.

FDA Drugs at FDA, Revlimid: http://www.accessdata.fda.gov/Scripts/cder/DrugsatFDA/: http://www.revlimid.com/pdf/REVLIMID_PI.pdf.

FDA Food and drug Autority, Kymriah: https://www.fda.gov/vaccines-blood-biologics/cellular-gene-therapy-products/kymriah-tisagenlecleucel.

FDA Food and drug Autority, Yescarta: https://www.fda.gov/vaccines-blood-biologics/cellular-gene-therapy-products/yescarta-axicabtagene-ciloleucel.

FDA: Food and Drug Authority Imlygic: https://www.fda.gov/vaccines-blood-biologics/cellular-gene-therapy-products/imlygic-talimogene-laherparepvec.

Ferlay, J., et al. 2020 Global cancer observatory. Cancer Today. International Agency for Research on Cancer: Lyon.

Fischer, K., Al-Sawaf, O., Hallek, M. 2020 'Preventing and monitoring for tumor lysis syndrome and other toxicities of venetoclax during treatment of chronic lymphocytic leukemia.' Hematology Am. Soc. Hematol. Educ. Program, 2020, 357–362.

Flanagan, R.J., Brown, N.W., Whelpton, R. 2008 Therapeutic drug monitoring (TDM). CPD Clin. Biochem., 9, 3–20.

Fletcher, C.D., Hogendoorn, P., Mertens, F., Bridge, J. 2013. WHO classification of tumors of soft tissue and bone, 4th ed. IARC Press: Lyon, France.

Floros, T., Tarhini, A.A. 2015 Anticancer cytokines: biology and clinical effects of interferon-a2, interleukin (IL)-2, IL-15, IL21 and IL-12. Semin. Oncol., 42, 539–548.

Freise, K.J., Shebley, M., Salem, A.H. 2017 'Quantitative prediction of the effect of CYP3A inhibitors and inducers on venetoclax pharmacokinetics using a physiologically based pharmacokinetic model.' J. Clin. Pharmacol., 57, 796–803.

Gage, A.A. In: Lucas L, ed. Paris: Int. inst. referring. 140 pp 1995. History Cryosurgery: mechanisms and applications.

Galpin, A.J., Evans, W.E. 1993 Therapeutic drug monitoring in cancer management. Clin. Chem., 39, 2419–2429.

Gebski, V., Lagleva, M., Keech, A., Simes, J., Langlands, A.O. 2006 Survival effects of postmastectomy adjuvant radiation therapy using biologically equivalent doses: a clinical perspective. J. Natl Cancer Inst., 98, 26–37.

Gerber, D.E. 2008 Targeted therapies: a new generation of cancer treatments. Am. Fam. Phys., 77, 311–318.

Ghiculescu, R.A. 2008 'Therapeutic drug monitoring: which drugs, why, when and how to do it.' Australian Prescriber, 31.2.

Gibson, T. D. 1999 "Biosensors: The stabilité problem." *Analusis* 27.7: 631-638.

González-Fernández, E., de-los-Santos-Álvarez, N., Lobo-Castañón, M.J., Miranda-Ordieres, A.J., and Tuñón-Blanco, P. (2011). Impedimetric aptasensor for tobramycin detection in human serum. *Biosens. Bioelectron.* 26, 2354–2360.

Gopinath, S.C.B. 2007 Methods developed for selex. Anal. Bioanal. Chem., 387, 171–181.

Görög, K., Görög, S. 1988 Difference enzyme spectrophotometric determination of 6-mercaptopurine in urine. J. Pharm. Biomed. Anal., 6, 109–113.

Griffin, E.G., Nelson, J.M. 1916 The influence of certain substances on the activity of invertase. J. Am. Chem. Soc., 38, 722–729.

Gross, A.S. 2001 'Best practice in therapeutic drug monitoring.' Br. J. Clin. Pharmacol., 52(Supplement 1), 5–9.

Guglieri-López, B. et al. 2016 'A wide linearity range method for the determination of lenalidomide in plasma by high-performance liquid chromatography: application to pharmacokinetic Studies.' J. Lab. Autom., 21, 806–810.

Guilbault, G.G., Montalvo Jr, J.G. 1969 Urea-specific enzyme electrode. J. Am. Chem. Soc., 91, 2164–2165.

Haji-Fatahaliha, M. et al. 2016 CAR-modified T-cell therapy for cancer: an updated review. Artif. Cells Nanomed. Biotechnol., 44, 1339–1348.

Hamilton, L., Elion, G.B. 1954 The fate of 6- mercaptopurine in man. Ann. N. Y. Acad. Sci., 60, 304–313.

Hatamluyi, B., Es'haghi, Z. 2018 Electrochemical biosensing platform based on molecularly imprinted polymer reinforced by ZnO–graphene capped quantum dots for 6-mercaptopurine detection. Electrochim. Acta, 283, 1170–1177.

Hawwa, A.F., Millership, J.S., Collier, P.S., McElnay, J.C. 2009 Development and validation of an HPLC method for the rapid and simultaneous determination of 6- mercaptopurine and four of its metabolites in plasma and red blood cells. J. Pharm. Biomed. Anal., 49, 401–409.

Haymart, M.R. et al. 2011 Use of radioactive iodine for thyroid cancer. JAMA, 306, 721–728.

Heineman, W.R., Jensen, W.B. 2006 Leland C. Clark Jr. (1918–2005). Biosens. Bioelectron., 21, 1403–1404.

Heinzerling, L., Goldinger, S.M. 2017 A review of serious adverse effects under treatment with checkpoint inhibitors. Curr. Opin. Oncol., 29, 136–144.

Helman, L.J., Meltzer, P. 2003 Mechanisms of sarcoma development. Nat. Rev. Cancer, 3, 685–693.

Herbrink, M. et al. 2018 'Development and validation of a liquid chromatography–tandem mass spectrometry analytical method for the therapeutic drug monitoring of eight novel anticancer drugs.' Biomed. Chromatogr., 32.

Hermann, T., Patel, D.J. 2000 Adaptive recognition by nucleic acid aptamers. Science, 287, 820–825.

Hermanson, Greg T. Bioconjugate techniques. Academic press, 2013.

Herr, H.W., Morales, A. 2008 History of bacillus Calmette–Guerin and bladder cancer: an immunotherapy success story. J. Urol., 179, 53–56.

Homola, J., Yee, S.S., Gauglite, G. 1999 Surface plasmon resonance sensors: review. Sens. Actuat. I, 54, 3–14.

Hon, Y.Y., Evans, W.E. 1998 Making TDM work to optimize cancer chemotherapy: a multidisciplinary team approach. Clin. Chem., 44, 388–399.

Hudson, P.J. 1999 Recombinant antibody constructs in cancer therapy. Curr. Opin. Immunol., 11, 548–556.

Hughes, W.S. 1922 The potential difference between glass and electrolytes in contact with the glass. J. Am. Chem. Soc., 44, 2860–2867.

Huynh, H.H. et al. 2017 ‘Development and validation of a simultaneous quantification method of 14 tyrosine kinase inhibitors in human plasma using LC-MS/MS.’ Ther. Drug Monit., 39, 43–53.

Imai, K., Takaoka, A. 2006 Comparing antibody and small-molecule therapies for cancer. Nat. Rev. Cancer, 6, 714–726.

Innocenti, F. et al. 2000 Variable correlation between 6-mercaptopurine metabolites in erythrocytes and hematologic toxicity: implications for drug monitoring in children with acute lymphoblastic leukemia. Ther. Drug Monit., 22, 375–381.

Jarmoskaite, Inga, et al. 2020 "How to measure and evaluate binding affinities." *Elife* 9: e57263.

Jeong, In Hwa, et al. "Development of aptamers for rapid airborne bacteria detection." *Analytical and Bioanalytical Chemistry* 414.27 (2022): 7763-7771.

Jia, Y.; Chen, S.; Wang, Q.; Li, J. Recent Progress in Biosensor Regeneration Techniques. *Nanoscale* 2024, 16, 2834–2846.
Jia, Y.; Chen, S.; Wang, Q.; Li, J. Recent Progress in Biosensor Regeneration Techniques. *Nanoscale* 2024, 16, 2834–2846.
Jing, Meng, and Michael T. Bowser. "Methods for measuring aptamer-protein equilibria: a review." *Analytica chimica acta* 686.1-2 (2011): 9-18.

Jonathan, E.C., Bernhard, E.J., McKenna, W.G. 1999 How does radiation kill cells? Curr. Opin. Chem. Biol., 3, 77–82.

Juárez-Salcedo, L.M., Desai, V., Dalia, S. 2019 ‘Venetoclax: evidence to date and clinical potential.’ Drugs Context, 8, 212574.

Kang, J.S., Lee, M.H. 2009 Overview of therapeutic drug monitoring. Korean J. Intern. Med., 24, 1–10.

Kato, Y., Matsushita, T., Yokoyama, T., Mohri, K. 1991 Determination of 6-mercaptopurine in acute lymphoblastic leukemia patients plasma by high performance liquid chromatography. Ther. Drug Monit., 13, 220–225.

Kaufman, J.L. et al. 2021 ‘Targeting BCL-2 with venetoclax and dexamethasone in patients with relapsed/refractory (11;14) multiple myeloma.’ Am. J. Hematol., 96, 418–426.

Kershaw, M.H., Westwood, J.A., Darcy, P.K. 2013 Gene engineered T cells for cancer therapy. Nat. Rev. Cancer, 13, 525–540.

Kim, Y.S., Gu, M.B. 2014 Advances in aptamer screening and small molecule aptasensors. Adv. Biochem. Eng. Biotechnol., 140, 29–66.

Kirkwood, J.M., Ernstoff, M.S. 1984 Interferons in the treatment of human cancer. J. Clin. Oncol., 2, 336–351.

Klener, P. Jr, Otáhal, P., Lateckova, L., Klener, P. 2015 Immunotherapy approaches in cancer treatment. Curr. Pharm. Biotechnol., 16, 771–780.

Kohlhapp, F.J., Kaufman, H.L. 2016 Molecular pathways: mechanism of action for talimogene laherparepvec, a new oncolytic virus immunotherapy. Clin. Cancer Res., 22, 1048–1053.

Krens, S.D., van der Meulen, E., Jansman, F.G.A., Burger, D.M., van Erp, N.P. 2020 'Quantification of cobimetinib, cabozantinib, dabrafenib, niraparib, olaparib, vemurafenib, regorafenib and its metabolite regorafenib M2 in human plasma by UPLC–MS/MS.' Biomed. Chromatogr., 34, e4758.

Krylov, Sergey N. "Underestimation of the Complexity of K d Determination: Causes, Implications, and Ways to Improve." *ACS Measurement Science Au* 4.3 (2024): 232-233.

Kushwaha, Ankita, et al. "Competitive non-SELEX for the selective and rapid enrichment of DNA aptamers and its use in electrochemical aptasensor." *Scientific Reports* 9.1 (2019): 1-11.

Lange, M.M., et al 2013 Long-term results of rectal cancer surgery with a systematical operative approach. Ann. Surg. Oncol., 20, 1806–1814.

Lasica, M., Anderson, M.A. 2021 'Review of Venetoclax in CLL, AML and multiple myeloma.' J. Pers. Med., 11, 463.

Lavi, L.E., Holcenberg, J.S. 1985 A rapid and sensitive high-performance liquid chromatographic assay for 6-mercaptopurine metabolites in red blood cells. Anal. Biochem., 144, 514–520.

Lazcka, O., Del Campo, F.J., Muñoz, F.X. 2007 Pathogen detection: A perspective of traditional methods and biosensors. Biosens. Bioelectron., 22, 1205–1216.

Le, Q.T., Shirato, H., Giaccia, A.J., Koong, A.C. 2015 Emerging treatment paradigms in radiation oncology. Clin. Cancer Res., 21, 3393–3400.

Lea, W.A., Simeonov, A. 2011 'Fluorescence polarization assays in small molecule screening.' Expert Opin. Drug Discov., 6, 17–31.

Lee, S.J., Chinen, J., Kavanaugh, A. 2010 Immunomodulator therapy: monoclonal antibodies, fusion proteins, cytokines, and immunoglobulins. J. Allergy Clin. Immunol., 125(Supplement 2), S314–S323.

Lee, Su Jin, et al. "Design and prediction of aptamers assisted by in silico methods." *Biomedicines* 11.2 (2023): 356.

Lenalidomide market outlook 2025-2034: Market share, and growth analysis, Research and Markets - Market Research Reports - Welcome. Available at: http://www.marketpublishers.com/report/drugs/oncology-drugs/lenalidomide-market-og.html

Lennard, L. 2001 Therapeutic drug monitoring of cytotoxic drugs. Br. J. Clin. Pharmacol., 52(Supplement 1), 75S–87S.

Lennard, L., Singleton, H.J. 1992 High-performance liquid chromatographic assay of the methyl and nucleotide metabolites of 6 – mercaptopurine: quantitation of red blood cell 6-thioguanine nucleotide, 6-thioinosinic acid and 6-methylmercaptopurine metabolites in a single sample. J. Chromatogr., 583, 83–89.

Leone, R.D., Lo, Y.C., Powell, J.D. 2015 A2aR antagonists: next generation checkpoint blockade for cancer immunotherapy. Comput. Struct. Biotechnol. J., 13, 265–271.

Lewandrowski, K.U., Anderson, M.E., McLain, R.F. In: Herkowitz HN, Garfin SR, Eismont FJ, Bell GR, Balderston RA, eds. 2011. Elsevier Saunders: Philadelphia, Tumors of the spine: 1480–1511.

Li, A.P., Peng, J.D., Zhou, M., Zhang, J. Six-mercaptopurine coupled with HPLC technique 2016. Spectrochim. Acta A Mol. Biomol. Spectrosc., 154, 1–7.

Li, A.P., Peng, J.D., Zhou, M.Q., Zhang, J. Resonance light scattering determination of.

Li, H., Sun, D.- E., Liu, Y., and Liu, Z. (2014). An ultrasensitive homogeneous aptasensor for kanamycin based on up conversion fluorescence resonance energy transfer. *Biosens. Bioelectron.* 55,149–156.

Li, M.-G., Wang, Y.-L., Wang, G.-F., Fang, B. Six-mercaptopurine at silver microdisk electrodes 2005. Ann. Chim., 95, 685–692.

Liedberg, B., Nylander, C., Lunström, I. 1983 Surface plasmon resonance for gas detection and biosensing. Sens. Actuators, 4, 299–303.

Lipson, E.J., Drake, C.G. 2011 Ipilimumab: an anti-CTLA-4 antibody for metastatic melanoma. Clin. Cancer Res., 17, 6958–6961.

Liu, H. et al. 2017 'Metabolism and disposition of a novel B-cell lymphoma-2 inhibitor Venetoclax in humans and characterization of its unusual metabolites.' Drug Metab. Dispos., 45, 294–305.

Lu, G., Goodman, A.M., Ayres, B., Builta, Z., Haes, A.J. 2015 Near real-time determination of metabolic parameters for unquenched 6-mercaptopurine and xanthine oxidase samples using capillary electrophoresis. J. Pharm. Biomed. Anal., 111, 51–56.

Lu, G., Goodman, A.M., Ayres, B., Builta, Z., Haes, A.J. Near real-time determination.

Manea, Ioana, et al. "A review on magnetic beads-based SELEX technologies: Applications from small to large target molecules." *Analytica Chimica Acta* 1297 (2024): 342325.

Mayer, L.D., Janoff, A.S. 2007 Optimizing combination chemotherapy by controlling drug ratios. Mol. Interv., 7, 216–224.

McBride, A. et al. 2019 'The role of inhibition of apoptosis in acute leukemias and myelodysplastic syndrome.' Front. Oncol., 9, 192.

McCormack, J., Johns, D. In: Chabuer B, ed., cd Pharmacologic principles of cancer treatment. W. B. Saunders Co.: Philadelphia 1982 Purine antimetabolitcs: 213–228.

Mehrotra, Parikha. 2106 'Biosensors and their applications–A review.' *Journal of oral biology and craniofacial research* 6(2): 154-159.

Meijer, R.P., Boon, T.A., van Venrooij, G.E.P.M., Wijburg, C.J. 2007 Long-term follow-up after laser therapy for penile carcinoma. Urology, 69, 759–761.

Mellman, I., Coukos, G., Dranoff, G. 2011 Cancer immunotherapy comes of age. Nature, 480, 480–489.

Meneghello, Anna, et al. 2018 "Biosensing technologies for therapeutic drug monitoring." Current medicinal chemistry 25.34 (2018): 4354-4376.

Menzies, A.M., Long, G.V., Murali, R. 2012 'Dabrafenib and its potential for the treatment of metastatic melanoma.' Drug Des. Dev. Ther., 6, 391–405.

Merienne, C. et al. 2018 'High throughput routine determination of 17 tyrosine kinase inhibitors by LC–MS/MS.' J. Pharm. Biomed. Anal., 150, 112–121.

Mikus, G., Foerster, K.I. 2017 'Role of CYP3A4 in kinase inhibitor metabolism and assessment of CYP3A4 activity.' Transl. Cancer Res., 6(Supplement 10), S1592–S1598.

Milone, M.C. 2024. 'Analytical techniques used in therapeutic drug monitoring.' Therapeutic Drug Monitoring. Academic Press, 67–91.

Mouridsen, H., Overgaard, M. 1990. In: Proceedings of 15th international cancer congress. BRD: Hamburg. Springer International, The role of adjuvant radiotherapy added to systemic therapy.

Mukherjee, D. et al. 2023 'Impact of multiple concomitant CYP3A inhibitors on venetoclax pharmacokinetics: a PBPK and population PK-Informed analysis.' J. Clin. Pharmacol., 63, 119–126.

Murphy, G. et al., 2018. In: Elder D, Massi D, Scolyer R, Willemze R, eds. WHO classification of skin tumors, 4th ed. IARC: Lyon, Squamous cell carcinoma: 35–45.

Narang, P.K., Yeager, R.L., Chatterji, D.C. 1982 Quantitation of 6-mercaptopurine in biologic fluids using high-performance liquid chromatograph: a selective novel procedure. J. Chromatogr., 230, 373–381.

Nelson, J.M., Griffin, E.G. 1916 Adsorption of invertase. J. Am. Chem. Soc., 38, 1109–1115.

Ni, X., Castanares, M., Mukherjee, A., Lupold, S.E. 2011 Nucleic acid aptamers: clinical applications and promising new horizons. Curr. Med. Chem., 18, 4206–4213.

Nijenhuis, C.M., Haverkate, H., Rosing, H., Schellens, J.H., Beijnen, J.H. 2016 'Simultaneous quantification of dabrafenib and trametinib in human plasma using high-performance liquid chromatography–tandem mass spectrometry.' J. Pharm. Biomed. Anal., 125, 270–279.

Nishiyama, K., Sugiura, K., Kaji, N., Tokeshi, M., Baba, Y. 2019 'Development of a microdevice for facile analysis of theophylline in whole blood by a cloned enzyme donor immunoassay.' Lab Chip, 19, 233–240.

Old, L.J. 1996 Immunotherapy for cancer. Sci. Am., 275, 136–143.

Ouellet, D. et al. 2014 'Population pharmacokinetics of dabrafenib, a BRAF inhibitor: effect of dose, time, covariates, and relationship with its metabolites.' J. Clin. Pharmacol., 54, 696–705.

Philippe, M. et al. 2022 'Venetoclax Pharmacokinetics in Real World AML patients: A real Candidate for therapeutic drug monitoring.' Blood, 140(Supplement 1), 6178–6180.

Puszkiel, A. et al. 2018 'Clinical pharmacokinetics and pharmacodynamics of dabrafenib.' Clin. Pharmacokinectics, 58, 451–466.

Rabel, S.R., Stobaugh, J.F., Trueworthy, R. 1995 Six-mercaptopurine metabolites in erythrocytes utilizing capillary electrophoresis with laser induced fluorescence detection. Anal. Biochem., 224, 315–321.

Rai, M., Gade, A., Gaikwad, S., Marcato, P.D., Durán, N. 2012 Biomedical applications of nanobiosensors: the state-of-the-art. J. Braz. Chem. Soc., 23, 14–23.

Rai, S.K., Gunnam, A., Mannava, M.K.C., Nangia, A.K. 2020 'Improving the dissolution rate of the anticancer drug dabrafenib.' Cryst. Growth Des., 20, 1035–1045.

Reddy, A., Jadav, T., Sahu, A.K., Sengupta, P. 2022 'LC–MS/MS bioanalytical method for quantification of binimetinib and venetoclax, and their pharmacokinetic interaction.' Bioanalysis, 14, 75–86.

Reddy, S.M., Higson, S.P.J., Vadgama, P.M. 1994 Enzyme and other Biosensors: evolution of a technology. Eng. Sci. Educ. J., 3, 41–48.

Reynolds, D.J.M., Aronson, J.K. 1993 ABC of monitoring drug therapy. Making the most of plasma drug concentration measurements. Br. Med. J., 306, 48–51.

Rheault, T.R. et al. 2013 'Discovery of dabrafenib: A selective inhibitor of Raf kinases with antitumor activity against B-Raf-Driven tumors.' ACS Med. Chem. Lett., 4, 358–362.

Ribas, A., Wolchok, J.D. 2018 Cancer immunotherapy using checkpoint blockade. Science, 359, 1350–1355.

Richardson, P., Anderson, K. 2004 Immunomodulatory analogs of thalidomide: an emerging new therapy in myeloma. J. Clin. Oncol., 22, 3212–3214.

Ried, L.D., Horn, J.R., McKenna, D.A. 1990 Therapeutic drug monitoring reduces toxic drug reactions: a meta-analysis. Ther. Drug Monit., 12, 72–78.

Rodríguez, J.M.F., Castañeda, G., Muñoz, L., Lizcano, I., Berciano, M.A. 2016 'Micellar electrokinetic chromatographic method for the dabrafenib determination in biological samples.' Electrophoresis, 37, 1296–1301.

Rosenberg, S.A. 2014 IL-2: the first effective immunotherapy for human cancer. J. Immunol., 192, 5451–5457.

Rosenberg, S.A. et al. 1988 Use of tumor-infiltrating lymphocytes and interleukin-2 in the immunotherapy of patients with metastatic melanoma. A preliminary report. N. Engl. J. Med., 319, 1676–1680.

Rosenfeld, J.M., Taguchi, V.Y., Hillcoat, B.L. & Kawal, M. (1977). Determination of 6-mercaptopurine in plasma by mass-spectrometry. Analyt. Chem., 49, 725-727.

Rousset, M., et al. 2017 'An UPLC-MS/MS method for the quantification of BRAF inhibitors (vemurafenib, dabrafenib) and MEK inhibitors (cobimetinib, trametinib, binimetinib) in human plasma. Application to treated melanoma patients.' Clin. Chim. Acta, 470, 8–13.

Rowe, A. A., Miller, E. A., and Plaxco, K. W. (2010). Reagent less measurement of aminoglycoside antibiotics in blood serum via an electrochemical, ribonucleic acid aptamer-based biosensor. *Anal. Chem*. 82,7090–7095.

Salamone, S.J., Courtney, J.B., Clarke, W.A. 2023 'New immunoassays in therapeutic drug monitoring: where is the journey heading?' Ther. Drug Monit., 45, 11–13.

Salem, A.H. et al. 2017 'Pharmacokinetics of Venetoclax, a novel BCL-2 inhibitor, in patients with relapsed or refractory chronic lymphocytic leukemia or non-Hodgkin lymphoma.' J. Clin. Pharmacol., 57, 484–491.

Salem, A.H. et al. 2019 'Pharmacokinetics of the BCL-2 inhibitor venetoclax in subjects with hepatic impairment.' Clin. Pharmacokinet., 58, 1091–1100.

Sato, Y. et al. 2005 Highly-sensitive determination of 6- mercaptopurine and its metabolites by electrochemical reductive desorption measurements. Electroanalysis, 17, 965–967.

Schultz, J.S. 1982 Optical sensor of plasma constituents. U.S. Pat. 4,344,438 A.

Scott, Duncan E., et al. 2016 "Small molecules, big targets: drug discovery faces the protein–protein interaction challenge." *Nature Reviews Drug Discovery* 15.8: 534-550.

Shaikh, A.S., Guo, R. 2017 'Therapeutic drug monitoring of phenytoin by simple, rapid, accurate, highly sensitive and novel method and its clinical applications.' Curr. Pharm. Biotechnol., 18, 1098–1104.

Sharma, P., Wagner, K., Wolchok, J.D., Allison, J.P. 2011 Novel cancer immunotherapy agents with survival benefit: recent successes and next steps. Nat. Rev. Cancer, 11, 805–812.

Singh, N.K.; Chung, S.; Chang, A.-Y.;Wang, J.; Hall, D.A. A Non-Invasive Wearable Stress Patch for Real-Time Cortisol Monitoring Using a Pseudoknot-Assisted Aptamer. *Biosens. Bioelectron*. 2023, 227, 115097

Sirohi, B., Powles, R. 2004 Multiple myeloma. Lancet, 363, 875–886.

Sletten, E., Sletten, J.T., Jensen, L.H. 1969 ‘The crystal and molecular structure of 6-mercaptopurine monohydrate.’ Acta Crystallogr. B Struct. Crystallogr. Cryst. Chem., 25, 1330–1337.

Snyder, L.R., Kirkland, J.J., Dolan, J.W. 2016. Introduction to modern liquid chromatography. John Wiley & Sons: Song, Zhaorui et al. "A validated chemiluminescence immunoassay for methotrexate (MTX) and its application in a pharmacokinetic study." Analytical Methods 8.1: 162–170.

Song, Min, et al. "Materials and methods of biosensor interfaces with stability." *Frontiers in Materials* 7 (2021): 583739.

Spector, R., Park, G.D., Johnson, G.F., Vesell, E.S. 1988 Therapeutic drug monitoring. Clin. Pharmacol. Ther., 43, 345–352.

Srinivas, T.R., Meier-Kriesche, H.U. 2008 Minimizing immunosuppression, an alternative approach to reducing side effects: objectives and interim result. Clin. J. Am. Soc. Nephrol., 3(Supplement 2), S101–S116.

Stafford, R.J., Fuentes, D., Elliott, A.A., Weinberg, J.S., Ahrar, K. 2010 Laser-induced thermal therapy for tumor ablation. Crit. Rev. Biomed. Eng., 38, 78–100.

Stangherlin, Stefen, Yuzhe Ding, and Juewen Liu. 2025 "Dissociation Constant (Kd) Measurement for Small-Molecule Binding Aptamers: Homogeneous Assay Methods and Critical Evaluations." *Small Methods*, 2401573.

Strategic insights for venetoclax market growth.Comprehensive Market Research & Forecast Analysis. Available at: http://www.datainsightsmarket.com/reports/venetoclax-306780#summary.

Stubbe, C.E., Valero, M. 2013 Complementary strategies for the management of radiation therapy side effects. J. Adv. Pract. Oncol., 4, 219–231.

Sun, H. et al. 2014 Oligonucleotide aptamers: new tools for targeted cancer therapy. Mol. Ther. Nucleic Acids, 3, e182, doi:10.1038/mtna.2014.32.

Sun, H., Wang, T., Liu, X., Chen, P. 2013 A sensitive inhibition chemiluminescence method for the determination of 6-mercaptopurine in tablet and biological fluid using the reaction of luminol Ag (III) complex in alkaline medium. J. Lumin., 134, 154–159.

Supandi, S., Harahap, Y., Harmita, H., R. 2018 Andalusia, Quantification of 6-mercaptopurine and its metabolites in patients with acute lympoblastic leukemia using dried blood spots and UPLC MS/MS. Sci. Pharm., 86.

Suttle, A.B. et al. 2015 ‘Assessment of the drug interaction potential and single- and repeat-dose pharmacokinetics of the BRAF inhibitor dabrafenib.’ J. Clin. Pharmacol., 55, 391–400.

Suzuki, S., Takahashi, F., Satoh, I., Sonobe, N. 1975 Ethanol and lactic acid sensors using electrodes coated with dehydrogenase–collagen membranes. Bull. Chem. Soc. Jpn, 48, 3246–3248.

Swerdlow, S.H., et al 2016 The 2016 revision of the World Health Organization classification of lymphoid neoplasms. Blood, 127, 2375–2389.

Syam, R., Davis, K.J., Pratheesh, M.D., Anoopraj, R., Surej Joseph, B. 2012 Biosensors: A novel approach for pathogen detection. VetScan, 7, 14–18.

Szeghalmi, A.V. et al. 2005 Adsorption of 6-mercaptopurine and 6-mercaptopurine-ribosideon silver colloid: a pH-dependentsurface-enhanced Raman spectroscopy and density functional theory study. II. 6-mercaptopurine-riboside. Biopolymers, 78, 298–310.

Tariman, J.D. 2007 Lenalidomide: a new agent for patients with relapsed or refractory multiple myeloma. Clin. J. Oncol. Nurs., 11, 569–573.

Tett, S., Ray, J., Morris, R. Best practice in therapeutic drug monitoring 1995. Published.

Thevendran, Ramesh, and Marimuthu Citartan. "Assays to estimate the binding affinity of aptamers." *Talanta* 238 (2022): 122971.

Trapani, J.A., Darcy, P.K. 2017 Immunotherapy of cancer. Aust. Fam. Phys., 46, 194–199.

Tuerk, C., Gold, L. 1990 Systematic evolution of ligands by exponential enrichment: RNA ligands to bacteriophage T4 DNA polymerase. Science, 249, 504–510.

Tzouvadaki, I., Aliakbarinodehi, N., De Micheli, G., and Carrara, S. (2017). The memristive effect as a novelty in drug monitoring. Nanoscale 9 (27), 9676–9684.

Ullman, E.F. In: Wild D, ed. 2013 The immunoassay handbook, 4th ed. Elsevier: Oxford, UK, Chapter 2.3 Homogeneous immunoassays: 67–86.

Usman, M., Hempel, G. 2016 'Development and validation of an HPLC method for the determination of vancomycin in human plasma and its comparison with an immunoassay (PETINIA).' Springerplus, 5, 124.

Van Eeckhaut, A., Lanckmans, K., Sarre, S., Smolders, I., Michotte, Y. 2009 'Validation of bioanalytical LC–MS/MS assays: evaluation of matrix effects.' J. Chromatogr. B Analyt. Technol. Biomed. Life Sci., 877, 2198–2206.

Van Erp, N.P., Gelderblom, H., Guchelaar, H.J. 2009 'Clinical pharmacokinetics of tyrosine kinase inhibitors.' Cancer Treat. Rev., 35, 692–706.

Verheijen, R.B. et al. 2017 'Practical recommendations for therapeutic drug monitoring of kinase inhibitors in Oncology.' Clin. Pharmacol. Ther., 102, 765–775.

Vestergaard, M.C., Kerman, K., Hsing, I.M., Tamiya, E. (eds) 2015. Nanobiosensors and nanobioanalyses. Springer: Tokyo.

Vikingsson, S., Dahlberg, J.O., Hansson, J., Höiom, V., Gréen, H. 2017 'Simple and cost-effective liquid chromatography-mass spectrometry method to measure dabrafenib quantitatively and six metabolites semi-quantitatively in human plasma.' Anal. Bioanal. Chem., 409, 3749–3755.

Vogeser, M., Seger, C. 2010 'Pitfalls associated with the use of liquid chromatography–tandem mass spectrometry in the clinical laboratory.' Clinical Chemistry, 56(8), 1234–1243.

Vonderheide, R.H., Nathanson, K.L. 2013 Immunotherapy at large: the road to personalized cancer vaccines. Nat. Med., 19, 1097–1100.

Waggoner, M., Katsetos, J., Thomas, E., Galinsky, I., Fox, H. 2022 'Practical management of the VenetoClax-Treated patient in chronic lymphocytic leukemia and acute myeloid leukemia.' J. Adv. Pract. Oncol., 13, 400–415.

Wang, C., Wu, J., Zong, C., Xu, J., Ju, H.-X. 2012 'Chemiluminescent immunoassay and its applications.' Chin. J. Anal. Chem., 40, 3–10.

Wang, J. et al. 1997 DNA electrochemical biosensors for environmental monitoring: a review. Anal. Chim. Acta, 347, 1–8.

Wang, Wenjing, et al. "A brief review of aptamer-based biosensors in recent years." *Biosensors* 15.2 (2025): 120.

Wang, Z., Liu, Q. 2017 Clinical pharmacological considerations on CAR-T cell therapy for cancer. J. Pharmacol. Clin. Res., 3, 001–004.

Wang, Z., Wu, Z., Liu, Y., Han, W. 2017 New development in CAR-T cell therapy. J. Hematol. Oncol., 10, 53.

Watts, H.J., Lowe, C.R., Pollard-Knight, D.V. 1994 Optical biosensor for monitoring microbial cells. Anal. Chem., 66, 2464–2470.

Whalen, C.E., Soldin, S.J., Sulk, H. et al 1986 Pharmacokinetic determinants of 6-mercaptopurine. Myelotoxicity and therapeutic failure in children with acute lymphoblastic leukemia (ALL). Clin. Chem., 31, 1092.

Wherry, E.J. 2011 T cell exhaustion. Nat. Immunol., 12, 492–499.

Wilhelm, A.J., den-den Burger, J.C.G., Swart, E.L. 2014 Therapeutic drug monitoring by dried blood spot: progress to date and future directions. Clin. Pharmacokinet., 53, 961–972.

Willoughby, R.C., Sheehan, E., Mitrovich, S.. 2002 A global view of LC/MS: how to solve your most challenging analytical problems (No Title).

Wilson, D.S., Szostak, J.W. 1999 In vitro selection of functional nucleic acids. Annu. Rev. Biochem., 68, 611–646.

Xiao, Xueran, et al. Oligonucleotide aptamers: Recent advances in their screening, molecular conformation and therapeutic applications. *Biomedicine & Pharmacotherapy*, 2021, 143: 112232.

Yang, Ge, et al. "Pressure controllable aptamers picking strategy by targets competition." *Chinese Chemical Letters* 32.1 (2021): 218-220.

Yang, H. et al. 2005 Raman mapping and in situ SERS spectroelectrochemical studies of 6-mercaptopurine SAMs on the gold electrode. J. Phys. Chem. B, 109, 2738–2744.

Yang, X. et al. 2022 'Quantification of Venetoclax for therapeutic drug monitoring in Chinese acute myeloid leukemia patients by a validated UPLC-MS/MS method.' Molecules, 27, 1607.

Yang, Y. 2015 'Cancer immunotherapy: harnessing the immune system to battle cancer.' J. Clin. Invest., 125, 3335–3337.

Yang, Y.L. et al. 2023 'LC–MS/MS methods for determination of venetoclax in human plasma and cerebrospinal fluid.' Biomed. Chromatogr., 37, e5738.

Ye, C.;Wang, M.; Min, J.; Tay, R.Y.; Lukas, H.; Sempionatto, J.R.; Li, J.; Xu, C.; Gao,W. AWearable Aptamer Nanobiosensor for Non-Invasive Female Hormone Monitoring. *Nat. Nanotechnol*. 2024, 19, 330–337.

Yip, A., Webster, R.M. 2018 The market for chimeric antigen receptor T cell therapies. Nat. Rev. Drug Discov., 17, 161–162.

Yoo, E.H., Lee, S.Y. 2010 Glucose biosensors: an overview of use in clinical practice. Sensors (Basel), 10, 4558–4575.

Yu, H.; Alkhamis, O.; Canoura, J.; Liu, Y.; Xiao, Y. Advances and Challenges in Small-Molecule DNA Aptamer Isolation, Characterization, and Sensor Development. *Angew. Chem. Int. Ed*. 2021, 60, 16800–16823.

Zhao, Y.T., et al. 2022 'Comparison of LC-MS/MS and EMIT methods for the precise determination of blood sirolimus in children with vascular anomalies.' Front. Pharmacol., 13, 925018.

Zhong, L. et al. 2021 'Small molecules in targeted cancer therapy: advances, challenges, and future perspectives.' Signal Transduct. Target. Ther., 6, 201.

Zhou, Jiehua; Rossi, John. Aptamers as targeted therapeutics: current potential and challenges. *Nature reviews Drug discovery*, 2017, 16.3: 181-202.

Zhou, Yuying, et al. 2025 "Recent advances in enhancing the sensitivity of biosensors based on field effect transistors." *Advanced Electronic Materials* 11.7: 2400712.

Appendix: Potential secondary structures for each selected aptamer

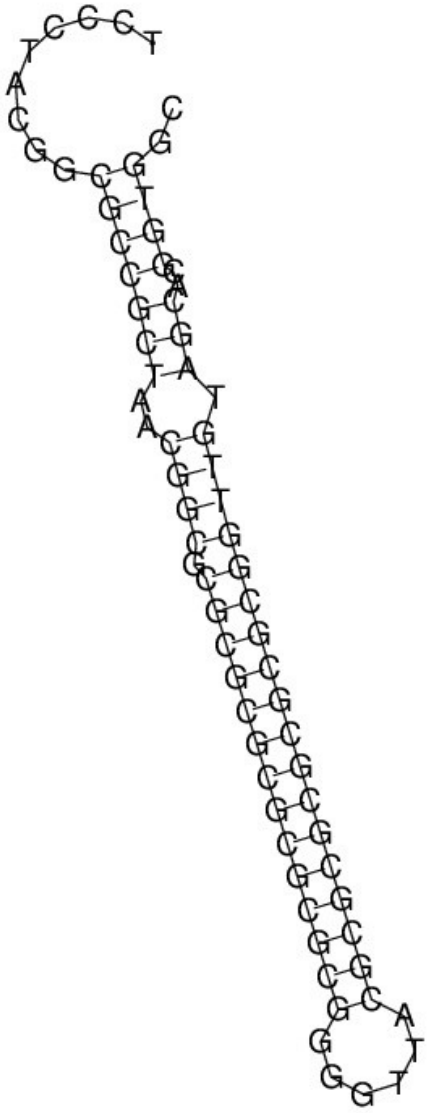

Aptamer code: LDM 1 (Δ = - 49.20 kcal/mol)

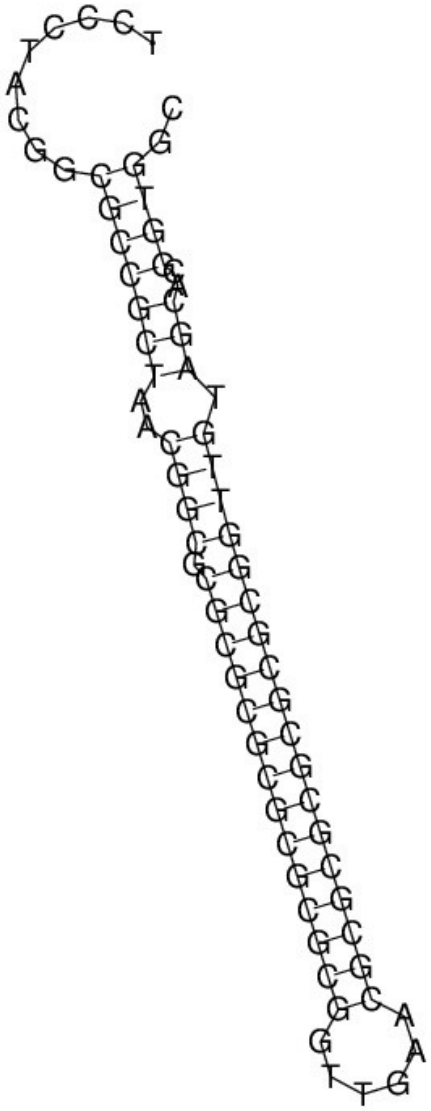

Aptamer code: LDM 2 (Δ = - 49.20 kcal/mol)

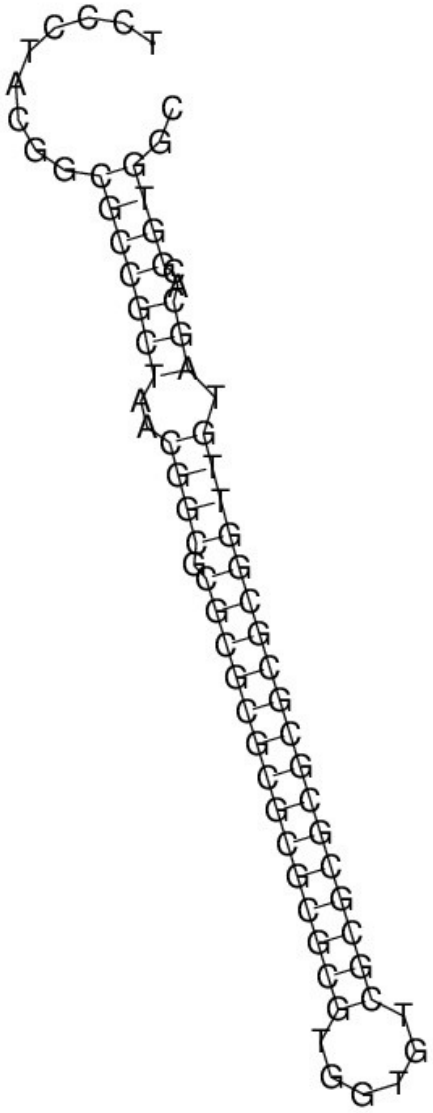

Aptamer code: LDM 3 (Δ = - 48.30 kcal/mol)

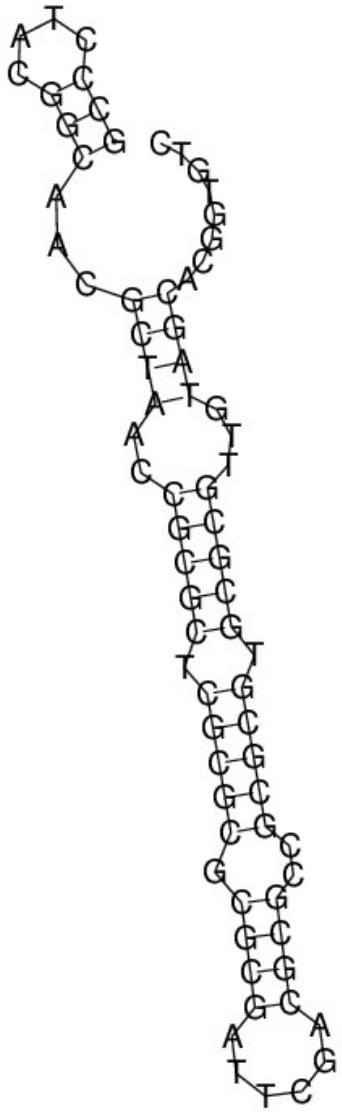

Aptamer code: 6-MP 1 (∆ = - 38.10 kcal/mol)

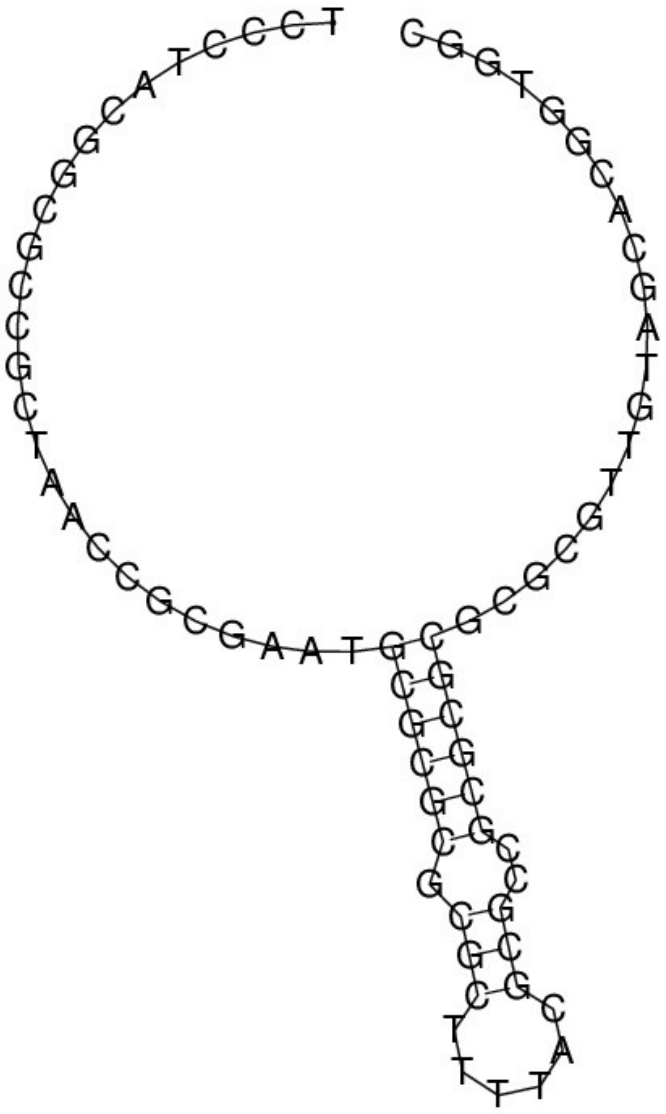

Aptamer code: 6-MP 2 (∆ = - 34.80 kcal/mol)

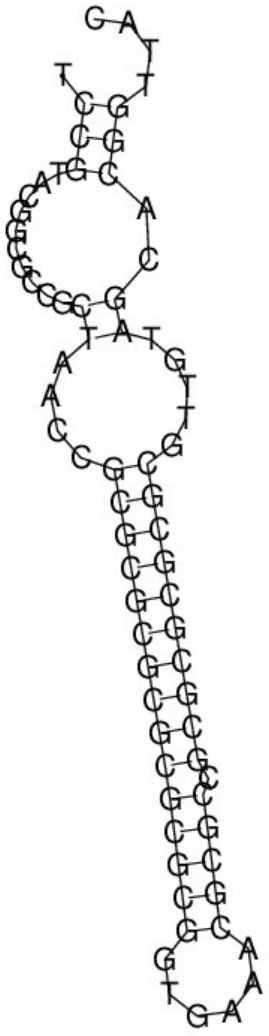

Aptamer code: 6-MP 3 (Δ = -43.50 kcal/mol)

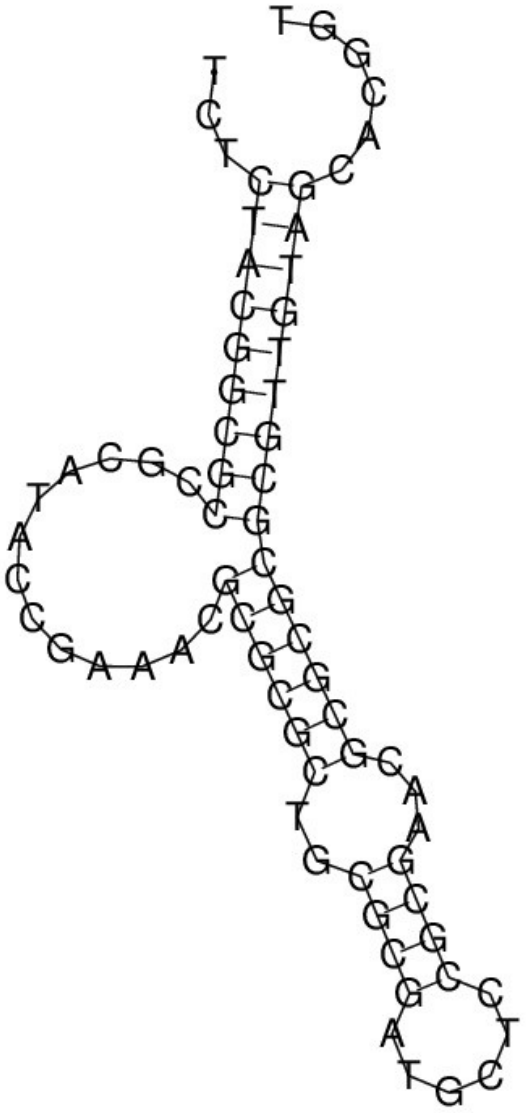

Aptamer code: DFB 1 (Δ = -27.90 kcal/mol)

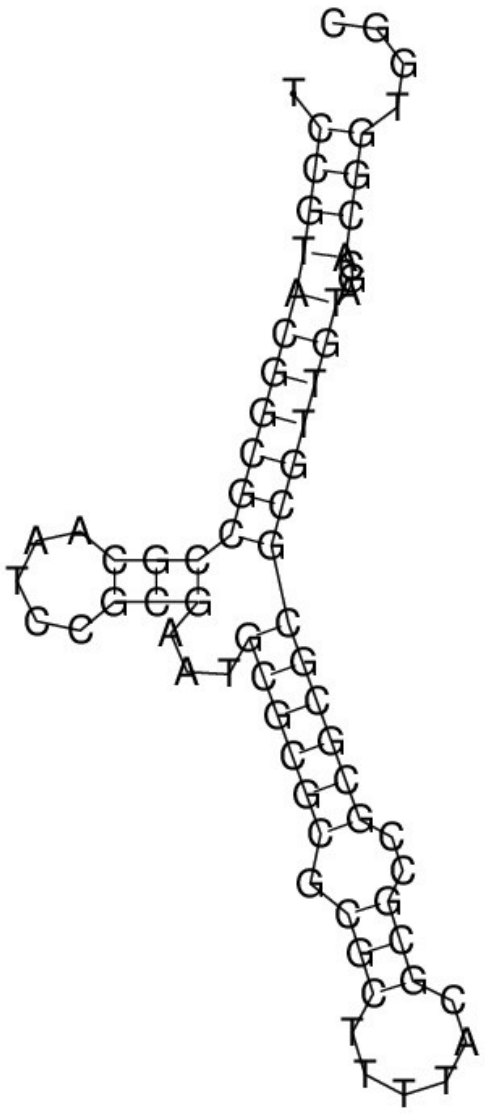

Aptamer code: DFB 2 (∆ = -34.70 kcal/mol)

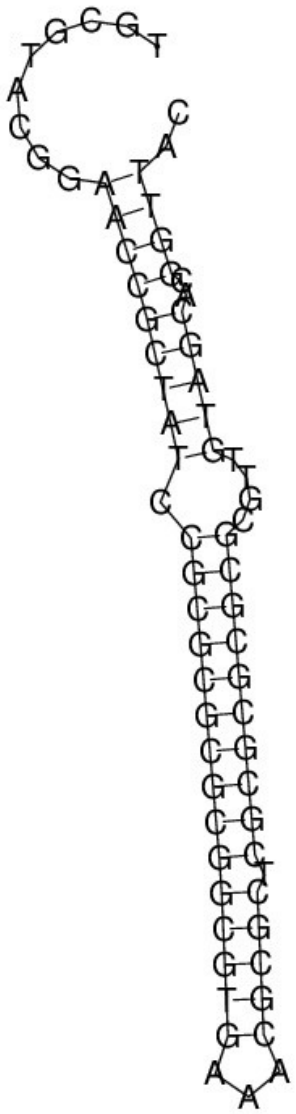

Aptamer code: DFB 3 (Δ = -37.30 kcal/mol)

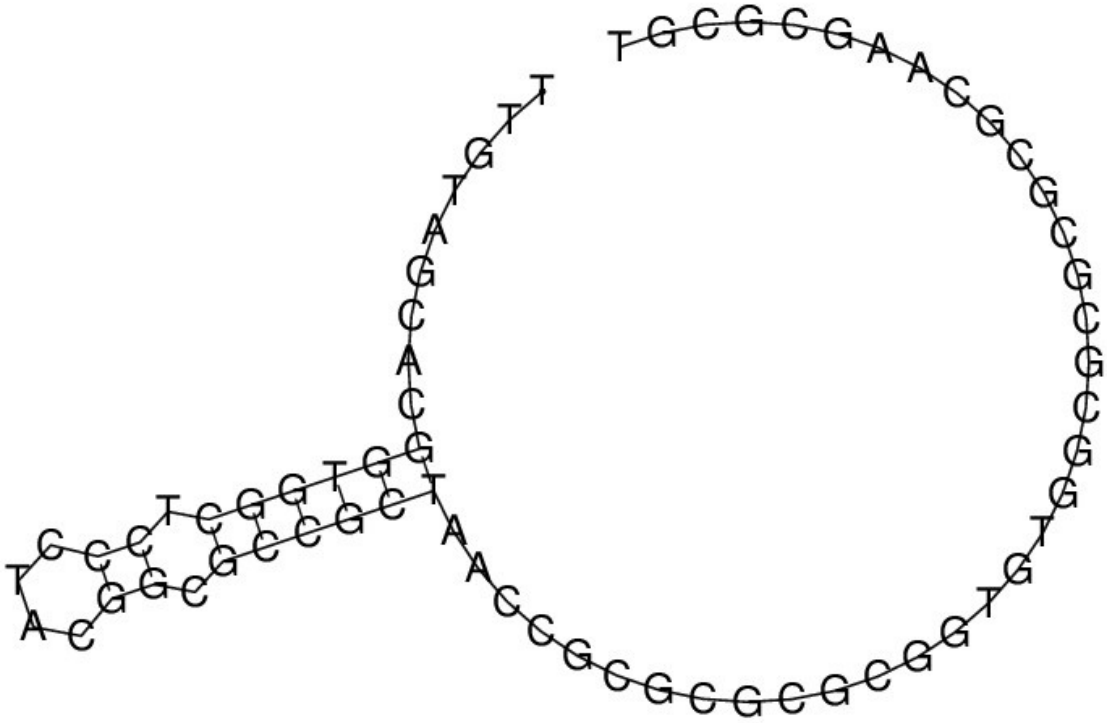

Aptamer code: VENX 1 (∆ = -33.30 kcal/mol)

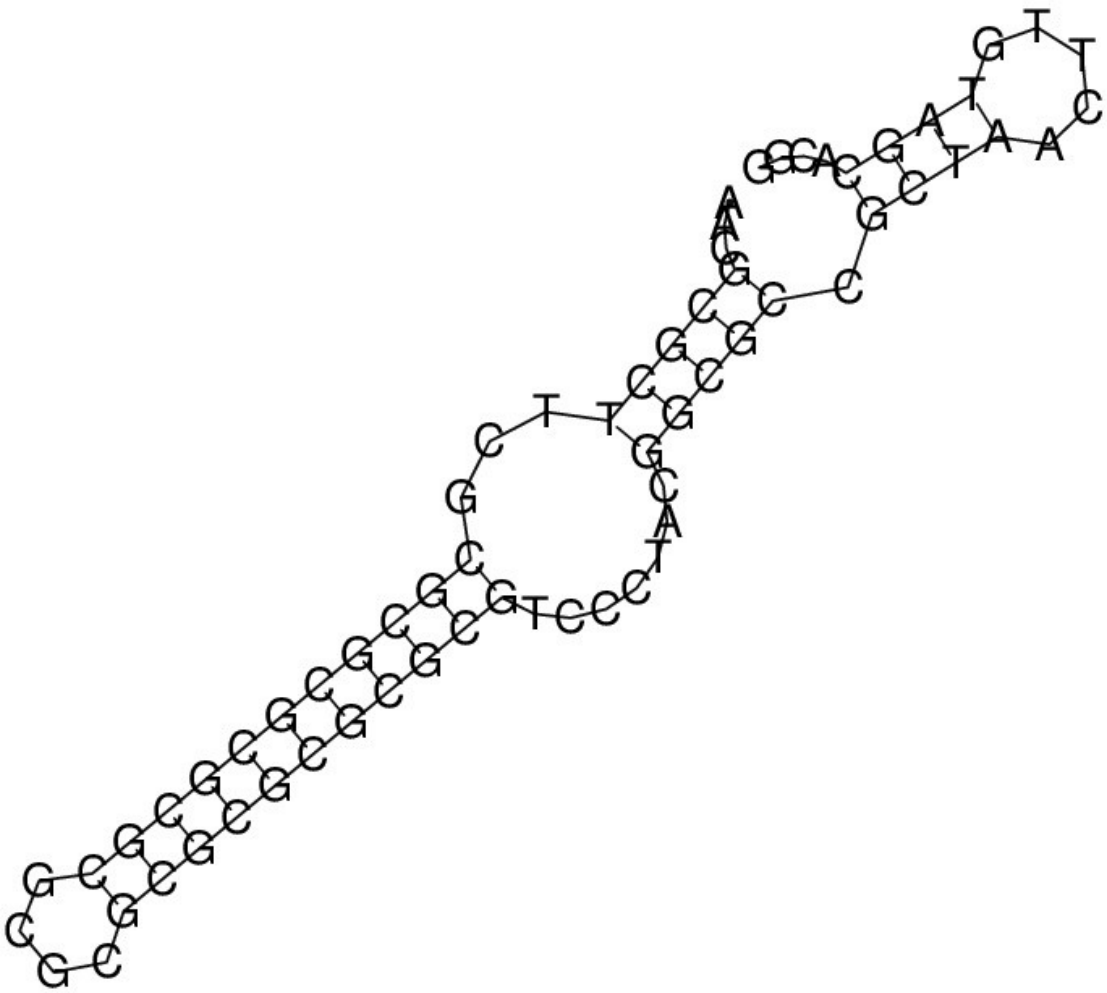

Aptamer code: VENX 2 (∆ = -36.60 kcal/mol)

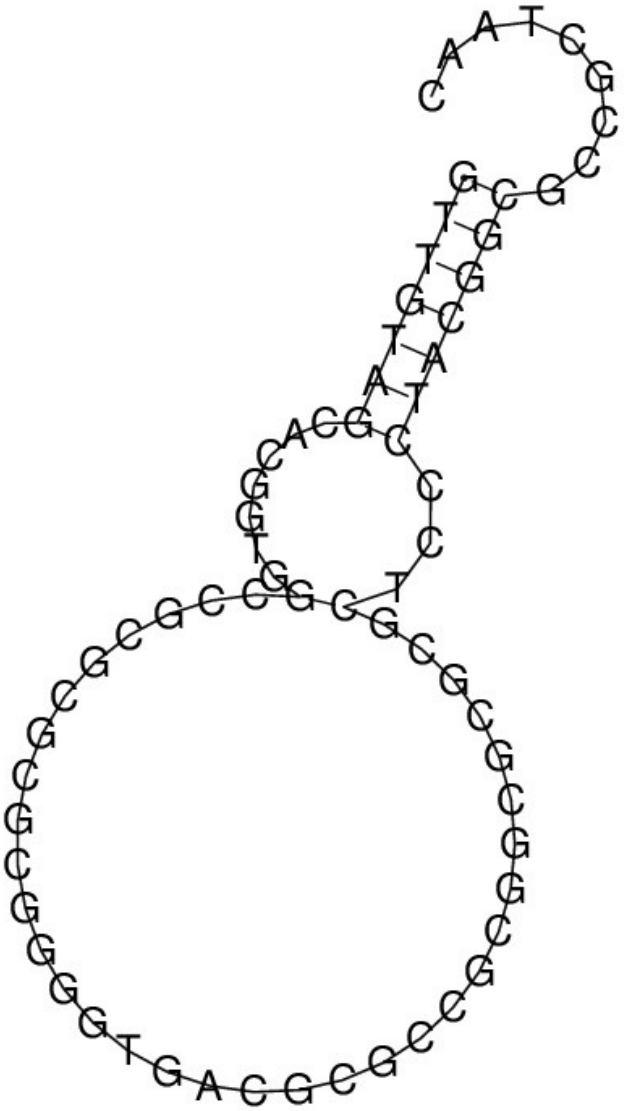

Aptamer code: VENX 3 (∆ = --36.20 kcal/mol)